



UNIVERSITÀ DEGLI STUDI DI MILANO

Dipartimento di Scienze Farmacologiche e Biomolecolari

Dottorato di ricerca in Scienze Farmacologiche Sperimentali e Cliniche  
Ciclo XXIX

SNX27 REGULATES GPR17 RECYCLING AND THE KINETICS OF  
OLIGODENDROCYTE DIFFERENTIATION: IMPLICATION IN  
DOWN SYNDROME

Settore Scientifico Disciplinare BIO/14

Tesi di Dottorato di:  
ALESSANDRO FRANCESCO ULIVI

Tutor: Prof. ALBERTO EMILIO PANERAI

Co-Tutor: Dott.ssa PATRIZIA ROSA

Coordinatore del Dottorato: Prof. ALBERTO CORSINI

Anno Accademico 2015/2016

# INDEX

ABBREVIATIONS	3
ABSTRACT	5
RIASSUNTO	6
INTRODUCTION	8
<b>From immature precursors to myelinating cells: factors that regulate OL development</b>	8
<i>Intrinsic factors</i>	10
<i>External cues</i>	12
<i>Neuronal activity</i>	15
<i>Epigenetic mechanisms</i>	15
<b>Slow and steady wins the race, an intrinsic timer for OL development: GPR17</b>	16
<b>Receptor endocytosis</b>	19
<i>The endosomal network</i>	19
<i>Biochemical properties of endosomes</i>	24
<i>Molecular mechanisms underlying endosomal sorting</i>	26
<b>Delivery to LE and lysosome</b>	26
<b>Retromer complex-regulated recycling and retrograde transport</b>	27
The different structures of retromer complexes	27
The sorting nexin family	27
The functions of retromer complexes	28
Molecular mechanisms underlying protein sorting in the endosomal pathways	30
<b>SNX27, an adaptor protein for receptor sorting into the short loop recycling</b>	33
<i>SNX27 retromer and pathologies</i>	36
<b>GPR17 PDZ-binding motif is required for receptor accurate localization at the cell surface by mediating a putative interaction with SNX27</b>	37
AIMS OF THE WORK	43
MATERIALS AND METHODS	44
<b>Antibodies and reagents</b>	44
<b>Plasmids, oligonucleotides and site-directed mutagenesis</b>	44
<b>Cell culture</b>	45
<b>Cell transfection</b>	46
<b>Cell lysis and fractionation of nuclei/cytosol</b>	47
<b>Protein purification from bacteria extracts</b>	48
<b>Protein pulldown</b>	48
<b>Western blotting</b>	49
<b>Immunolabeling of live cells and cell fixation</b>	49
<b>Immunofluorescence</b>	50
<b>Mouse colony</b>	50

<b>Immunohistochemistry</b>	51
<b>Total RNA purification, retrotranscription and qRT-PCR</b>	51
<b>Image acquisition and analysis</b>	52
<b>Statistical analysis</b>	53
RESULTS	54
<b>A PDZ-binding motif is specifically required for endosomes to plasma membrane recycling of GPR17</b>	54
<b>SNX27 interacts with GPR17 at the level of endosomal compartments</b>	59
<b>SNX27 regulates GPR17 recycling and levels of expression</b>	64
<b>SNX27 is required for the correct kinetics of OL differentiation</b>	71
<b>Altered OL differentiation and myelin defects in Ts65Dn mouse model of DS correlate with a decrease of SNX27 levels</b>	76
<b>mir-155 overexpression inhibits Oli-neu differentiation</b>	83
DISCUSSION	85
<b>SNX27 interacts with the PDZ-binding motif of GPR17 and is required for receptor recycling to the plasma membrane</b>	86
<b>Loss of SNX27 accelerates OL differentiation kinetics</b>	88
<b>OL development in SNX27-deficient Ts65Dn brains</b>	89
<b>mir-155 up-regulation inhibits OL differentiation</b>	91
CONCLUSIONS	92
ACKNOWLEDGMENTS	93
REFERENCES	94
TABLES	106

# ABBREVIATIONS

A $\beta$ , amyloid  $\beta$  peptide

AMPA,  $\alpha$ -amino-3-hydroxy-5-methyl-4-isoxazolepropionic acid receptor

APP, amyloid precursor protein

BAR, bin/amphiphysin/rvs

$\beta_2$ AR,  $\beta_2$ -adrenergic receptor

BMP, bone morphogenic protein

C/EBP $\beta$ , CCAAT/enhancer binding protein  $\beta$

CI-MPR, cationic-independent mannose-6-phosphate receptor

CM, conditioned medium (1:1 Sato medium and neuron-conditioned medium)

CNS, central nervous system

CREB, cAMP response element-binding protein

DS, Down syndrome

EE, early endosomes

EEA1, early endosome antigen 1

ERK1/2, extracellular signal-regulated kinases 1 and 2

FAM21, family with sequence similarity 21

GRK2, G protein-coupled receptor kinase 2

GPR17, G protein-coupled receptor 17

Id2/Id4, inhibitor of DNA binding proteins 2 and 4

ILV, intra-lumenal vesicles

LE, late endosomes

MAG, myelin associated glycoprotein

MBP, myelin basic protein

mir-155, micro-RNA 155

MS, multiple sclerosis

mTOR, mammalian target of rapamicin

MVB, multivesicular bodies

NHERF1, Na<sup>+</sup>/H<sup>+</sup> exchanger regulatory factor 1

NMDA, N-methyl-D-aspartate receptor

NPC, neural precursor cell

NRG-1, neuregulin-1

OL, oligodendrocyte

OPC, oligodendrocyte precursor cell

PDGF-AA, platelet derived growth factor-AA  
PI, phosphatidylinositol  
PI3P, phosphatidylinositol 3-monophosphate  
PLC $\gamma$ , phospholipase C gamma  
Rab4/Rab7/Rab11, Rab GTPase isoforms 4, 7 and 11  
RE, recycling endosomes  
SCAR, suppressor of cAMP receptor  
SHH, sonic hedgehog  
SNARE, snap receptor  
SNX, sorting nexin  
SNX27, sorting nexin 27  
SorLA, sortilin receptor  
T3, triiodothyronine  
TF, transcription factor  
TfR, transferrin receptor  
UDP-Gluc, uridine diphosphate-glucose  
VPS, vacuolar protein sorting  
WASH, Wiskott-Aldrich syndrome protein and SCAR homolog  
WLS, wntless

# ABSTRACT

Oligodendrocytes (OLs) are specialized glial cells of the central nervous system (CNS) responsible of myelin formation and trophic support of neurons. The understanding of mechanisms regulating OL differentiation may have fundamental implications in the development of therapeutic strategies for demyelinating and neurological diseases. In this respect, the G protein-coupled receptor 17 (GPR17) is considered a promising pharmacological target, in the light of its well-established role in the regulation of OL differentiation by acting as an intrinsic timer of the process. GPR17 is specifically and transiently expressed by a subset of NG2-positive OL precursors (OPCs) that exit mitosis and undergo cell differentiation. However, GPR17 expression has to be down-regulated before cells enter the terminal myelinating phases. Despite the many efforts that were made, the mechanisms controlling GPR17 expression are still unclear. To shed light on these mechanisms we have focused on the control of GPR17 intracellular trafficking. A process that regulates GPR17 levels at the cell surface and also its global expression. Our previous characterization of GPR17 endocytic trafficking had shown that upon endocytosis GPR17 is subjected to endosomal sorting between lysosomal degradation or recycling via the short loop pathway. In the light of this observation we decided to understand the molecular machineries that regulate GPR17 endosomal sorting. We here have demonstrated that the PDZ-binding motif expressed at GPR17 C-terminal is fundamental for receptor recycling, by mediating an interaction of GPR17 with SNX27. SNX27 is an accessory protein of the retromer complex that is emerging as a master regulator of receptor short loop recycling. We observed that loss of SNX27 unbalances GPR17 endosomal sorting and determines an increased receptor degradation and down-regulation. Interestingly, GPR17 precocious down-regulation was accompanied by an increased expression of myelin proteins, indicating an accelerated kinetics of OL differentiation in SNX27-silenced samples. Notably, we also found decreased GPR17 expression levels in Ts65Dn mouse brains, which are characterized by decreased levels of SNX27. Ts65Dn mice are the most used murine model of Down syndrome (DS). In accordance with what observed for DS patients, we found also a reduced amount of myelin fibers in Ts65Dn brains. The mechanism underlying myelination defects in DS brain is unknown. On the basis of the observation that SNX27 down-regulation was determined by reduced levels of C/EBP $\beta$  transcription factor, which are due to overexpression of trisomic micro-RNA 155 (mir-155), we decided to better characterize the role of mir-155 in OLs. Our preliminary results indicated that mir-155 is expressed at low levels in the oligodendroglial lineage and that its overexpression (mimicking pathological condition) determines a sustained inhibition of OL differentiation. This effect, however, is not dependent on SNX27 down-regulation, suggesting that other mechanisms may be involved.

## RIASSUNTO

Gli oligodendrociti sono un particolare tipo di cellula gliale del sistema nervoso centrale, responsabile della formazione della guaina mielinica e di fornire supporto trofico per i neuroni. La comprensione dei meccanismi che ne regolano il differenziamento è di fondamentale importanza per lo sviluppo di strategie terapeutiche per malattie demielinizzanti e neurologiche. In questo senso, GPR17, un recettore associato a proteina G, è considerato un promettente target farmacologico, sulla base del suo ruolo ben stabilito di timer intrinseco del differenziamento degli oligodendrociti. GPR17 è espresso in maniera specifica e transiente da un sottogruppo, NG2-positivo, di precursori degli oligodendrociti, i quali escono dalla mitosi e incominciano a differenziarsi. Tuttavia, l'espressione di GPR17 deve essere down-regolata prima che le cellule entrino nelle fasi finali di mielinizzazione. Nonostante i numerosi sforzi che sono stati compiuti, i meccanismi che regolano l'espressione di GPR17 non sono ancora del tutto conosciuti. Per comprendere meglio questo aspetto, ci siamo concentrati sui meccanismi che ne controllano il traffico intracellulare, un processo importante per la regolazione sia dei livelli di recettore esposti alla superficie cellulare, che di quelli globali. La nostra iniziale caratterizzazione del traffico endocitotico del recettore, ci ha permesso di rivelare che, dopo endocitosi, GPR17 è sottoposto a un processo di smistamento tra degradazione a livello lisosomiale e riciclo in membrana. Sulla base di queste osservazioni, abbiamo quindi deciso di studiare i meccanismi molecolari che regolano tale smistamento endosomiale. In questo lavoro abbiamo dimostrato che il "PDZ-binding motif" espresso al C-terminale di GPR17, è essenziale per il riciclo del recettore, poiché permette un'interazione con SNX27. SNX27 è una proteina accessoria del complesso del retromero, che negli ultimi anni sta emergendo come il principale regolatore del riciclo recettoriale attraverso la via di riciclo rapido. Abbiamo inoltre osservato che in assenza di SNX27 lo smistamento endosomiale di GPR17 è sbilanciato, e si ha una maggiore degradazione e down-regolazione del recettore. Questa prematura down-regolazione di GPR17 è accompagnata da un aumento nell'espressione di alcune proteine della mielina, indicando un'accelerazione nella cinetica di differenziamento degli oligodendrociti nei campioni silenziati per SNX27. Inoltre, abbiamo individuato un ridotto numero di cellule GPR17-positive in cervelli di topi Ts65Dn, che sono caratterizzati da una riduzione nell'espressione di SNX27. I topi Ts65Dn sono il modello murino più utilizzato per studiare la sindrome di Down. In analogia con quanto osservato nei pazienti Down, abbiamo individuato una ridotta presenza di fibre mieliniche nei cervelli di tali topi. I meccanismi alla base di ciò sono sconosciuti. Per chiarire meglio tali meccanismi, abbiamo quindi deciso di iniziare a caratterizzare il ruolo del micro-RNA 155 negli oligodendrociti, sulla base del fatto che la down-regolazione di SNX27 è determinata da una diminuzione del fattore di trascrizione C/EBP $\beta$ , a sua volta dovuta alla

sovra-espressione del micro-RNA 155 (trisomico). I nostri risultati preliminari indicano che il micro-RNA 155 è espresso a bassi livelli negli oligodendrociti, e che la sua sovra-espressione (mimando le condizioni patologiche) determina una forte inibizione del differenziamento oligodendrocitario. Questi effetti, tuttavia, non sembrano dipendere dalla down-regolazione di SNX27, suggerendo che altri meccanismi potrebbero essere coinvolti.



# INTRODUCTION

OLs are a specialized type of glial cell of the CNS. OLs are responsible of a number of different functions. They produce myelin, a multi-layered compact sheath that surrounds axons and allows action potential saltatory conduction. Moreover, they physically and metabolically sustain neurons. Given the roles that OLs hold, it is easy to understand why their degeneration or dysregulation affect the physiological functioning of CNS, leading to pathological conditions. In particular, OL degeneration is the main etiology of pathologies that for this reason are collectively referred to as demyelinating diseases of the CNS and include leukodystrophic disorders and the most known multiple sclerosis (MS). OL dysregulation on the other side is now reported for a number of different neurological and psychiatric disorders such as autism, DS, schizophrenia and depression among the others (Fields, 2008).

Myelinating OLs derive from the differentiation of OPCs. Interestingly, OPCs are still present in the adult brain, scattered in the different brain areas either in the white or in the grey matter. Adult brain OPCs are arrested in a quiescent state but, differently from neuronal precursors, their activation has been described in response to stimuli such as brain injuries and ischemia. The fundamental implication of these observations is that if we learn how to promote and control adult brain OPC development, a strategy arises for the treatment of pathologies where OL physiological functioning is compromised.

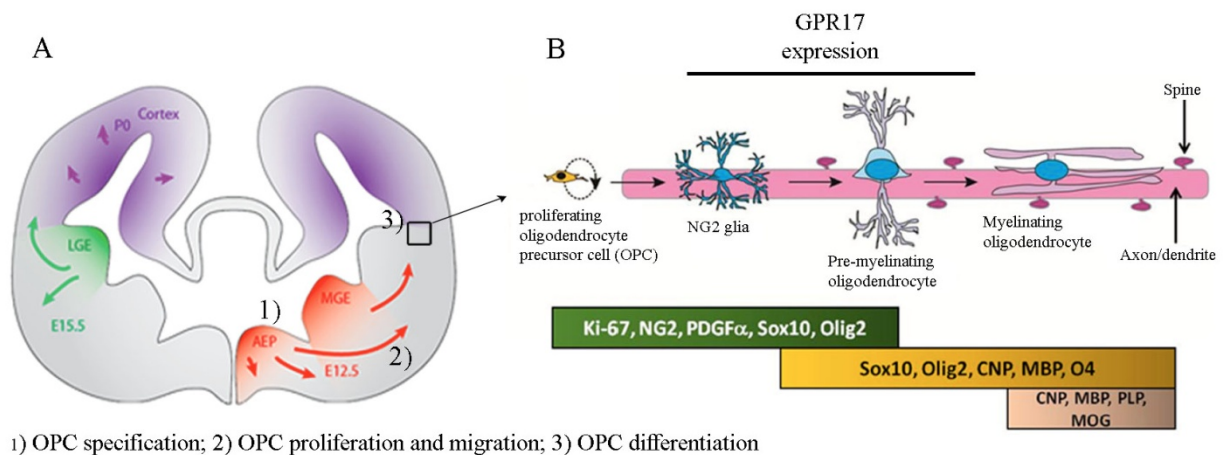
The first step to understand how OL differentiation is modified in response to pathologies is to characterize in details the mechanisms that physiologically underlie and regulate their development.

## **From immature precursors to myelinating cells: factors that regulate OL development**

The majority of OLs present in the adult brain derives from specification and differentiation of neural precursor cells (NPCs) of the neural tube. OL development is a highly specialized process, temporally and spatially restricted, finely tuned with the development of the CNS. It can be basically divided into three phases: firstly, NPCs are committed towards oligodendroglial lineage (OPC specification); secondly, OPCs proliferate and spread in the developing brain (OPC proliferation and migration); finally, immature cells differentiate giving rise to mature OLs able, when get contacts with neurons, to produce myelin and wrap neuronal axons (Emery, 2010) (Intro.Fig. 1).

Myelination is a late-occurring process. Furthermore, the time period over which it occurs is long too. OPC development begins nearly at embryonic days 12-13 in mice (embryonic week 5 for humans) and continues after birth until the first two weeks (first two months for humans), with evidences of *de novo* synthesis and remodeling also during adulthood (Mitew et al., 2014).

OPCs originate, proliferate and migrate from specific germinal niches, and the process occurs in three sequential waves. The first precursors are formed at around E12.5 (in mice) in the ventral neural tube, specifically in the medial ganglionic eminence (MGE, Intro.Fig. 1A) and the closely associated enteropeduncular area (AEP, Intro.Fig. 1A). Ventrally-derived OPCs spread to most of the developing telencephalon until E18, when the majority is surrounded and replaced by a second wave of dorsally-derived OPCs, originating in the lateral and caudal ganglionic eminences (LGE/CGE, Intro.Fig. 1A). A final third wave of OPCs begins after birth from cortical progenitor cells (Richardson et al., 2006; Lopez Juarez et al., 2016). Some studies suggested that adult-brain OPCs mainly derive from NPCs located in the subventricular zone of the lateral ventricles (Zuchero and Barres, 2013). Interestingly, it was reported that the genetic ablation of either ventral or dorsal-derived OPCs results in a compensatory effect of the counterpart-derived precursors that leads to a normal final complement of OLs and myelin (Mayoral and Chan, 2016).



**Intro. Figure 1. Schematic representation of the different phases of OL development.**

**A** The first wave of OPCs originates from NPCs localized in the AEP and VGE areas of the ventral neural tube at E12.5. They are then surrounded and replaced by a second wave of precursor cells that originates in the LGE, a more dorsal area compared to AEP and VGE. **B** After migration OPCs undergo through different phases of differentiation to become mature myelinating OLs. The expression windows of GPR17 and of some intrinsic TFs involved in OL differentiation regulation are reported. Figure is adapted from Somkuvar et al., 2014 and Traiffort et al., 2016.

After specification OPCs undergo to different phases of maturation from precursors to pre-myelinating and myelinating OLs and a number of different factors attend at the regulation of OL differentiation (Intro.Fig.1B). They are basically divided in extrinsic and intrinsic factors. The impact of extrinsic and intrinsic factors and whether OL development is essentially driven by extracellular signals, internal controls or a combination of the two is still object of discussion. An important consideration is that studies of gene expression profiling revealed a high grade of heterogeneity in the gene expression pattern of OPC populations derived from different brain areas, suggesting that intrinsic differences may guide OPC development. However, it is still not resolved whether this diversity depends on either a differential genetic commitment of OPCs or different maturation stages and/or different external cues (Mayoral and Chan, 2016). It is also unresolved whether distinct sub-populations of precursor cells originate specialized OL subtypes with peculiar molecular and/or functional properties (Zuchero and Barres, 2013).

Among the factors described to regulate OL development, many have multiple (and sometimes contrasting) roles over the subsequent phases of the process. Since it is not aim of this introduction to describe all the mechanisms underlying OL development (please refer to reviews He and Lu, 2013; Mitew et al., 2014), while it is thought to contextualize our experimental work in the complexity of myelination, I will describe the many aspects that concur to the complex scenario of OL development, focusing on factors whose roles are more established. In doing this, I will firstly summarize intrinsic controls of OL maturation, describing in a second part how external signals modify OL development by acting on intrinsic regulator activity.

### *Intrinsic factors*

All the most important transcription factors (TFs) involved in OL development belong to the basic-helix-loop-helix (bHLH) superfamily. Among them OLIG1, NKX2.2, SOX10, TFC4 and ASCL1 are known to be positive regulators of OL development, while Id2, Id4, HES5 and SOX6 are well-established inhibitors of maturation (Emery, 2010). However, the most characterized TF involved in the promotion of OL development is OLIG2. Although its expression is reported also in precursors of motor neurons, OLIG2 is a reliable marker of the oligodendroglial lineage, and is expressed at all the stages of the development. Accordingly, OLIG2 functions span the whole process of OL maturation, and OLIG2 is probably the master TF onto which convey signaling pathways of external cues. The knockout of the gene determines a failure of OPC generation, while OLIG2 overexpression in NPCs forces cell specification towards OPCs (Lu et al., 2002). Different strategies were reported to regulate OLIG2 activity. As for many other TFs, enhancers and

inhibitors influence OLIG2-dependent transcription. In addition, Id2 and Id4 (inhibitor of DNA binding proteins 2 and 4) were shown to directly bind OLIG2, blocking DNA transcription. Furthermore, OLIG2 activity was suggested to depend on phosphorylation. In particular, some studies proposed that different oligodendrogenic pathways might merge their signaling on the regulation of OLIG2 phosphorylation state (Mitew et al., 2014). Once activated, OLIG2 may directly promote gene transcription, while some studies suggest that it exerts its functions also by recruiting chromatin-remodeling factors such as SMARCA4/BRG1 (Zuchero and Barres, 2013). In addition to OLIG2, another TF shown to promote myelination is OLIG1. In particular OLIG1 is thought to regulate the terminal myelination of differentiating OLs, due to observation that OLIG1-knockout mice express early OLs with complex branched-shapes that fail to myelinate (Xin et al., 2005). Despite this observation, the mechanism by which OLIG1 exerts its functions is unclear. It has been shown that OLIG1 re-localizes from nucleus to cytosol in coincidence with myelination beginning. Whether this translocation is required for the recruitment of promoter factors present in the cytosol, or for the removal of inhibitory factors is still unresolved (Mitew et al., 2014). OLIG1 was proposed to co-operate with SOX10, a TF shown to control the expression of a number of genes tightly correlated to myelin formation and among them MBP promoter activity. In accordance, OLs are arrested in a pre-myelinating stage in SOX10 conditional-null mice (Li et al., 2007).

Other important TFs involved in OL myelination promotion are: NKX2.2, MYRF (MRF; myelin gene regulatory factor) and ZFP488 (He and Lu, 2013; Mitew et al., 2014).

Concerning inhibitory intrinsic controls of OL development, well established is the role of Id2 and Id4. During OL differentiation Id2 and Id4 are activated by many different signals among which are BMP/SMAD signaling pathway, GPR17 signaling, and Wnt/ $\beta$ -catenin. Once activated Id2 and Id4 conformations change leading to their translocation from cytosol to nucleus where Id2/Id4 directly regulate gene transcription and also inhibit OLIG2 activity (Chen et al., 2009). In addition to Id2/Id4 OL maturation is under the negative control of HES1 and HES5. These TFs are activated downstream to the NOTCH signaling pathway and act directly as TF but also by inhibiting SOX10 (Wang et al., 1998).

A number of studies were conducted to decipher the role of TFC4/TCF7L2 complex, which mediates the effects of Wnt/ $\beta$ -catenin signaling pathway. Although some aspects are still unclear, it is now accepted that the complex has a dual role in OL differentiation. In accordance with the Wnt/ $\beta$ -catenin signaling, TFC4/TCF7L2 are transiently activated during OL differentiation: while their activation arises at the onset of the process, their signaling requires to be down-regulated before terminal differentiation, otherwise myelination fails. TFC4/TCF7L2 were shown to activate

a number of inhibitory genes, including Id2. Surprisingly, however, TCF4 knockout was shown to arrest myelination (He and Lu, 2013).

Interestingly, despite the number of intrinsic mechanisms controlling OL development, no one of the listed factors appears to be essential. This conclusion is suggested by the observation that knocking-out each of the above described TFs does not completely abolish OL development. Thus, we may assume that mechanisms underlying OL development are highly intertwined and redundant.

### *External cues*

A number of different external cues have been implicated in guiding OL maturation in the complex scenario of CNS development.

OPCs are generated by a progressive specification of NPCs present in specific germinal niches. An important cue described to drive ventrally-derived OPC specification is sonic hedgehog (SHH), which acts by means of different intracellular pathways. SHH activates NKX6.1 and NKX6.2 TFs that, in turn, promote the OLIG2-dependent expression of genes involved in NPC commitment towards OPCs. In addition, SHH favors the formation of GLI1/2 complex and counteracts GLI3 repressor activity, thus finally leading to the activation of OLIG2 (He and Lu, 2013). Notably, the floor plate and the notochord specifically secrete SHH to drive the formation of ventrally-derived OPCs, and the ectopic grafting of SHH-expressing tissue results in the generation of ectopic OPCs (Yu et al., 2013). Dorsally-derived OPCs are too far to sense the SHH-driving signal. This observation suggested that other factors might also be involved in OPC specification. Accordingly, Bone Morphogenic Protein (BMP)/SMAD and Wnt/ $\beta$ -catenin signaling pathways were also shown to regulate OPC generation, although with inhibitory roles (Richardson et al., 2006). BMP is a family of growth factors that belong to the TGF $\beta$  superfamily. BMP signaling is mediated by the SMAD complex, which is composed by SMAD1/SMAD5/SMAD8 proteins. Once activated the SMAD complex leads to an increased expression of Id2 and Id4, which, as previously reported, negatively regulate OL differentiation (He and Lu, 2013). The FGF family of proteins also plays important roles in OL development. In particular, during the different phases of OL development FGF-2, FGF-8, FGF-17 and FGF-18 were shown to control many and differential aspects. FGFs act on specific receptors (FGFRs) expressed on developing OPC cell surface. The ERK1/2 (extracellular signal-regulated kinases 1 and 2) and MAPK signaling pathways are then activated downstream to FGFR stimulation. With specific regards to OPC specification, FGF-2 was shown to promote OLIG2 activity, via activation of ERK1/ERK2 pathway (He and Lu, 2013; Mitew et al., 2014).

Committed OPCs, before differentiate into mature myelinating cells, spread in the whole brain areas. In doing this, OPCs undergo a process of proliferation and migration. It is interesting to note that migration and proliferation are commonly considered pathways alternative to OPC differentiation. By proliferating and migrating, OPCs populate different brain areas with immature cells, whose differentiation will be context-dependent and driven by environmental-specific cues. It is indeed commonly accepted that mitogens and motility-promoting factors have also anti-differentiating properties, while, on the contrary, promoters of OPC differentiation also determine cell exit from mitosis (Mayoral and Chan, 2016). A master regulator of OPC proliferation is PDGF-AA (platelet derived growth factor-AA) by acting on its receptor PDGFR $\alpha$ . Once engaged by PDGF-AA, PDGFR $\alpha$  seems to activate many intracellular pathways, including MAPK signaling cascade, phospholipase C gamma (PLC $\gamma$ ) and the PI3K/AKT signaling pathways (He and Lu, 2013). FGF-2 in addition to promote OPC specification was also reported to sustain cell proliferation by working in concert with IGF-1 to activate cyclinD1 (He and Lu, 2013). OPC survival is also increased by neuregulin-1 (NRG-1), which is either expressed on the surface of neurons or secreted as an extracellular peptide. NRG-1 acts by activating PI3K/AKT pathway by means of activation of ERB B tyrosine-kinase receptor, expressed on OPC cell membranes.

Three categories of molecules drive OPC migration: chemokinetic secreted molecules, chemotactic cues present in the extracellular matrix, and contact molecules expressed on the surface of developing neurons and glial cells. The most important chemokinetic cues are the already described PDFG-AA and FGF-2 (Mitew et al., 2014). In addition to these, molecules of the extracellular matrix play a very important role. Among them are laminins (in particular laminin-2), fibronectins, merosin, tenascin and anosmin-1. These molecules are mainly sensed by integrins expressed on the surface of migrating OPCs and a particularly relevant role has integrin  $\alpha 6\beta 1$  (He and Lu, 2013). Finally, with regards to adhesion molecules expressed on cell surface by OPCs and other cell types, PSA-NCAM, ephrins, NG2 and N-chaderins have all been associated to the control OPC migration. Notably, contact sites between OPC themselves are thought to regulate cell migration so that the final result would be a homogeneous distribution of cells in brain parenchyma (Mitew et al., 2014).

Among the phases that OLs tread during their development, the terminal differentiation is probably the most characterized and studied. This is due to the implications that OL differentiation control may have for the development of strategies to contrast demyelinating diseases and to

promote recovery of myelin degeneration. A number of mechanisms are now well established to exert regulatory effects on differentiation process. Interestingly, many of these mechanisms have inhibitory effects. Among these are the LINGO1/NOGO signaling axis and NOTCH signaling pathway (Emery, 2010). LINGO1 is expressed by both neuronal axons and adjacent differentiating OLs and binds NOGO receptor on OL cell surface. It exerts its inhibitory functions by decreasing the activity of FYN kinase, which, consequently, increases RHOA activity leading to anti-differentiating effects (Mitew et al., 2014). NOTCH signaling is also activated by neuronal expression of JAGGED1 and DELTA1 ligands. OPCs express both NOTCH1/NOTCH2/NOTCH3 receptors (He and Lu, 2013). NOTCH1 activation upon ligand-binding is the best characterized pathway, which was demonstrated to determine the cleavage of NOTCH cytoplasmic tail, thus leading to the release of a soluble peptide (NICD), that enters the nucleus and promotes the expression of HES1 and HES5 TFs. As previously reported, HES1 and HES5 are well-characterized negative regulators of OPC differentiation (Mitew et al., 2014).

The Wnt/ $\beta$ -catenin signaling pathway is also one of the most studied mechanisms underlying OPC differentiation. As described previously, Wnt/ $\beta$ -catenin effects are mediated by TCF4/TCF7L2 TFs (He and Lu, 2013). It is now thought that Wnt signaling may promote the initial differentiation stages but it must be shut down before OL terminal myelination (Emery et al., 2010). BMP and FGF families, which were both described to be important for the control of OPC specification, also concur to the negative regulation of differentiation process (He and Lu, 2013). Among FGF family members FGF-8, FGF-17 and FGF-18 inhibit OPC differentiation, while FGF-9 enhances differentiating OPC ramification and processes extension (He and Lu, 2013).

Few signals have been reported to sustain OL differentiation. Among them a very relevant role has triiodothyronine (T3) hormone. Even if not essential for the developmental process, T3 seems to be particularly important for the correct timing of OL maturation. Consistent with this hypothesis, congenital hypothyroidism patients have defective myelination while hyperthyroidism determines precocious myelination and an elevated number of mature OLs (Mitew et al., 2014).

As well as for OL differentiation, the majority of extracellular signals identified to date as regulators of OL myelination are inhibitory. Thus, they are deputed at preventing myelination of wrong axons or excessive myelination. The already mentioned axonal molecules PSA-NCAM, JAGGED1 and LINGO1 are well-characterized examples. On the contrary, examples of pro-myelinating factors are laminin- $\beta$ 2 and NRG-1. Laminin- $\beta$ 2 is expressed by neurons just before being myelinated and binds to  $\beta$ 1-integrin expressed by OLs. NRG-1, by binding ERB B3 on OL membranes, was proposed to be important for both the regulation of myelin thickness and for

myelin remodeling process that occurs in the postnatal period (and also in adulthood) (Zuchero and Barres, 2013). All these extracellular signals finally converge on the modification of actin cytoskeleton. In particular, many downstream signaling pathways involve the activation of FYN kinase that results in the inhibition of anti-differentiation factor RHOA (Wolf et al., 2001). This observation suggests FYN/RHOA pathway as a possible general effector of myelination process (Mitew et al., 2014).

### *Neuronal activity*

Neuronal activity was largely described to control OL differentiation and myelination. Different mechanisms have been proposed to explain the observed effects. A first possibility is that electrical activity may regulate the expression of cell surface ligands on neuronal axons. In addition, active neurons may release adenosine in the extracellular matrix, thus acting on purinergic receptors, known to be expressed by OLs (Emery, 2010). It has also been proposed that OPCs may form functional synapses regulated by neuronal activity. In this respect it is important to note that OLs express both ionotropic glutamate receptors ( $\alpha$ -amino-3-hydroxy-5-methyl-4-isoxazolepropionic acid receptor, AMPA; and N-methyl-D-aspartate receptor, NMDA) and voltage-gated ion channels that may be directly stimulated by glutamate secreted by neuronal synapses (De Biase et al., 2010). However, the exact role of AMPA and NMDA receptors in OL differentiation and whether their stimulation is a pro- or anti- differentiating cue is still controversial (De Biase et al., 2011). Despite are still incompletely resolved the molecular mechanisms it is mediated by, OL differentiation and myelination driven by neuronal activity is an interesting candidate suggested to exert an important role in the regulation of OL remodeling and plasticity associated to learning (Zuchero and Barres, 2013).

### *Epigenetic mechanisms*

The role of epigenetic mechanisms is starting to be studied in the context of OL development. Chromatin remodeling hystone acetylase and deacetylase (HDAC) family members 1 and 2 (HADAC1 and HADAC2) were reported to act upstream and regulate Wnt/ $\beta$ -catenin signaling pathway (Ye et al., 2009). Furthermore, SWI/SNF and SMARCA4/BRG1 are examples of ATP-dependent chromatin remodeling complexes which control transcription of genes associated to OL development by regulating hystone positioning (Emery, 2010). Few is known regarding micro-RNA involvement in the regulation of OL maturation. Functions have been proposed for mir-219, mir-338, mir-7a and mir-125-3p (Duglas et al., 2010; Zhao et al., 2010; Lecca et al., 2016).



## ***Slow and steady wins the race, an intrinsic timer for OL development: GPR17***

In 2006 Ciana and colleagues described for the first time the pharmacological properties of a G protein-coupled receptor with an intermediate phylogenetic position between P2Y and CysLT receptor families: GPR17 (Ciana et al., 2006). A growing number of studies indicate that GPR17 is transiently expressed during OL differentiation and may have opposite stage-specific roles: a positive function in the early phase of OPC differentiation and a negative role in pre-myelinating OLs (Ceruti et al. 2009; Chen et al., 2009; Boda et al., 2011; Fumagalli et al., 2011; Fratangeli et al. 2013, Hennen et al., 2013, Viganò et al., 2016). In myelin lesions associated to MS, stroke and stab wound injuries an abnormal overexpression of GPR17 was described in OPCs that surround myelin degeneration. These GPR17-expressing cells are arrested in a quiescent state and fail to repair myelin defects (Lecca et al., 2008; Chen et al., 2009; Boda et al., 2011). The down-regulation of GPR17 was proposed to force quiescent OPCs to overcome differentiation arrest and complete their maturation (Hennen et al., 2013; Simon et al., 2016). On the other hand, GPR17 stimulation could also be useful for promoting OL differentiation (Lecca et al., 2008; Fumagalli et al., 2011; Daniele et al., 2014; Fumagalli et al., 2015). For these reasons GPR17 is a putative (and promising) pharmacological target for the treatment of demyelinating diseases and MS in particular (Ceruti et al., 2009; Boda et al., 2011).

Although GPR17 is mainly studied in the oligodendroglial lineage, it is also expressed at lower levels by neurons and, under specific conditions, also by microglia. Moreover, its expression was confirmed in heart and kidney, while the transcript was found in lung and liver (Ciana et al., 2006). With regards to OLs, GPR17 decorates a specific subset of NG2-positive precursor cells that under physiological conditions are scattered in the brain parenchyma both in the white and in the grey matter (Ceruti et al., 2009; Boda et al., 2011). GPR17-expressing cells could also be found in typical neurogenetic areas such as hippocampus, ependymal layer and subependymal cells of the lateral ventricles (Lecca et al., 2008; Ceruti et al., 2009). GPR17 begins to be expressed once cells exit mitosis and undergo cell differentiation, and its expression continues and arises until differentiating cells reach premyelinating stages. After that GPR17 is down-regulated, thus no expression was found in mature, myelinating OLs (Boda et al., 2011). Consistent with this kinetics, early after birth GPR17 mainly decorates immature precursor cells (PDGFR $\alpha$ <sup>+</sup>, NG2<sup>+</sup>, MBP<sup>-</sup>) while during the first postnatal weeks GPR17 expression increases and is found in differentiating OLs. Its expression reaches a peak around postnatal day P24 in cells co-expressing markers of premyelinating stages such as PLP/DM20 and CD9, but then progressively diminishes in

concomitance with myelin production (Boda et al., 2011). Despite this pattern, GPR17-expressing OPCs are still present in the adult brain, distributed in both the white and grey matter and they have been extensively described to increase in number in response to brain injuries (Lecca et al., 2008; Ceruti et al., 2009; Boda et al., 2011 and 2015; Viganò et al., 2015).

From a pharmacological point of view GPR17 is endogenously stimulated by extracellular uracil- and sugar-nucleotides (UTP, UDP, UDP-glucose and UDP-galactose) and by cysteinyl-leukotrienes (LTC<sub>4</sub> and LTD<sub>4</sub>). Extracellular nucleotides are associated to many different processes: from regulation of homeostasis to embryogenesis; while cysteinyl-leukotrienes are well-established inflammatory mediators (Ciana et al., 2006). A number of studies were conducted to determine the intracellular signaling pathways associated to GPR17 activation. Using pertussis toxin (PTX), which is a well-known inhibitor of G $\alpha$ i-protein, and forskolin activator of adenylyl cyclase, Abbracchio and colleagues demonstrated that GPR17 is coupled by a G $\alpha$ i-protein. Consequently, when activated GPR17 leads to inhibition of adenylyl cyclase and increases intracellular calcium concentration (Ciana et al., 2006). More recent studies used a small molecule proposed to be a selective agonist of GPR17: MDL29,951. These studies reported that GPR17 can engage the entire repertoire of GPCR intracellular adaptor proteins including G proteins of subfamilies G $\alpha$ i, G $\alpha$ s and G $\alpha$ q and also  $\beta$ -arrestins. It follows that GPR17 stimulation perturbs cyclic adenosine monophosphate (cAMP) levels, as well as inositol phosphate and intracellular calcium concentrations, and also the ERK1/2 signaling pathway (Hennen et al., 2013). The activation of ERK kinase signaling was also shown by an independent study that described activation of alternative transduction pathways in response to the two classes of agonists. When stimulated by CysLTs GPR17 conformational change leads to recruitment of G protein-coupled receptor kinase 2 (GRK2) isoform and a transient binding by  $\beta$ -arrestin. This determines a rapid phosphorylation of ERK kinase via a G protein-dependent mechanism and a sustained re-localization of cAMP response element-binding protein (CREB) into the nucleus. On the other side, upon purinergic ligands stimulation GPR17 recruits GRK5 isoform and forms a stable complex with  $\beta$ -arrestin. ERK kinase activation is slower and sustained while CREB is less activated (Daniele et al., 2014). However, CREB activation downstream of GPR17 stimulation is still controversial. MDL29,951-mediated GPR17 activation reduces the activity of the cAMP/PKA/CREB cascade and also of exchange protein directly activated by cAMP (EPAC) (Simon et al., 2015). In addition Chen and colleagues showed that GPR17 overexpression has no effects on CREB re-localization (Chen et al., 2009). On the contrary, they demonstrated that GPR17 overexpression correlates with increased

translocation of Id2 and Id4 to nucleus where they strongly inhibit OL maturation (Chen et al., 2009).

Due to its phylogenetic relationship with both P2Y and CysLT receptors and to the observation that extracellular nucleotides and CysLT levels are increased in injured areas, GPR17 was firstly associated to the response to CNS injury (Lecca et al., 2008). It was described that early after the onset of an ischemic episode (from 24 to 48 hours after ischemia onset), neurons that surround the damaged area increase the expression of GPR17 in concomitance with heat shock protein 70 expression. However, at later stages (48 to 72 hours after ischemia) the number of GPR17-positive neurons was drastically diminished, most probably due to cell death since pharmacological and biotechnological inhibition of GPR17 correlated with an attenuation of cell death. At this time point on the other side, GPR17 was expressed by microglial-macrophagic cells that infiltrate the injured area, while 72 hours after ischemia onset GPR17 decorated proliferating OPCs, recruited to repair damaged parenchyma. Based on these observations it was proposed a dual role for GPR17, firstly as a “sensor of damage”, while at later stages as a director of the response to brain damage by being sequentially expressed in different cell types (Lecca et al., 2008).

GPR17 is mainly studied for its role in OL differentiation. Many efforts have been made to clarify the role of GPR17 during the process, and some aspects are still controversial. It was firstly suggested that GPR17 may be an important promoter of the early stages of differentiation due to the observations that primary OLs or co-cultures of primary cortical neurons and OLs treated with UDP-glucose (UDP-Gluc) and LTD<sub>4</sub> expressed increased levels of MBP myelin protein (Fumagalli et al., 2011; Daniele et al., 2014). In addition, *in vitro* studies showed that GPR17 knock-down arrests OPC differentiation at early stages (Fumagalli et al., 2011). On the other hand, *in vivo* studies of GPR17 functioning described that receptor knockout in mice determines precocious myelination onset. Furthermore, GPR17 forced overexpression leads to impaired OL differentiation and myelin defects, suggesting an inhibitory role for GPR17 during OL differentiation (Chen et al., 2009). This conclusion was also supported by *in vitro* studies showing that GPR17 activation using MDL29,951 inhibits OL differentiation. Hennen and colleagues also proposed GPR17 inhibition as a strategy to promote myelination repair in MS (Hennen et al., 2013).

Altogether these studies indicate that GPR17 may have a positive function in the early phase of OL differentiation but a negative role on final OL maturation, suggesting that GPR17 down-regulation is needed to allow axonal myelination. Thus, the mechanisms underlying receptor

synthesis and stability may play an important role in controlling OPC/OL-differentiation stages and myelination.

To get more insights in the mechanisms that control GPR17 functioning, our research has focused on mechanisms underlying receptor intracellular trafficking. Intracellular trafficking impacts on many aspects of receptor expression/stability and signaling: i) it determines receptor levels at the plasma membrane, thus its availability to agonist/antagonist stimulation; ii) it regulates the total amount of receptor levels of expression, mainly by controlling receptor degradation and turnover rates; iii) it controls the temporal and spatial desensitization and resensitization upon drug administration. In recent studies we have characterized the endocytic transport of GPR17 and demonstrated that it undergoes both constitutive and agonists (LTD<sub>4</sub> and UDP-Gluc) induced endocytosis. GPR17 endocytosis occurs via clathrin-coated vesicles. After internalization receptors are collected into Transferrin receptor (TfR)/early endosome antigen 1 (EEA1)-positive early endosomes (EE), a well-known station of sorting into different intracellular routes. From EE a portion of internalized receptors is sorted to lysosome for degradation, while a minor amount is recycled back to the plasma membrane. We also showed that GPR17 recycling mainly occurs through the so-called “short loop” pathway (see the following section) as indicated by the co-localization with Rab4-positive vesicles (Fratangeli et al., 2013). In the light of these observations we extended our research on the molecular mechanisms underlying GPR17 endocytic sorting, by focusing our attention on the role of the class I post-synaptic density protein 95 - Drosophila disc large tumor suppressor protein - zonula occludens protein 1 (PDZ) binding motif expressed at GPR17 C-terminal. PDZ-binding motifs are a class of short sequence-specific domains largely associated to the regulation of receptor signaling, subcellular localization and transport (Romero et al., 2011).

## **Receptor endocytosis**

### *The endosomal network*

As many other receptors and membrane integral proteins, GPR17, once internalized, undergoes trafficking into the endosomal network where is sorted between lysosomal degradation or plasma membrane recycling.

Endosomes are an ensemble of tubular and vesicular structures distributed in the cellular cytoplasm and associated to many cellular processes. Molecules, lipids and solutes that are internalized by cells traffic through the endosomal pathways. Moreover, endosomal sorting

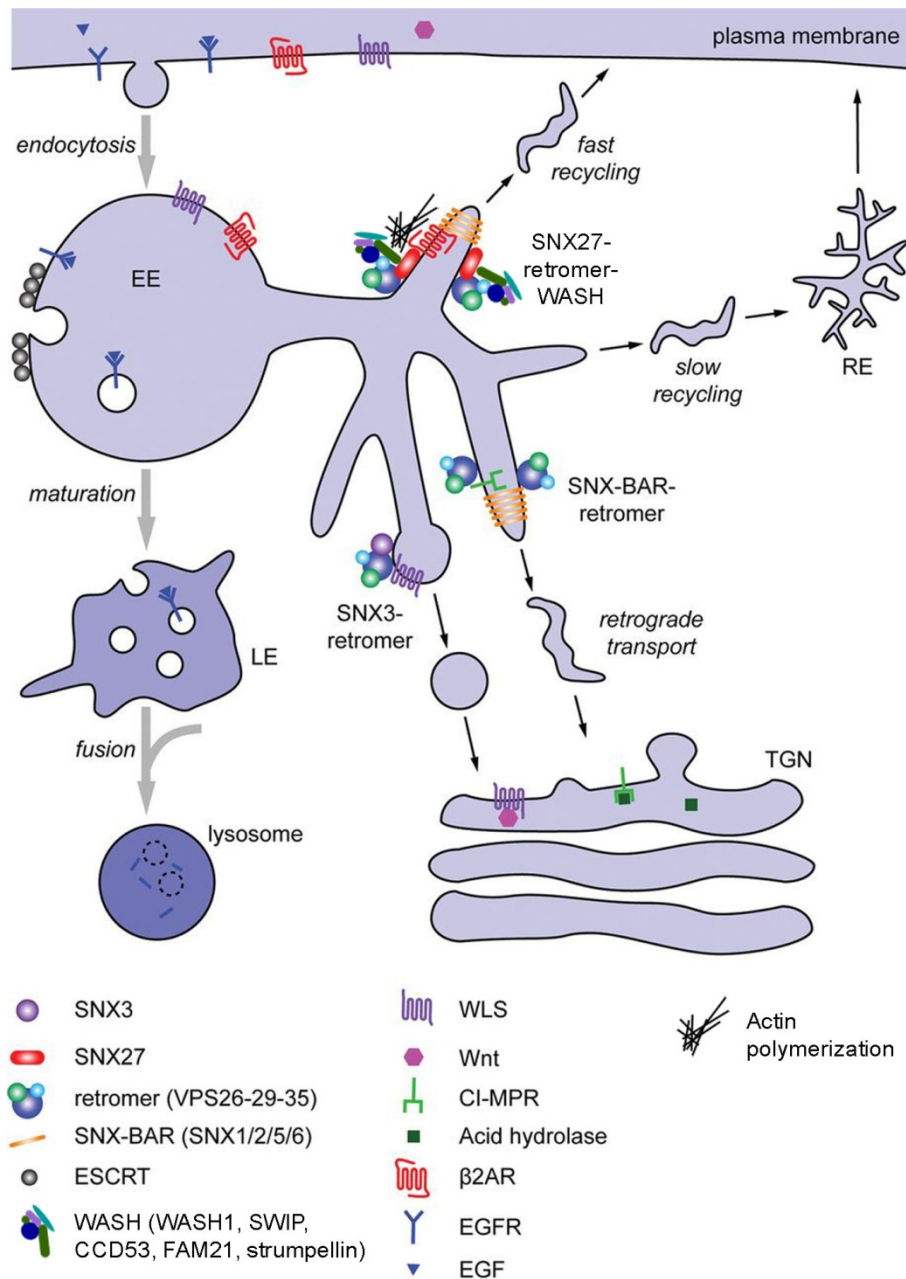
regulates receptor expression at the cell surface, receptor turnover, as well as receptor desensitization and resensitization after agonist stimuli (Hanyaloglu and von Zastrow; 2008). Endosomes constitute a spatial restricted compartment with peculiar biochemical/biophysical properties that allows the correct activity of many different enzymes, thus the processing of peculiar enzymatic reactions (Scott et al., 2014). Related to this, is also the new emerging view of endosomal compartments as important hubs for receptor signaling (Irannejad et al., 2015). The above reported are only a small part of the numerous functions that endosomes are beginning to be associated with and give an idea of why the regulation of endosomal network is emerging as an important topic in the regulation of cellular functioning in physiological and pathological conditions. Although endosomes are associated with many processes, I will describe their organization and regulation focusing on their role in the control of receptor transport and signaling. In doing this, I will use the word “cargo” to refer to the union of receptor and its ligand or the receptor alone without discriminate between the two, except when it is specifically required.

Most of the studies that were conducted to characterize receptor traffic into the endocytic compartments relied on the use of transferrin (Tf) and TfR for tracking the recycling routes, while the EGF and EGF receptor (EGFR) were used to study the degradative pathway (Houtari and Helenius, 2011). On the base of these studies the “classic” view of endocytic transport assumes that cargo molecules reach endosomes after being internalized at the cell surface. Although it was demonstrated that this is not always true (refer to the following section), I will start to present cargo distribution in endosomal pathways considering that they enter endocytic compartments by endocytosis.

Many different mechanisms mediate the initial step (internalization) of receptor endocytosis. They are generally divided in clathrin-dependent endocytosis (CDE), caveolae-dependent endocytosis (CavDE) and clathrin-independent endocytosis (CIE) mechanisms. Whether the endocytic pathway of cargo internalization also impacts on the endocytic sorting is still object of discussion (Grant and Donaldson, 2009).

After internalization cargo molecules generally reach a tubulovesicular compartment called early endosomes (EE). Due to their peculiar biochemical/biophysical characteristics EE determine the release of receptor-ligand complex. Moreover EE are the first station of sorting into different pathways (Bissig and Gruenberg, 2013). EE are “classically” seen as the epicenter of all endosomal pathways and the progenitors of the other sub-compartments (Gruenberg, 2001). They are characterized by a mild-acidic pH concentration (pH 6.2 – 6.5) and their membranes are enriched in cholesterol and phosphatidylinositol 3-monophosphate (PI3P). Examples of EE-anchored proteins

are EEA1, Rab5 GTPase and PI3-kinase VPS34. It has been reported that in some cases cargo receptors that arrive at EE do not release their ligands and continue to signal for a prolonged period. Despite this observation, EE are never the ultimate destination of endocytic cargos. On the contrary, cargo molecules are generally sorted between two opposite destinies: degradation which occurs via late endosomes (LE)/lysosome pathway, or recycling which occurs by a number of different routes (Intro.Fig. 2) (Hanyaloglu and von Zastrow, 2008).



**Intro. Figure 2. Schematic representation of the “classic” endocytic pathways.**

After endocytosis EGFR,  $\beta_2$ AR, CI-MPR and WLS are sorted into different endosomal pathways. EGFR and its ligand (EGF) are internalized into ILV and sorted to LE/lysosome for degradation. On the contrary,  $\beta_2$ AR is recycled to the plasma membrane via the short-loop recycling pathway.

$\beta_2$ AR sorting in the recycling pathway depends on the SNX27-retromer-WASH macromolecular complex. WLS and CI-MPR are examples of cargos that are transported to the Golgi apparatus via retrograde transport. However, the two cargo molecules traffic through different pathways: while CI-MPR transport depends on the SNX-BAR retromer complex, the transport of WLS to the Golgi is regulated by the SNX3 retromer complex. Figure is adapted from Gallon and Cullen, 2015.

Cargo receptors that are transported to LE are internalized into intra-luminal vesicles (ILV) generated by a process of invagination of the EE membrane. It is not clear whether these ILV may reach LE also by free transport. However, a number of data established the formation of a multivesicular structure called multivesicular bodies (MVB), which is then transported to LE. Meanwhile MVB undergo a series of modifications that are collectively called “EE maturation” and contribute to determine the biochemical properties of LE (Houtari and Helenius, 2011). The most characteristic modifications are i) pH acidification (LE pH is around 5.0–5.5), determined by the activity of vacuolar-type protonic pump  $H^+$ -ATPase; ii) Rab-associated protein switch from isoform 5 to isoform 7; iii) phosphatidylinositol conversion from PI3P to PI(3,5)P<sub>2</sub>, although PI3P is still found in ILV (Bissig and Gruenberg, 2013). Cargo receptors that enter LE are generally (but not always) committed to lysosome for degradation (Houtari and Helenius, 2011).

Notably, whereas the vacuolar part of EE undergoes membrane invagination and forms ILV committed to degradative pathway, the EE tubular structures are associated to cargo recycling (Gruenberg, 2001). Recycling may occur via different pathways that are tightly correlated with the biological functions of the cargo molecules. A basic distinction is between constitutive recycling and regulated recycling. Constitutive recycling is associated with molecules that are involved in the intake of substrates required for cellular metabolism such as cholesterol and its receptor (LDL receptor). These receptors of metabolites are supposed to be continuously in service to supply cells with essential metabolites, thus they do not require a regulated recycling (Grant and Donaldson, 2009). Little information is available about constitutive recycling except that occurs via a bulk membrane flow. Some studies suggested that this pathway might exploit the Rab4-dependent regulated recycling pathway (Pfeffer, 2013). On the contrary, signaling receptors, for which the balance and the timing of cell surface re-exposure may impact on cell functioning, undergo a process of regulated recycling (Hanyaloglu and von Zastrow, 2008; Grant and Donaldson, 2009). This process is better characterized than the constitutive one and involves the sorting of different cargos into distinct intracellular pathways. The fastest regulated recycling pathway occurs by means of vesicles that bud from EE and directly reach the plasma membrane. This pathway is also called “short loop” recycling pathway and is regulated by the Rab GTPase isoform 4 (Rab4). A slower

way of recycling implies the traffic through tubule-vesicular compartments intermediate between EE and plasma membrane, which are called recycling endosomes (RE). This pathway is also referred to as “long loop” recycling and depends on the activity of Rab11 GTPase (Intro.Fig. 2). RE are generally (but not always) localized more proximal to the nucleus in respect to EE and have a less acidic pH than EE. However, it is important to remember that in some cell lines it is difficult to distinguish Rab4-positive vesicles, Rab11-associated RE and also EE as clearly separated compartments (Gruenberg, 2001).

Finally, it is important to note that some cargos leave EE and are transported to the trans-Golgi network (Intro.Fig. 2). Cargo return from EE to trans-Golgi is known as retrograde transport (Gallon and Cullen, 2015). The number of cargos described to traffic from endosomes to the Golgi complex is rapidly increasing. Probably the most characterized example of retrograde transport is the traffic of Wntless (WLS) that is required for Wnt transport to the plasma membrane, where is secreted. Thus, WLS recruits Wnt at the trans-Golgi, after that WLS/Wnt complex is transported to the plasma membrane (where the change of pH in the extracellular space determines Wnt release). WLS is then internalized in the EE and transported to the trans-Golgi via retrograde pathway. Similar mechanisms were also described for some other proteins and in particular for proteins involved in the transport of enzymes and proteins associated to endosomal compartments (EE, LE and lysosome) (Johannes and Popoff, 2008).

The above described is the “classic” representation of endosomal organization. This view is rapidly evolving because of new evidences showing an extremely high interconnection between different endosomal pathways and between endosomes and many cellular processes. Endosomes receive material not only from the endocytic pathway, but also from the biosynthetic pathway (Golgi complex and also endoplasmic reticulum) and even the autophagic pathway (plasma membrane or autophagosomes). Endosomal transport is not anymore unidirectional: from EE to recycling, degradation or retrograde pathways. New evidences highlight a high interweaving between different compartments with cargos that although already internalized in LE are retrieved from degradation and re-directed to Golgi, RE, and extracellular secretion (exocytosis). Also RE were shown to receive cargos from biosynthetic pathway and re-direct them to EE and LE or plasma membrane (Johannes and Popoff, 2008; Houtari and Helenius, 2011; Scott et al., 2014). An important implication of this high grade of interconnectivity is that compartment biochemical/biophysical composition is extremely dynamic and constantly under remodeling.

From compartments deputed at the regulation of intracellular trafficking, endosomes are now considered central elements in the regulation of many cellular processes: from



autophagocytosis, to regulation of focal adhesion and cell motility (Scott et al., 2014). Due to their peculiar biochemical and biophysical properties EE, LE and also lysosome are emerging as important hubs for the execution of specific enzymatic reactions. Related to this, is also the new concept of “signaling endosomes”, which considers endosomes master organizers of signaling pathways. Endocytic trafficking regulates the cell surface amount of receptors available for external signals and it is important to consider that receptors must reach endosomes (and a different pH) to rid of their ligands. Endocytic transport gives the opportunity for a fine, temporal and spatial regulation of receptor desensitization and resensitization. Moreover, endosomal sorting between degradation and recycling is a crucial crossroad determining signaling sustainment or down-regulation. Endosomal membranes represent a microenvironment highly different from plasma membrane both in the lipid and protein composition. There are now increasing evidences of receptors whose signaling is activated upon endocytosis or that after internalization activate alternative signaling pathways. Finally, due to the spatial limitation of endosomal lumen, receptor activation in some cases may be more efficient when internalized in endosomal compartments (Scita and Di Fiore, 2010).

Given the important role of endocytic trafficking in a number of cellular processes, it is not surprising that defects in the endosomal functioning are emerging to be associated to pathological conditions and development defects. Mutations in the molecular machineries that control endosomal sorting have been associated to neurological diseases such as Alzheimer and Parkinson diseases (Small and Petsko, 2015; Elkin et al., 2016; refer also to the following section). Furthermore, endosomal transport is exploited by different pathogens for their mechanisms of infection and reproduction (*Salmonella*, *Coxiella burnetii*, *Legionella pneumophila*, human papillomavirus, herpesvirus saimiri and also human immunodeficiency virus). Some toxins were also identified to target endosome sorting mechanisms. Examples are Shiga toxin produced by bacterium *Shigella dysenteriae*, and Cholera toxin produced by *Vibrio cholera* (Johannes and Popoff, 2008).

### *Biochemical properties of endosomes*

What regulates such a highly complex network? The biochemical properties of different endosomal sub-compartments are fundamental for the correct functioning of endosome-associated processes (Scott et al., 2014). As previously reported, during maturation endosomes undergo a progressive acidification (Elkin et al., 2016). The peculiar pH concentration of endosomal compartments allows the release of ligands by internalized receptors and also the correct functioning of endosomal resident enzymes. This second consideration is also an important

regulatory mechanism that prevents the ectopic progression of enzymatic reactions outside their correct subcellular localization (Houtari and Helenius, 2011).

Membrane lipid composition has a fundamental role in the regulation of endosomal network. Lipids present in distinct sub-compartments allow the organization of membrane micro-domains that are fundamental for the correct sorting of endosomal cargos (Bissig and Gruenberg, 2013). Furthermore, lipid composition determines the biophysical properties of different sub-compartments, favoring the formation of vesicular and tubular structures. Membrane lipids attend at protein recruitment, and control the distribution and turnover rate of enzymes (Bissig and Gruenberg, 2013). Each endosomal compartment is characterized by a specific repertoire of phosphatidylinositols (PIs), which has been proposed to constitute a specific phosphoinositide-based code. Different PIs are univocally recognized by proteins that express specific domains as well as by unstructured protein regions where cluster of basic amino acids are present. Examples of PI-binding domains are the FYVE domain, the pleckstrin homology (PH) and the phox homology (PX) domains expressed by EE-associated proteins and recognizing PI3P-enriched membranes (Bissig and Gruenberg, 2013). Thus, the PI composition of each endosomal sub-compartment cooperates in recruiting the pattern of peculiar membrane-associated proteins that characterize each compartment. The repertoire of PIs is composed of seven molecules, which can be rapidly interchanged between each other by activity of different subtypes of PI kinases and PI phosphatases. The subcellular localization of these enzymes is tightly regulated. Thus, the regulation of PI composition by PI kinases and PI phosphatases constitutes an additional highly dynamic level of regulation. The functions in which PIs are implicated vary from regulation of signal transduction to the regulation of membrane-cytoskeleton interaction, membrane permeability and trafficking, among the others (Di Paolo and De Camilli, 2006).

Each endosomal compartment also associates to specific members of the Rab family of small GTPases. As well as PIs Rab proteins exert essential functions for the maintaining of structural and functional endosomal compartment peculiarity by recruiting specific sets of proteins at the different endosomal membranes. As the other small GTPases Rab proteins switch between two different states: GTP association activates Rab GTPase, while its catalysis to GDP determines Rab inactivation. The activation state is controlled by Rab association to regulatory factors. In particular, guanine-nucleotide exchange factors (GEFs) promote GDP release and GTP binding, thus leading to Rab activation. On the contrary GTPase-activating proteins (GAPs) favor Rab-dependent GTP hydrolysis and consequent Rab inactivation. This mechanism of control allows Rab protein spatial and temporal regulation, and consequential spatial and temporal regulation of Rab-dependent processes (Elkin et al., 2016).

SNARE (Snap receptor) proteins were associated to the regulation vesicles docking and fusion between different endosomal compartments by working in concert with Rab GTPases. SNARE proteins described to be involved in endocytic trafficking are syntaxins 13 and 6, VTI1a and VAMP5 (Gruenberg J., 2001).

### *Molecular mechanisms underlying endosomal sorting*

#### **Delivery to LE and lysosome**

Endosomal sorting between different pathways is a highly regulated process that requires the recruitment of complex macro-molecular machineries. The observation that impairment of either recycling or retrograde pathways results in a prominent increase of cargo delivery to lysosome led to the speculation that LE/lysosome is the dominant destiny of cargos that are retained longer in the EE (Gruenberg J., 2001; Hanyaloglu and von Zastrow, 2008). Cargo entering into the degradative pathway requires a process of ubiquitination that is the covalent binding of a polyubiquitin chain to a residue of lysine in receptor cytoplasmic domain. This reaction is catalyzed by a series of ubiquitin-activating enzymes (E1), ubiquitin-conjugating enzymes (E2) and ubiquitin ligases (E3). In particular for E3 ligases a large number of isoforms has been found, which are specific for different substrates. Ubiquitinated cargos are internalized into ILV and delivered to LE via MVB (Houtari and Helenius, 2011). Although alternative mechanisms have been described, sorting to LE/lysosome is commonly considered a process regulated by the Endosomal Sorting Complexes Required for Transport (ESCRTs) I, II and III that are required for the formation of ILV (Bissig and Gruenberg, 2013). The process is initiated by ESCRT 0 complex, which localizes at the EE due to the presence of a PI3P-binding FYVE domain in one of its subunit, named HRS. HRS also contains an ubiquitin-interacting motif that allows its interaction with ubiquitinated cargos. ESCRT 0 directly interacts with ESCRT I complex and is thought to load cargos to ESCRT I. ESCRT II and III are then responsible of membrane invagination and cargo delivery in ILV. Another element thought to be important for ILV formation is sorting nexin 3 (SNX3) due to the observation that its knockout impairs ILV formation. However, the exact role of SNX3 in ILV formation is still unclear (Bissig and Gruenberg, 2013; Hanyaloglu and von Zastrow, 2008).

In addition recent data have demonstrated that MVB-LE-lysosome fusions are regulated also by specific macro-molecular complexes: HOPS (late endosomal/lysosomal homotypic fusion and vacuole protein sorting) and COVERT (class C core vacuole/endosome tethering factor) (Houtari and Helenius, 2011; Scott et al., 2014).

## **Retromer complex-regulated recycling and retrograde transport**

### The different structures of retromer complexes

Cargo recycling, retrograde transport and retrieval from LE are all commonly regulated by macro-molecular machineries that share a core complex: the retromer. All these pathways have the plasma membrane as common final destination, although during their delivery cargo molecules may traffic through intermediate compartments.

The retromer complex evolved with the primary role of regulating cargo retrograde transport. Accordingly, it was firstly identified in yeast to regulate endosome-to-Golgi retrieval of the CYP receptor (Vps10p). Despite this initial role, the retromer complex is an evolutionary conserved protein complex, which in mammals is described to regulate not only retrograde transport, but also recycling pathways. Furthermore, in mammals it seems that retromer has diversified into at least two distinct complexes. The “core” complex (common to all retromer complexes and also referred to as the retromer itself) is a heterotrimer composed by the association of vacuolar protein sorting 29 (VPS29), VPS35 and VPS26a or VPS26b. It is also known as the heterotrimeric sub-complex or the cargo-selective sub-complex. The core component of the complex is VPS35, to which VPS26 and VPS29 associate at the distal ends and in an independent way. It is generally accepted that the cargo-selective sub-complex works in concert with a heterodimeric sub-complex known as the membrane deformation sub-complex, or SNX-BAR sub-complex. SNX-BAR sub-complex is constituted by any combination of SNX1 or SNX2 and SNX5 or SNX6. When working in concert heterodimeric and heterotrimeric sub-complexes are collectively referred to as the SNX-BAR retromer complex.

The observation that the cargo-selective sub-complex may regulate retrograde transport also independently by the SNX-BAR complex (e.g. by recruiting SNX3 protein) had led to the proposal that when interacting with SNX3 the retromer complex is called SNX3-retromer. This nomenclature was also suggested for other retromer complexes formed by the combination of the retromer “core” complex with different accessory proteins. An example is the complex formed by cargo-selective sub-complex/SNX-BAR sub-complex and SNX27 (Seaman, 2012).

### The sorting nexin family

As reported above, sorting nexins (SNXs) are a large family of proteins characterized by the expression of a PX domain and involved in many endocytic functions. The PX domain mediates interaction with PI3P, thus, SNXs are cytoplasmic globular proteins that are enriched at EE membranes. SNX family can be divided into at least five groups: SNX-PX, SNX-BAR, SNX-

FERM, SNX-PXA-RGS-PSX and SNX-MIT. The last two groups are very few characterized. As already mentioned, i) SNX1, SNX2, SNX5 and SNX6 (members of the SNX-BAR sub-complex), ii) SNX3 (member of the SNX-PX sub-family) and iii) SNX27 (member of the SNX-FERM sub-family) have particular importance for retromer functioning.

i) The members of the SNX-BAR sub-family are characterized by the expression of a Bin/Amphiphysin/Rvs (BAR) domain at the C-terminal. This domain is characterized by a concave surface in which are exposed positively-charged (basic) residues. Characteristics that make BAR domain particularly adapt to “sense” membrane curvature. Moreover, BAR domains allow the homo- and hetero-dimerization of SNX-BAR members (in particular of one SNX1/SNX2 with one SNX5/SNX6). A condition proposed to stabilize and even promote the formation of highly curved membrane tubular structures by forming higher helical complexes. These tubular structures have been described in EE micro-domains committed to recycling and in RE.

ii) SNX3 is the most characterized member of the SNX-PX subfamily. SNX3 is important to mediate retromer recruitment at endosomal membrane by directly interacting with VPS35. In addition SNX3 was demonstrated to regulate WTL retrograde transport to the TGN independently from the SNX-BAR sub-complex (Intro.Fig. 3) (Carlton et al., 2005).

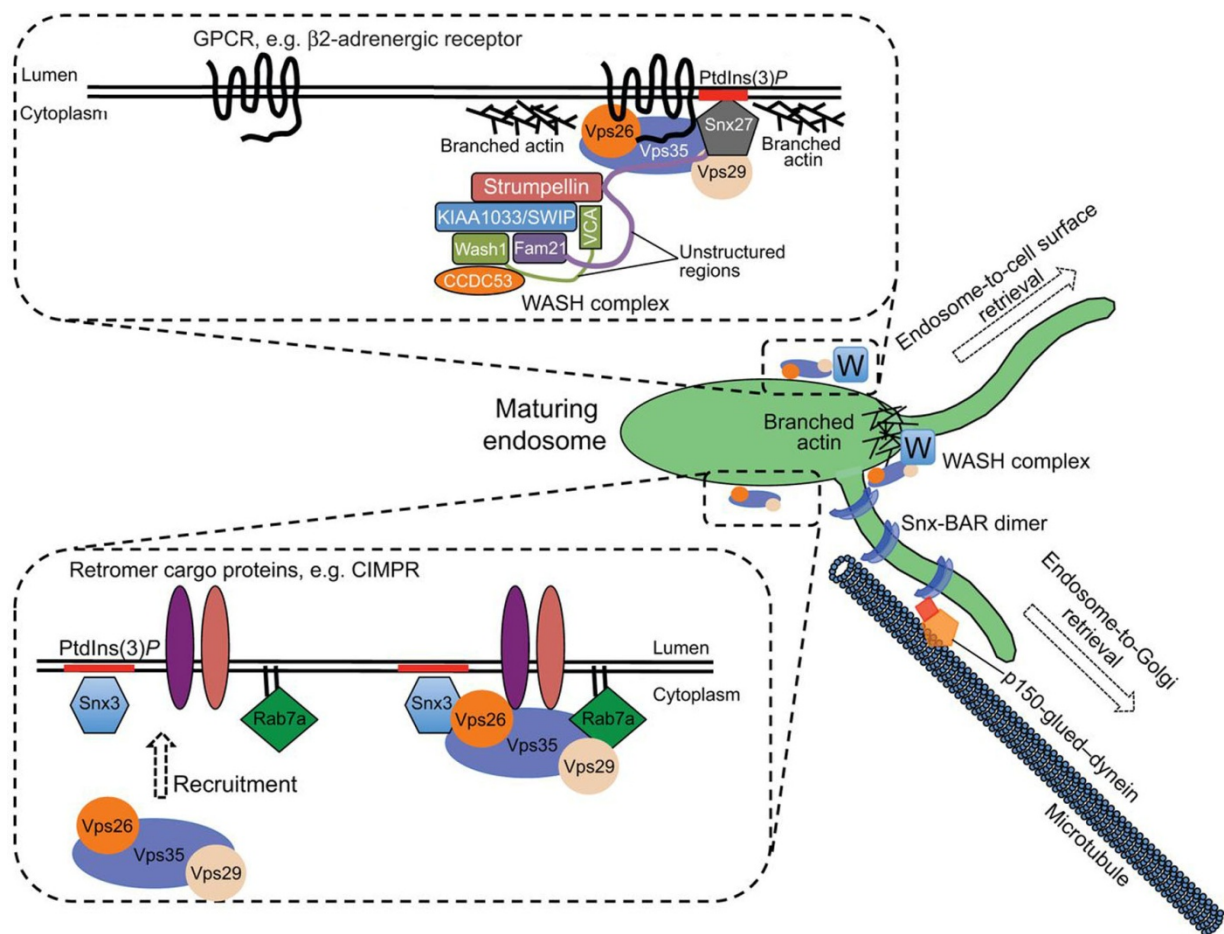
iii) Three proteins belong to the SNX-FERM sub-family. They are SNX27, SNX17 and SNX31. These proteins are characterized by the expression of a FERM-like domain at their C-terminal. SNX27 is unique among all SNXs because in addition to the FERM-like domain it also expresses a PDZ-domain. Thus, it has been shown to interact with a large number of different receptors and ion channels that express a PDZ-binding motif and to regulate their sorting into the recycling pathway. SNX17 has also been shown to regulate protein recycling. In particular it associates transmembrane proteins that express a NPXY motif in their cytoplasmic domain, by direct binding via its FERM-like domain. An established SNX17 cargo is the  $\alpha 5\beta 1$ -integrin. Whether SNX17-mediated recycling depends on the association with the retromer complex and if it travels through the Rab11-dependent recycling is still unclear (Pfeffer, 2013).

### The functions of retromer complexes

The retromer complex is considered the master regulator of sorting of many different cargos. More than hundred different receptors, transporters and ion channels were demonstrated to require retromer complex for their recycling (Steinberg et al., 2013). In addition, retromer-dependent retrograde transport has been demonstrated for cargos such as the cationic-independent mannose-6-phosphate receptor (CI-MPR), sortilin receptor (SorLA) and WLS (Intro.Fig. 2). The current view of retromer complex functioning proposes that it serves as a general hub to which associate a

number of different proteins deputed to different tasks, from selection of cargos to micro-domain localization and membrane deformation. Among these proteins essential roles have SNXs.

Although other mechanisms are now known (i.e. SNX17-mediated recycling), cargo recycling is largely considered to depend on retromer association with SNX-BAR sub-complex and with SNX27 adaptor protein (refer to the following section) (Intro.Fig. 2 and 3). With regards to retrograde transport on the other side, different complexes were proposed for different cargos. SorLA transport was shown to be mediated by retromer association to the SNX-BAR sub-complex, while as already mentioned WLS retrograde transport depends on SNX3-retromer (Intro.Fig. 2 and 3) (Bissig and Gruenberg, 2013). An interesting observation is that the interaction with Rab7 GTPase determines retromer localization also in the LE. Accordingly, in LE retromer was proposed to continue to recover cargos from degradation and re-direct them to the trans-Golgi. This trafficking pathway, which is also a form of retrograde transport, was shown to be necessary for the recovery of cargos that from the *de novo* synthesis pathway (i.e. the Golgi) transport lysosomal enzymes and resident proteins such as the mannose-6-phosphate receptor (Elkin et al., 2016).



**Intro. Figure 3. Schematic representation of retromer complexes that regulate short loop recycling and retrograde transport.**

Cargos (e.g.  $\beta_2$ AR) committed to short-loop recycling are recruited by the retromer complex through SNX27, which functions as an adaptor protein for cargos that express a type I PDZ-binding motif. The WASH complex is also required for the process by promoting actin polymerization. Cargos committed to retrograde transport (e.g. CI-MPR) are directly bound by the cargo-selective retromer sub-complex that is recruited to EE membranes by the concomitant actions of SNX3 and Rab7. The SNX-BAR sub-complex and microtubules are then required for membrane deformation and tubules stabilization, respectively. Figure is adapted from Seaman, 2012.

Molecular mechanisms underlying protein sorting in the endosomal pathways

The mechanistic details of retromer sorting into recycling/retrograde pathways are now starting to be characterized. The mechanism requires the following elements: i) Rab GTPases; ii) scaffolding and tubulation machineries; iii) motor proteins for vesicular transport; iv) a cargo selective machinery.

i) Rab proteins are fundamental for many aspects of recycling pathway. Rab7 mediates retromer recruitment at endosomal membranes by acting in concert with SNX3 (Intro.Fig. 3), while

Rab4 and Rab11 are crucial regulators of the recruitment of complexes required for tubules stabilization, vesicles fission and fusion over the “short” and “long loop” pathways, respectively.

ii) A number of studies have unveiled the mechanistic details of recycling tubules formation. As previously reported SNX-BAR due to the peculiar characteristics of the BAR domain and to the possibility of forming helical complexes has an important role in stabilizing and, probably, also promoting the curvature of tubular membranes. In detail, it was proposed that amphipathic helices expressed at the amino-terminal of SNX1 and SNX2 BAR domains, when anchored to the membrane, generate surface tension between membrane leaflets. To accommodate this tension the membrane is warped generating a positive curvature, which is immediately stabilized by the curvature-sensing properties of BAR domains. Despite this model of SNX-BAR-mediated membrane deformation, WLS and SNX3-retromer-associated retrograde transport was shown to do not depend neither on SNX-BAR complex nor on tubular structures. On the contrary, the process occurs via transport of vesicles that are generated by clathrin coating (Intro.Fig. 3) (Cullen and Korswagen, 2011). Another element shown to be required for tubular structures stabilization and vesicles fission is the Eps15-homology domain (EHD) family of proteins (EHD1-4). However, the molecular bases of EHD proteins functioning as well as of their interaction with the retromer complex are still undefined (Seaman, 2012).

iii) Strictly required for endosomal sorting are microtubules and actin cytoskeleton. Microtubules have been joined to the regulation of vesicle transport. Notably, SNX5 and 6 associate retromer complex to the dynein-dynactin minus-end-directed motor complex by binding of its component p150<sup>glued</sup>. Far better characterized is the association of retromer-regulated sorting with actin cytoskeleton polymerization. Actin polymerization, at the endosomes, is regulated by the WASH (Wiskott-Aldrich syndrome protein and SCAR homolog) complex that acts as a nucleation-promoting factor. The WASH complex is composed of five elements, which are WASH1, strumpellin, SWIP (strumpellin and WASH1 interacting protein), CCDC53 (coiled-coil domain-containing protein 53) and FAM21 (family with sequence similarity 21). FAM21 is WASH complex subunit responsible of interaction with the retromer by direct binding of VPS35 subunit. WASH1 was also reported to interact with VPS35, but with less affinity than FAM21 (Seaman, 2012). Moreover, FAM21 associates with CAPZ $\alpha/\beta$  heterodimer that is a known actin capping protein. Thus, FAM21 mediates the release of actin capping leading to an extensive polymerization in the proximity of retromer complex–decorated membrane micro-domains (Intro.Fig. 3). The role of actin polymerization is now beginning to be understood. The process is supposed to be important for many reasons: i) it may contribute to form membrane micro-domains; ii) it may generate forces required for the elongation of membrane tubules and final vesicle fission; iii) it may be exploited by



motor proteins (i.e. myosin VI) that contribute to vesicle transport; iv) it may contribute to the maintaining of endosomal architecture; v) it favors the scission of vesicles from endosomal tubules by association with dynamin-2. Accordingly, loss of WASH complex components results in increased endosomal tubulation (Seaman, 2012).

iv) How does retromer complex recognize cargos? Different mechanisms have been proposed. A first possibility involves the heterotrimeric cargo-selective sub-complex direct binding (and selection) of cargos. An example is CI-MPR and SorLA retrograde transport, which was demonstrated to depend on a direct interaction with VPS26. Notably, VPS26 in mammals is present in two isoforms (VPS26a and VPS26b), suggesting that different cargos may be recognized by different isoforms (Seaman, 2012). Also VPS35 is supposed to mediate the binding and sorting of some retromer cargos (Cullen and Korswagen, 2011). However a fundamental way for retromer to recruit cargos is by the use of adaptor proteins. Among these proteins a relevant role has SNX27 (Steinberg et al., 2013).

Short loop and long loop recycling pathways are supposed to share a similar mechanism and common machineries for cargo sorting at the level of EE. What are the factors that discriminate between the two pathways is beginning to be understood. SNX27 is now considered the main retromer adaptor protein for the recruitment of cargos that recycle via the Rab4-dependent pathway. The mechanism of SNX27 functioning will be detailed in the following part of this introduction. With regards to Rab11-dependent recycling, whether cargo sorting depends on SNX17, on a direct binding of cargo-selection sub-complex or is mediated by different adaptor proteins is still unclear. A putative candidate is SNX4, which was shown to decorate tubular-vesicular elements that from EE extend to the recycling compartments. SNX4 was also proposed to act in concert with dynein motor protein to regulate the entrance of TfR in the RE (Grant and Donaldson, 2009). Once transported to juxtannuclear RE cargos require to traffic to the plasma membrane. It was shown that tubular structures extending from RE towards the plasma membrane are also involved in the process. These tubules align along microtubules, and it was demonstrated that both microtubules and actin polymerization are required for their formation. An important factor shown to regulate RE-plasma membrane transport is ARF6. ARF6 activates both phospholipase D (PLD) and PI4P-kinase (PI4PK) to remodel membrane lipid composition. PI4PK in particular catalyzes the formation of PI(4,5)P<sub>2</sub> from PI4P, leading to recruitment of peculiar protein complexes required for tubule stabilization and elongation, and also for vesicle fission and fusion. A fundamental role in the recruitment of these complexes has also Rab11, which is specifically expressed into RE. In accordance RNA-interfering down-regulation of Rab11 or of its effectors affect recycling and alter

RE subcellular localization. Finally EHD1 was shown to be required for the stabilization and vesicular fission of recycling carriers involved in RE-to-plasma membrane traffic (Grant and Donaldson, 2009).

The dysregulation of retromer complex is now starting to be associated with the pathogenesis of different diseases. The knockout of retromer components VPS26a and VPS35 is lethal in mammals. Retromer deficiency has also been associated to the pathogenesis of neurodegenerative diseases like Alzheimer and Parkinson diseases (Seaman, 2012), and spastic paraplegia (Blackstone et al., 2011). The retrograde transport of APP relies on SorLA that, as previously said, is a retromer cargo. Notably, the levels of retromer protein expression are reduced in brain areas shown to be more prone to Alzheimer pathogenesis. Mutations in some components of the retromer machinery (i.e. SNX1, SNX3 and WASH) have also been associated to Alzheimer's disease. Furthermore, a mutation of VPS35 that disrupts interaction with the WASH complex was associated with Parkinson's disease. Accordingly, transgenic rats carrying this mutation show a degeneration of dopaminergic neurons (Small and Petsko, 2015).

## **SNX27, an adaptor protein for receptor sorting into the short loop recycling**

SNX27 belongs to the SNX-FERM sub-family of SNX proteins. There are two different isoforms of SNX27 named SNX27 a and b. They distinguish only for the terminal carboxyl tail since SNX27b is 13 amino acids shorter than SNX27a (Rincon et al., 2007). Both the two proteins are broadly expressed in human and murine tissues and are considered constitutively expressed proteins, although their expression was directly demonstrated only for brain, hematopoietic cells, lung, spleen, testis, liver, pancreas and kidney (Rincon et al., 2007; Cai et al., 2011).

As the other SNX members, SNX27 is characterized by the expression of a PX domain that is responsible for its recruitment to EE membranes. Furthermore, as well as SNX17 and SNX31, SNX27 also expresses a FERM-like domain at the C-terminal. However SNX27 is unique among SNXs, since it is the only member of the family that expresses a PDZ domain, which is localized at the N-terminal region (Rincon et al., 2007).

Before explaining the roles and characteristics of SNX27, it is important to give some information regarding PDZ domains and PDZ domain-containing proteins. PDZ domains are protein-protein recognition modules that mediate interactions of PDZ domain-containing proteins

(also referred to as only PDZ proteins) with short sequence-specific domains, named PDZ-binding motifs, and between each other (Romero et al., 2011; Lau and Hell, 2001). They have obtained great interest on the basis of the observation that PDZ domain-containing proteins are implicated in the regulation of receptor signaling, subcellular localization and trafficking. PDZ-binding motifs are classified into three main classes on the basis of the biochemical properties of the amino acids that constitute their consensus sequence. PDZ domains are classified into three classes too, on the basis of the class of PDZ-binding motifs they interact with. The consensus sequence of PDZ-binding motif is essentially constituted by four amino acids. The most C-terminal amino acid is generally indicated as the P<sub>0</sub> (position 0). The other ones are sequentially indicated as P<sub>-1</sub>, P<sub>-2</sub> and P<sub>-3</sub> starting from P<sub>0</sub> residue. Class I PDZ-binding motif consensus sequence is -X-[S/T]-X-Φ (Romero et al., 2011). The consensus sequences of type II and III PDZ-binding motifs are -X-Φ-X-Φ and -X-[D/E/K/R]-X-Φ, respectively. Different type I PDZ domains may prefer specific amino acids in the different positions of PDZ-binding motif (e.g. Na<sup>+</sup>/H<sup>+</sup> exchanger regulatory factor 1, NHERF1, prefers a leucine at position P<sub>0</sub> and an aspartate or a glutamate at position P<sub>-2</sub>; Harris and Lim, 2001; Donowitz et al., 2005). However, residues up to position P<sub>-7</sub> in the PDZ-binding motif –containing proteins have been shown to regulate interaction with PDZ domains. Furthermore, phosphorylation of either the PDZ-binding motif or the PDZ domain has been demonstrated to modulate the interaction (Harris and Lim, 2001; Donowitz et al., 2005).

The structure of PDZ domains and the mechanistic details of PDZ domain – PDZ-binding motif interaction have been studied in details. PDZ-binding motifs are generally located at the C-terminal end of protein chain, but in some cases have been described also internal PDZ-binding motifs. Interestingly, these internal motifs form a tridimensional structure that resembles that of a C-terminal tail. PDZ domains are compact, highly modular globular structures composed by six β-strands and two α-helices. PDZ-binding motifs interaction occurs by means of a mechanism called “strand addition”. This mechanism implies PDZ-binding motif positioning in an extended groove which is located between a β-strand and an α-helix, and is called “peptide-binding groove”. A loop named “carboxylate-binding loop” is responsible for the correct positioning of PDZ-binding motifs (Harris and Lim, 2001). A hydrophobic niche is present in all the three types of PDZ domains and coordinates the P<sub>0</sub> hydrophobic residue. On the other side, at the distal end of the second α-helix of the domain, different residues in the three types of PDZ domains are responsible for discrimination of different types of PDZ-binding motifs. In the type I PDZ domain of NHERF1 for example has been shown to be expressed a histidine residue (His<sup>212</sup>) to coordinate the hydroxyl group of S/T residue P<sub>-2</sub> of type I PDZ-binding motifs (Hanyaloglu and von Zastrow, 2008). On the contrary, a hydrophobic residue is expected in type II PDZ-binding groove to coordinate the hydrophobic

residue express at P<sub>2</sub> by type II PDZ-binding motifs. However, it has been demonstrated that amino acids adjacent to the peptide-binding groove also contribute to determine the specificity of PDZ domains for different PDZ-binding motif -expressing proteins (Sheng and Sala, 2001).

PDZ domains are frequently found in multiple copies on the same polypeptide. Moreover there are now strong evidences of PDZ domain-containing protein hetero- and homo-dimerization due to PDZ domain - PDZ ligand and PDZ domain – PDZ domain interactions. The important implication of this is the possibility to generate multi-protein networks below the plasma membrane that may be key regulators of cellular membrane signaling and of the maintenance of cell polarity (Sheng and Sala, 2001). These evidences led to the concept of “receptosomes” as an important element in receptor signaling. Receptosomes are complexes of different molecules that are aggregated in close proximity because they all contribute to a unique cellular process as, for example, signal transduction. They may include receptors, associated G-proteins, ion channels, kinases, and also proteins of the cytoskeleton and adhesion molecules (Bockaert et al., 2004). PDZ proteins may serve as scaffolds to maintain all proteins required for a signaling pathway in a spatial-restricted region, thus improving both the accuracy and the efficiency of the process. This is particularly important if we think at processes such as synaptic signaling. In addition to improve the activation of post-synaptic signaling pathways, post-synaptic density protein scaffold maintains receptors in the correct position so that neurotransmitters released in the synaptic space efficiently and rapidly activate their target receptors (Sheng and Sala, 2001). Receptosomes are only an example of the many processes PDZ proteins are involved in. PDZ domain-containing proteins have been largely studied for their roles in receptor endocytosis, intracellular sorting and trafficking. Furthermore, they regulate GPCR association to heterotrimeric G-proteins,  $\beta$ -arrestins and GTPase regulatory proteins. Finally, PDZ proteins modulate GPCR interaction to their intracellular effectors such as PLC and protein kinase A (PKA) (Romero et al., 2011).

SNX27 has been shown to prefer type I PDZ-binding motifs that express a valine at P<sub>0</sub> position or another amino acid with a small steric hindrance. Moreover, a positively charged or uncharged residue at position P<sub>5</sub> in PDZ-binding motifs is preferred. However SNX27 has been shown to interact also with PDZ ligands that do not respect these criteria and even with type II PDZ-binding motifs (Gallon and Cullen, 2015). Recently a bioinformatic work described the presence of a specific acidic amino acid sequence upstream at the PDZ-binding motif that is required (although not essential) for a high-affinity engagement by human-SNX27 PDZ domain. Notably, it was also reported that receptors that lack this sequence express a consensus sequence for

cargo phosphorylation, a post-translational modification that serves as a potent signal to induce SNX27 engagement (Clairfeuille et al., 2016).

SNX27 is a cytoplasmic protein anchored to EE membranes by means of its PX domain. At the endosomes SNX27 also interacts with VPS26 subunit of retromer complex via a direct atypical interaction between VPS26 and SNX27 PDZ domain in a site distinct from the PDZ ligand-binding groove. Moreover SNX27 by means of its FERM-like domain directly interacts with FAM21 subunit of the WASH complex and with SNX1 of the SNX-BAR sub-complex. The overall result is that SNX27, due to its peculiar characteristic of expressing a PDZ domain, interacts with cargos that express a type I PDZ-binding motif and constrains them into specific micro-domains where are also recruited the retromer complex, the SNX-BAR sub-complex and the WASH complex. In other words SNX27 recruits cargos in the short loop recycling pathway, functioning as an accessory protein of the retromer complex that adapts the machinery for the binding of specific proteins (i.e. proteins that express a type I PDZ-binding motif) (Intro.Fig. 3). Notably, it was shown that in the absence of FAM21 SNX27 cargos are redirected to the Golgi apparatus instead of the recycling pathway (Lee et al., 2016). A great number of receptors and ion channels have been shown to interact with and depend on SNX27 for their recycling, and SNX27 itself was proposed to be the major regulator of Rab4-dependent recycling at the level of EE (Steinberg et al., 2013). Among the cargos whose recycling was demonstrated to depend on SNX27 are G protein-gated inwardly rectifying potassium channel (Kir3) (Lunn et al., 2007), the glucose transporter GLUT1 (Steinberg et al., 2013), 5-hydroxytryptamine type 4 receptor (Rincon et al., 2007), diacylglycerol kinase  $\zeta$ -associated protein (Joubert et al., 2004), the  $\beta_2$ -adrenergic receptor ( $\beta_2$ AR) (Lauffer et al., 2010) and, importantly, the glutamate receptors AMPA and NMDA (Cai et al., 2011).

Due to its broadly role in regulating such a high number of cargos, it is not surprising that SNX27-knockout is lethal in the first weeks after birth. In particular SNX27 KO mice have a generalized growth defect that involves many different organs, suggesting that SNX27 function is fundamental for many tissues development (Cai et al., 2011).

### *SNX27 retromer and pathologies*

SNX27 deficiency in heterozygous-KO mice results in cognitive impairment and a pathological condition that resembles that of DS. Notably, SNX27 involvement in DS pathogenesis was strengthened by observation of SNX27 reduced levels of expression in DS brains, a defect determined by an impaired regulatory mechanism of SNX27 expression. SNX27 gene transcription is under the control of CCAAT/enhancer binding protein  $\beta$  (C/EBP $\beta$ ), whose levels of expression

are reduced in DS because are directly inhibited by hsa21-associated micro-RNA 155 (mir-155) overexpression. Thus, it was proposed that SNX27 deficiency may contribute to DS cognitive impairment by disregulating AMPA and NMDA receptors recycling and, consequently, their levels at hippocampal synapses (Wang et al., 2013). Furthermore, SNX27 impairment contributes to the early onset of Alzheimer's disease that is observed in DS patients. SNX27 was shown to associate with presenilin-1, a member of the  $\gamma$ -secretase complex. SNX27 binding of presenilin-1 determines  $\gamma$ -secretase complex dissociation, with the final consequence of decreasing  $\gamma$ -secretase activity and amyloid- $\beta$  peptide (A $\beta$ ) production. In DS reduced levels of SNX27 lead to an increased protease activity of  $\gamma$ -secretase and increased A $\beta$  production (Wang et al., 2014).

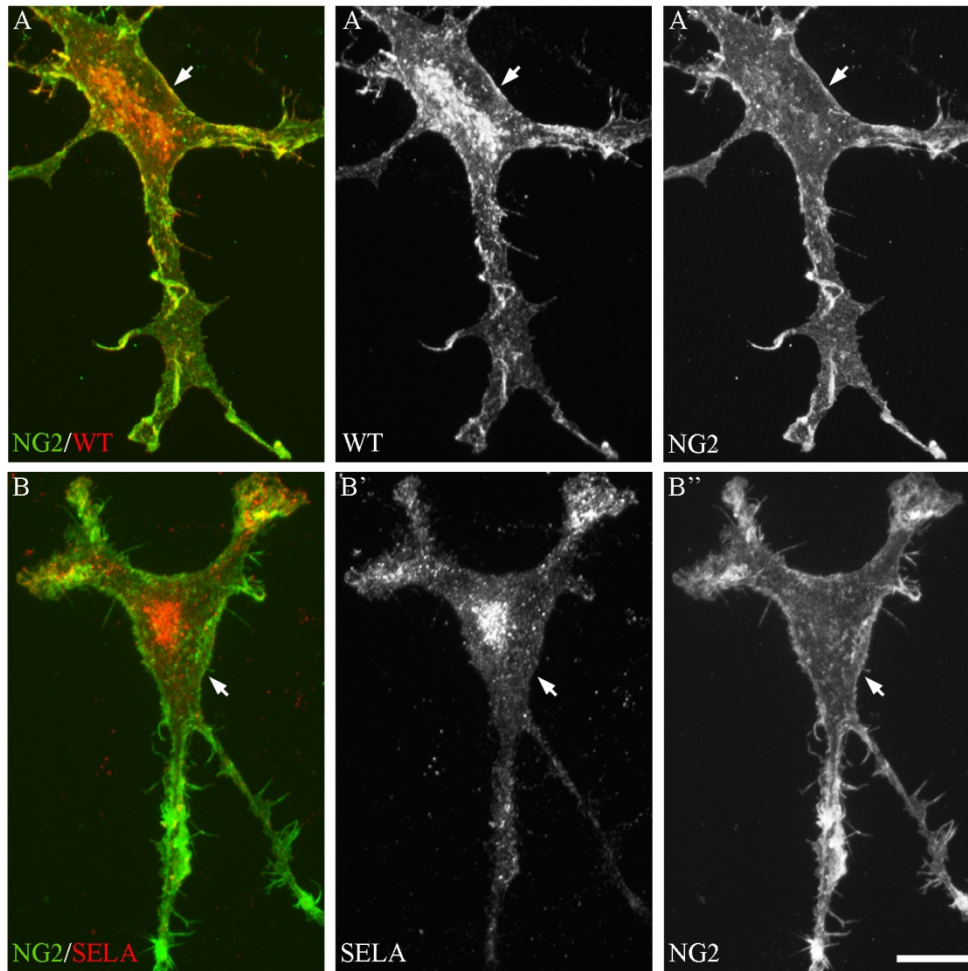
In addition to DS, SNX27 was associated to the pathogenesis of other diseases. McMillan and colleagues showed that a mutation in VPS26a retromer subunit previously characterized to be associated to atypical Parkinson affects endosomal transport of many different cargos by altering the association of retromer and SNX27 (McMillan et al., 2016). Finally it is important to note that a mutation in SNX27 gene was recently reported in humans, in a family affected by infantile myoclonic epilepsy and brain degeneration that determines an impairment of psychomotor development (Damseh et al., 2015).

## **GPR17 PDZ-binding motif is required for receptor accurate localization at the cell surface by mediating a putative interaction with SNX27**

The mechanisms controlling GPR17 levels of expression and at the cell surface are partially known and their characterization may allow a better understanding of OL differentiation, given the well-established function of GPR17 in the regulation of the process. Furthermore, it may provide cues to understand GPR17 dysfunction (Chen et al., 2009; Fumagalli et al., 2011; Boda et al., 2011; Viganò et al., 2016).

To gain more insights on the regulation of GPR17 expression and signaling, we have recently began to characterize the mechanisms underlying receptor endocytic transport. Our previous results showing GPR17 endocytic transport partially to recycling pathway and partially to lysosome (Fratangeli et al., 2013), brought us to focus our attention on the mechanisms that control GPR17 endosomal sorting. As was extensively described in previous sections, endosomal sorting is a crucial event that determines whether receptor would undergo recycling to the plasma membrane or degradation, two opposite destinies leading to signaling sustainment or down-regulation, respectively.

To shed light on these mechanisms we have focused our attention on the C-terminal PDZ-binding motif of GPR17. PDZ-binding motifs, as previously described, have been extensively associated to the regulation of receptor signaling, localization and trafficking (Romero et al., 2011). GPR17 expresses a class I PDZ-binding motif, which sequence, from P<sub>-2</sub> to P<sub>0</sub> residues, is -S-E-L. This motif is conserved in human and mouse receptors (Ciana et al., 2006), suggesting it has a functional role for association to class I PDZ domain-containing proteins (Harris and Lim, 2001). To understand the role of GPR17 PDZ-binding motif we generated receptor variants expressing site-directed mutations in residues important for association with PDZ proteins. In particular we generated: i) a stop codon before the -S-E-L sequence that leads to a truncated GPR17 (GPR17-stop); ii) a substitution of residues at P<sub>-2</sub> and P<sub>-1</sub> with two alanines (GPR17-AAL); iii) a substitution of the residue at P<sub>-2</sub> with an alanine (GPR17-AEL); iv) the addition of an alanine at the extreme C-terminal after the P<sub>0</sub> leucine (GPR17-SELA). The second and the third mutations target the P<sub>-2</sub> residue that is essential for the correct positioning of PDZ-binding motifs in the peptide binding groove of PDZ domains (Harris and Lim, 2001). The fourth mutation was previously described to disrupt PDZ ligand – PDZ domain interaction by steric hindrance (Lunn et al., 2007; Lauffer et al., 2010). The effects of these mutations on receptor trafficking were analyzed by transient transfection of mutant constructs in Oli-neu (an oligodendroglial murine cell line, see Materials and Methods; Intro.Fig. 4) and HEK293 (Intro.Fig. 5) cells, followed by immunolabeling with anti-GPR17 antibodies. As shown in introduction figure 4, labeling of Oli-neu with anti-GPR17-C-terminal antibody ( $\alpha$ GPR17-Ct) and anti-NG2 to decorate the plasma membrane, demonstrated that disruption of PDZ-binding motif results in the altered subcellular distribution of GPR17. Confocal images showed that GPR17 mutants were mainly detected in intracellular vesicles scattered in the cytosol (Intro.Fig. 4 for GPR17-SELA and data not shown), whereas wild type receptors colocalized with NG2, a marker of OPC plasma membrane.



**Intro. Figure 4. GPR17-WT and GPR17-SELA distribution in Oli-neu.**

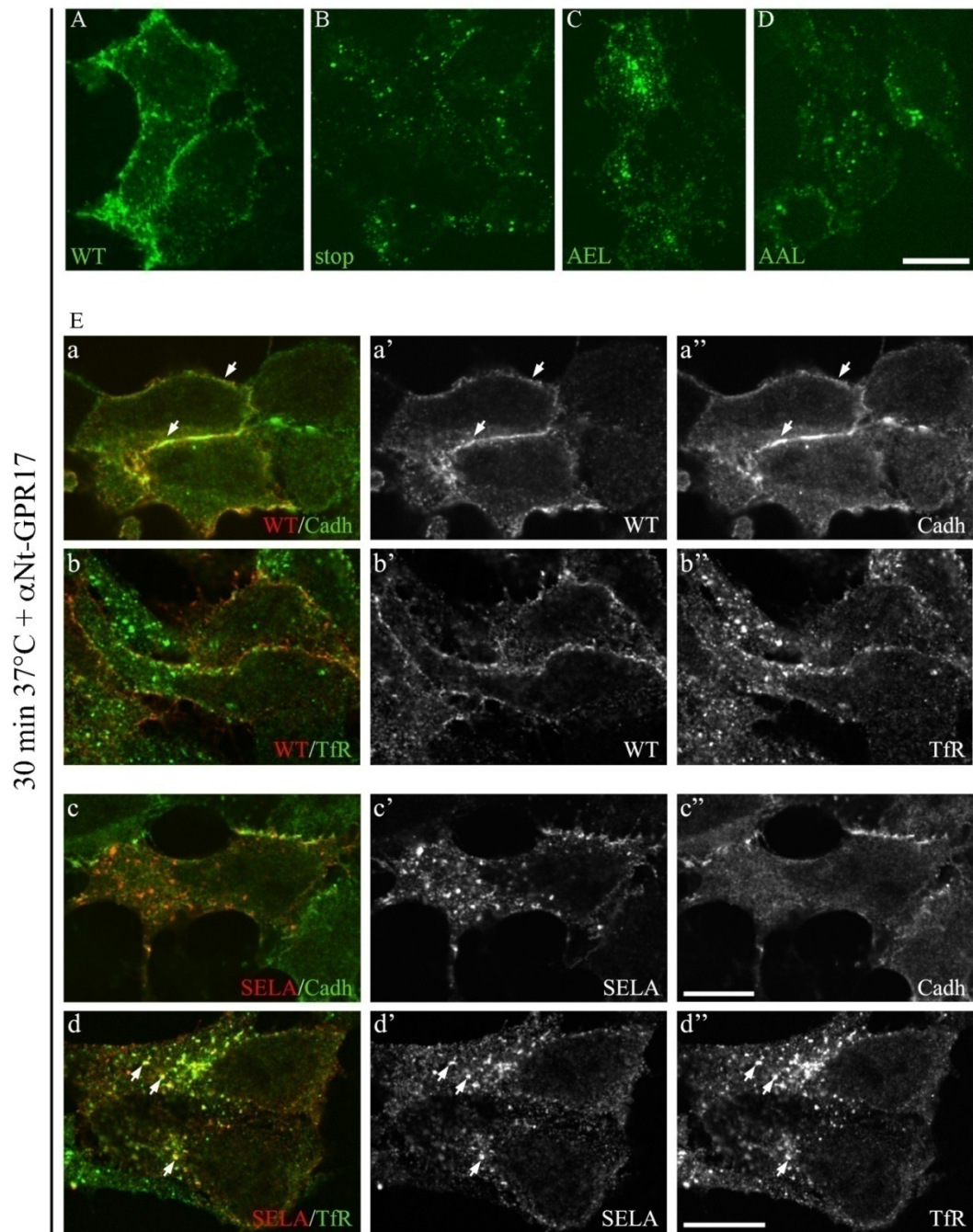
**A-B''** Oli-neu transfected with GPR17-wt or -SELA were fixed and double-labeled for GPR17 and NG2 (plasma membrane protein of immature OLs). Merges are shown in A and B. Note that almost no GPR17-SELA is detected at the cell surface (compare arrows in A-A'' and arrows in B-B''). Scale bar: 10  $\mu$ m.

To gain more insights into the defects found in the trafficking of GPR17 mutants, we took advantage of an antibody raised against GPR17 N-terminal extracellular domain ( $\alpha$ Nt-GPR17; Table 1) to label, at 37°C, wild type and mutant receptors expressed at the cell surface of living HEK293 cells. After 30 minutes (min) cells were fixed and GPR17 receptors were identified by labeling with the appropriated secondary antibody. Confocal microscopy analysis of samples revealed that wild type GPR17 was still retained at the cell surface as shown by co-localization with cadherins (markers of plasma membrane, arrows in Intro.Fig. 5E a-a''). Mutant GPR17 were also labeled with  $\alpha$ Nt-GPR17 antibody, suggesting that their synthesis and biosynthetic transport were not inhibited. However they were mainly detected into intracellular vesicles (Intro.Fig. 5A-E).



Double-immunostaining with anti-TfR antibody revealed that a number of these vesicles correspond to endosomes (Intro.Fig. 5E d-d''). Altogether these results suggested that GPR17 PDZ-binding motif mutants were mainly retained in endocytic vesicles, indicating that PDZ-binding motif is specifically involved in the regulation of receptor endocytic trafficking.

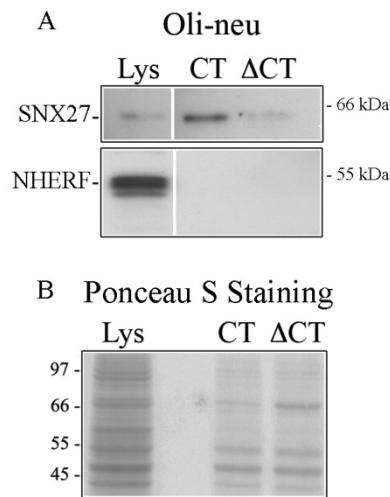
In the light of these data we looked for candidate proteins capable of interacting with the GPR17 PDZ-binding motif. Among PDZ domain-containing proteins known to regulate GPCR endosomal trafficking and/or signaling we selected SNX27 because: i) it interacts with type I PDZ-binding motifs (Lunn et al., 2007; Rincon et al., 2007); ii) it is a well-established regulator of Rab4-dependent recycling (Temkin et al., 2011; Steinberg et al., 2013), which is the pathway exploited by GPR17 (Fratangeli et al., 2013); iii) it has been shown to interact with a number of different receptors and ion channels and among them are also many GPCRs (Lauffer et al., 2010; Steinberg et al., 2013); and iv) its expression in the CNS is well established (Cai et al., 2011; Wang et al., 2013). In addition we analyzed the role of NHERF1, a widely expressed scaffold protein that has been reported to affect the trafficking and signaling of the purinergic receptor P2Y<sub>12</sub> (Nisar et al., 2012), which shares similarities with GPR17.



**Intro. Figure 5. PDZ-binding motif mutated GPR17 receptors are retained intracellularly.**

**A-D** Representative immunofluorescence micrographs showing HEK293 cells transfected with GPR17-wt (A) or with plasmids coding for GPR17 PDZ-binding motif mutants (i.e. stop, B; AEL, C; or AAL, D). Live cells were incubated 30min at 37°C with the  $\alpha$ Nt-GPR17, fixed and stained with anti-rabbit IgG conjugated to Cy2. **E** Representative immunofluorescence micrographs showing HEK293 cells transfected with GPR17-wt (a-b'') or GPR17-SELA (c-d''). Live cells were incubated 30min at 37°C with the  $\alpha$ Nt-GPR17 and double-immunostained for cadherins (marker of plasma membrane, a-a'' and c-c'', arrows) or TfR (marker of endosomes, b-b'' and d-d'', arrows). Scale bars: 10  $\mu$ m.

To test whether SNX27 and NHERF1 interact with GPR17 PDZ-binding motif we performed pulldown experiments using two different peptides covalently conjugated with Sepharose 4B resin beads: i) a peptide corresponding to the last 19 amino acids of GPR17 C-terminal tail (referred to as CT peptide) and ii) a second peptide identical to CT, but lacking the PDZ-binding motif (referred to as  $\Delta$ CT). Interestingly, neither CT nor  $\Delta$ CT peptide could isolate NHERF1 from Oli-neu cell extracts, whereas CT peptide isolated at least 10 times more SNX27 than  $\Delta$ CT (Intro.Fig. 6), suggesting that SNX27 may interact with the C-terminal PDZ-binding motif of GPR17.



**Intro. Figure 6. GPR17 PDZ-binding motif interacts with SNX27 *in vitro*.**

Oli-neu cell lysates (500  $\mu$ g of proteins) were incubated with CT or  $\Delta$ CT peptides conjugated to sepharose beads (20  $\mu$ L). Proteins eluted from the beads and aliquots of total lysates (30  $\mu$ g of proteins, Lys) were analyzed by Western blotting with antibodies against NHERF1 or SNX27. A Immunoblots representative of three independent experiments are shown. B Ponceau S staining of nitrocellulose membrane before immunolabeling.

## AIMS OF THE WORK

Altogether our results indicate that GPR17 PDZ-binding motif plays an important role in the endocytic trafficking and cell surface expression of GPR17 via a possible interaction with SNX27. Based on these observations we decided to definitively demonstrate the specific role of SNX27 in the regulation of GPR17 endosomal sorting, with specific regards to sorting between degradation and recycling. Furthermore, we investigated whether SNX27 down-regulation occurring in pathological conditions (e.g. DS or SNX27 gene mutation; Wang et al., 2013; Damseh et al., 2015) may have implications for OL differentiation, with the aims to reveal further mechanisms underlying defects of myelination (see DS) and to identify new pharmacological strategies to target GPR17 as therapy for pathological conditions where myelination is affected.

# MATERIALS AND METHODS

## *Antibodies and reagents*

Primary antibodies used in this study are listed in Table 1.  $\alpha$ Nt-GPR17 and  $\alpha$ GPR17-Ct antibodies were obtained by immunization of rabbits and affinity purification, and were characterized as previously described (Fratangeli et al., 2013). Anti-rabbit or anti-mouse IgG conjugated to horseradish peroxidase, anti-rabbit IgG-light chain conjugated to horseradish peroxidase, biotinylated anti-goat IgG, and reagents UDP-Gluc, dithiothreitol (DTT) and protease inhibitor cocktail were purchased from Sigma-Aldrich (Milan, Italy). AlexaFluor® 488-conjugated streptavidin, His-Pur-Ni-NTA resin and TurboFECT transfection reagent were from Thermo-Fisher Scientific (Waltham, MA, USA), while JetPei transfection reagent was purchased from Polyplus Transfection (Illkirch, France). The anti-rat IgG conjugated to horseradish peroxidase, AlexaFluor® 488 -conjugated goat anti-mouse or anti-rabbit IgGs and streptavidin conjugated to AlexaFluor® 555 were from Life Technologies (Monza, Italy). Goat anti-rabbit IgG and goat anti-mouse IgG conjugated to IR Dye 800 CW and IR Dye 680 RD, respectively, were from Li-Cor Biosciences (Cornaredo, Milan, Italy). We purchased the anti-mouse, anti-rabbit and anti-rat IgGs conjugated to Cy3-, Cy5-, Cy2-, DyLight488- or FITC-, from Jackson ImmunoResearch Laboratories (West Grove, PA, USA).

## *Plasmids, oligonucleotides and site-directed mutagenesis*

pCMVEntry-human(h)SNX27 was purchased from OriGene Technologies (Rockville, MD 20850). To remove Flag epitope SNX27 cDNA was sub-cloned in a pcDNA3.1 (SNX27 wild-type), while to conjugate hSNX27 with a poly-histidine epitope (his-SNX27) we sub-cloned SNX27 cDNA into a pRSET B vector (Life Technologies). The cloning of GPR17 cDNA into pcDNA3.1/V5-His-TOPO was previously described (Lecca et al., 2008), while for Flag epitope conjugation, GPR17 was sub-cloned in a pFLAG-CMV2 expression vector (Life Technologies). We also purchased from Life Technologies the pcDNA3 vector backbone. The pMGP-155 vector for mir-155 expression and pMGP vector control were from Addgene (O'Connell et al., 2009). Short-hairpin (sh)-RNAs scrambled (CSHCTR001-CU6) and targeting SNX27 mRNA sequences 1) catgaggctgataacctag, 2) ggccattctcattatcaga, 3) ctggcacctaataatgaatttc and 4) actctacgtccagaactat cloned into a psi-U6.1 expression vector, and carrying EGFP expression cassette, were purchased from GeneCopoeia (Rockville, MD). Mmu-miR-155-5p (5'-UUA AUGCUAAUUGUGAUAGGGGU-3') and hsa-miR-155-5p (5'-UUA AUGCUAAUCGUGAUAGGGGU-3') primer sets to analyze mir-155 expression by quantitative real time PCR (qRT-PCR) were purchased from Exiqon (Vedbaek, Denmark). Site directed mutagenesis of GPR17 cDNA in pcDNA3.1/V5-His-TOPO and in pFLAG-

CMV2 vectors and of the SNX27 cDNA cloned in pRSET B were done using the QuickChange Lighting Site-Directed Mutagenesis Kit (Agilent Technologies, La Jolla, CA, USA) accordingly to manufacturer's instructions. Primers used for the mutagenesis are here listed:

Stop For, 5'-CTCCCTGAGTGCCTGATCCGAGCTGTG-3';  
Stop Rev, 5'-CACAGCTCGGATCAGGCACTCAGGGAG-3';  
RAAL For, 5'-CCCTGAGTGCCCGAGCCGCGCTGTGAGAAGG-3';  
RAAL Rev, 5'-CCTTCTCACAGCGCGGCTCGGGCACTCAGGG-3';  
RAEL For, 5'-CCCTGAGTGCCCGAGCCGAGCTGTG-3';  
RAEL Rev, 5'-CACAGCTCGGCTCGGGCACTCAGGG-3';  
RSELA For, 5'-GTGCCCGATCCGAGCTGGCATAAGGGCAATTCTGCAGA-3';  
RSELA Rev, 5'-TCTGCAGAATTGCCCTTATGCCAGCTCGGATCGGGCAC-3';  
KSELA For, 5'-GCCAAGTCAGAGCTGGCATGATCTAGAGGATCCC-3';  
KSELA Rev, 5'-GGGATCCTCTAGATCATGCCAGCTCTGACTTGGC-3';  
KAEL For, 5'-GCTCGCTGAGTGCCAAGGCAGAGCTGTGATCTAGAGG-3';  
KAEL Rev, 5'-CCTCTAGATCACAGCTCTGCCTTGGCACTCAGCGAGC-3';  
SNX27 H114A For, 5'-GAATGTTGAGGGGGCGACAGCCAAGCAGGTGGTGGACC-3';  
SNX27 H114A Rev, 5'-GGTCCACCACCTGCTTGGCTGTGCCCCCTCAACATTC-3'.

Constructs were sent to Eurofins MWG Operon (Ebersberg, Germany) for sequencing.

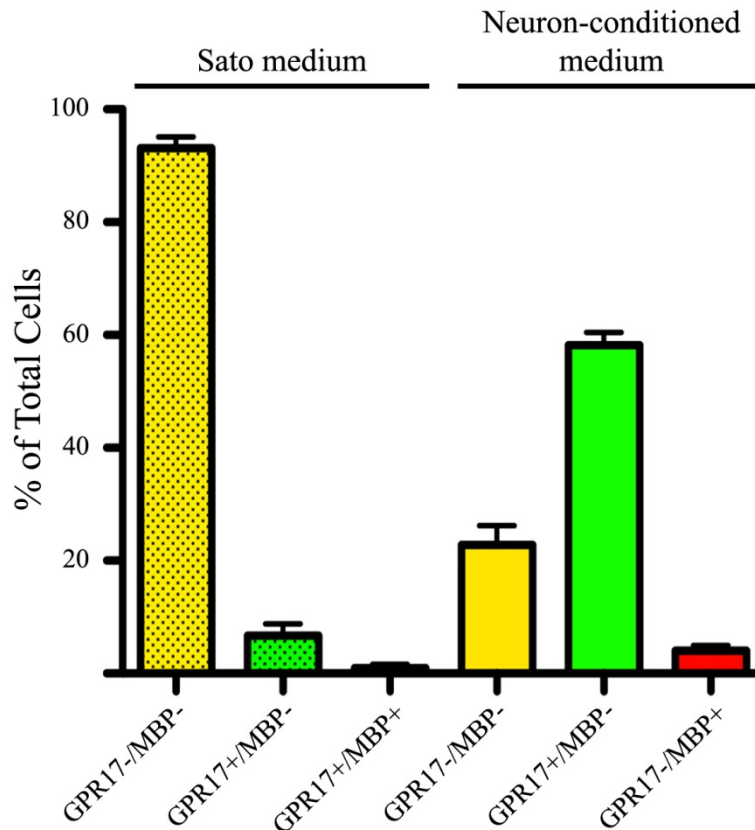
### *Cell culture*

Oli-neu is a cell line derived from immortalized murine OPCs and was kindly provided by Professor J. Trotter of the University of Mainz (Germany). Oli-neu were maintained in Sato medium (13,4 g/L DMEM powder, 2 g/L NaHCO<sub>3</sub>, 10 µg/mL Transferrin, 10 µg/mL Insulin, 100 µM Putrescine, 200 nM Progesterone, 500 nM TIT, 220 nM Na-selenium, 520 nM L-Thyroxin, 25 µg/mL Gentamicin) containing 1% horse serum (HS) (from here on I will refer to Sato containing 1% HS as only Sato medium) at 37°C and 10% CO<sub>2</sub> (Jung et al.; 1995). To allow Oli-neu differentiation cells were cultured in conditioned medium (CM) composed of 1:1 Sato and neuron conditioned medium. Neuron conditioned medium was obtained from 12 and 14-div (days in vitro) old neuronal cortical cultures from 18-day old rat embryos and was kindly provided by Dr. M. Passafaro (CNR, Institute of Neuroscience). As described in Fratangeli et al., 2013 exposure to CM promotes Oli-neu exit from mitosis and differentiation, in a manner that resemble that of primary OPCs. Our analysis and quantification of different markers of OL differentiation demonstrated that after 48-hours (hr) of culture in differentiating conditions nearly 80% of cells of the whole cell culture express GPR17, while at 72hr after CM exposure the percentage of cells expressing GPR17

is reduced and we observed a concomitant expression of MBP (Meth.Fig. 1 and Fratangeli et al., 2013). Thus we analyzed the expression of GPR17 in control (ctr) or plasmid transfected cells 72hr after transfection and 48hr after treatment with CM. HEK293 cells were maintained in DMEM medium containing 10% Fetal Bovine Serum (FBS), 1% Penicillin/Streptavidin (P/S) and 2 mM L-glutamine (from here on I will refer to 10%FBS 1%P/S 2mM L-glutamine in DMEM as only DMEM medium), at 37°C and 10% CO<sub>2</sub>. Primary cultures of fibroblasts derived from DS embryos and euploid controls were a kind gift of Professor Lucio Nitsch (University of Napoli Federico II; Department of Molecular Medicine and Medical Biotechnology) and were maintained in DMEM medium further containing 10 ng/μL FGF, at 37°C and 10% CO<sub>2</sub>. Primary cultures enriched in OPCs were prepared following previously described methodologies (Fumagalli et al., 2011; Medina-Rodriguez et al., 2013). In brief, cortices of postnatal day 3 (P3) C57BL/6 mice or P2 Sprague-Dawley rats were used to obtain mixed glial cultures which then underwent a process of selection based on selective detachment upon shaking on a rocking plate. OPCs were then transferred to Petri dishes or coverslips (previously treated with poly-L-lysine, Sigma-Aldrich, Milan) and expanded by maintaining in Sato medium without tyroxine and supplemented with 10 ng/mL bFGF and 10 ng/mL PDGF-AA. Cell transfection was done two days later. After transfection samples were incubated in differentiation conditions (i.e. Sato medium without growth factors).

### *Cell transfection*

JetPei (PolyPlus) or TurboFECT (Thermo Scientific, Rockford, Illinois) were used as transfection reagents in accordance with manufacturer's instructions. The appropriate amounts of cells were seeded onto 24x24 mm glass coverslips or 60 mm Petri dishes 24hr before the transfection. In particular we seeded 150,000 HEK293/coverslip, while Oli-neu cell number depended on the time span of the following differentiating treatments and ranged from 30,000 to 75,000/coverslip and from 130,000 to 150,000/petri dish for 72hr and 48hr of differentiation respectively. 0.5 μg and 1 μg of DNA were used respectively for Oli-neu and HEK293 cells onto 24x24 mm coverslips, while Oli-neu in 60 mm Petri dishes were transfected using 1 μg of DNA. For experiments of co-transfection, vectors were mixed in a 1:1 ratio. 24hr after transfection the medium was replaced with fresh medium or, in the case of Oli-neu, with CM to promote cell differentiation. HEK293 cells were fixed 48hr after transfection (see below), while Oli-neu cells were fixed or lysed as described below after 72hr or 96hr (48hr or 72hr of differentiation, respectively).



**Meth. Figure 1. Quantification of GPR17 and MBP expressing cells in 48hr-differentiated Oli-neu.**

Oli-neu cells were cultured in either Sato medium or CM (neuron-conditioned medium) to induce cell differentiation. After 48hr cells were fixed and double-immunolabeled with  $\alpha$ GPR17-Ct and anti-MBP antibodies. The numbers of GPR17 and of MBP –expressing cells were counted in twenty optical fields/coverslip and in a total of 6 coverslips for each group and results were then reported as a percentage of the total number of counted cells set to 100%. As indicated by histograms the percentage of GPR17-positive cells increases upon Oli-neu exposure to CM, and we also observed the appearance of MBP-expressing cells, suggesting that cells are under differentiation. The results are the means ( $\pm$ s.e.m.) of three independent experiments.

*Cell lysis and fractionation of nuclei/cytosol*

Different lysis buffers were used depending on the procedures used after extraction. For pulldown experiments we used buffer B (PBS, pH 7.4, 2.5 mM EDTA and 10% glycerol containing 0.5% Nonidet P40 and protease inhibitors). When pulldown was performed using His-Pur-Ni-NTA resin EGTA was removed from the buffer. For other experiments we lysed cells using buffer A (150 mM NaCl, 2 mM EGTA, 50 mM Tris-HCl, pH 7.5, containing 1% Triton X-100 and protease inhibitors). Cell extracts were harvested and incubated on ice for 30min, followed by 30min centrifugation at 12,000 rpm at 4°C. For nuclei/cytosol fractionation, buffer C (10 mM Hepes, 10



mM KCl, 1.5 mM MgCl<sub>2</sub>, 0.5 mM DTT, pH 7.9, containing protease inhibitors) was used to collect cells, while lysis was obtained mechanically using 2.5 mL syringes and 18Gx1.5'' needles (Terumo, Leuven, Belgium). Nuclei were pelleted by centrifuging samples at 800xg for 10min at 4°C and cytosolic fraction was collected. Buffer D (400 mM NaCl, 20 mM Hepes, 25% glycerol, 0.2 mM EDTA) was then used to resuspend the nuclear fraction. Samples were incubated on ice for 40min and finally centrifuged at 40,000 rpm and 4°C for 40min. To concentrate samples, when required, we precipitated proteins by means of 4-volumes of 100% acetone and overnight incubation at -20°C. The following day samples were centrifuged at 10,000 rpm 4°C for 30min and solubilized in Laemmli's sample buffer (3% SDS, 125 mM Tris-HCl pH 6.8, 6.6% glycerol, β-mercaptoethanol and bromophenol blue).

#### *Protein purification from bacteria extracts*

For expression of his-SNX27 in bacteria we used BL21DE3 *E. coli* strain. We cultured bacteria until OD<sub>600</sub> 0.6-0.8 and then induced expression of his-SNX27 by administration of 0.1 mM isopropyl β-D-1-thiogalactopyranoside (IPTG) to the culture followed by incubation for 3hr at 37°C. Bacteria were pelleted and resuspended in 20 mM phosphate buffer. Cell lysis was obtained by freeze-thaw cycles between liquid nitrogen and water bath at 42°C. For protein purification from bacteria extracts, we used nickel-nitrilotriacetic acid resin (His-Pur-Ni-NTA; Thermo-Fisher Scientific, Waltham, MA, USA) according to the manufacturer's instructions. 200 μL of resin were used to purify his-SNX27 derived from a 200 mL bacteria culture. Amicon® Ultra Centrifugal Filter (Millipore) were finally used to remove imidazole from the eluted samples.

#### *Protein pulldown*

For proteins pulldown we used a GPR17 C-terminal peptide (CT) or a GPR17 C-terminal peptide lacking the PDZ-binding motif (ΔCT) previously conjugated at a concentration of 2 mg/mL-of-matrix with CNBr-activated sepharose 4B resin beads. 500μg of Oli-neu protein extracts, 50μL of BL21DE3 bacteria extracts or 2μg of purified his-SNX27 were incubated overnight at 4°C with 20 (Oli-neu) or 10 (bacteria and purified his-SNX27) μL of the resins in buffer B containing 0.2% Nonidet P40 and protease inhibitors. The following day samples were washed with buffer B containing 0.2% Nonidet P40 (three times) and with buffer B without detergent (three times). Finally, proteins bound to the resins were eluted in Laemmli's sample buffer. When using His-Pur-Ni-NTA resin EGTA was removed from the buffer B.

### *Western blotting*

Proteins were separated by SDS-PAGE using 8% or 12% acrylamide/bisacrylamide gels, and transferred onto 0.45  $\mu\text{m}$  nitrocellulose membrane (Whatman, Dossel, Germany). Polyvinylidene Fluoride (PVDF) membranes (Amersham Hybond<sup>TM</sup>-P; GE Healthcare) were required for GPR17 immunostaining. For Odyssey Li-Cor detection we used either 0.22  $\mu\text{m}$  nitrocellulose membrane or PVDF (Immobilon<sup>®</sup>-FL; Millipore). We blocked aspecific binding sites by overnight incubation at 4°C in Tris Buffered Saline (TBS) (25 mM Tris-HCl, pH 7.4 and 150 mM NaCl) and 5% non-fat milk (blocking buffer). TBS containing 5% non-fat milk and 1% bovine serum albumin (BSA) was required for immunostaining using anti-SNX27 antibody. Primary and secondary antibodies were diluted in TBS containing 5% non-fat milk and 0.3% Tween 20, while 0.1% Tween 20 was used for SNX27, ID2 and GAPDH, and 0.05% Tween 20 was required for MBP staining. 5% non-fat milk in TBS was utilized for anti-GRK2, anti-mTOR, and anti-phospho-mTOR antibodies. Incubation was done for 2hr and 1hr for primary and secondary antibodies respectively, except for anti-MBP antibody which was incubated overnight at 4°C. Extensive washes were done between antibody incubations and after secondary antibody staining. Anti-rabbit or anti-mouse IgGs conjugated to horseradish peroxidase were diluted 1:50,000 with exceptions for SNX27 and ID2 immunostaining, for which dilution was 1:25,000, and horseradish peroxidase-conjugated anti-rat IgG which was used at 1:5,000 dilution. Chemiluminescent detection was done using SuperSignal WestPlus ECL substrate (Thermo-Fisher Scientific, Waltham, MA USA) and Amersham Hyperfilm ECL (GE Healthcare, Little Chalfont, UK). For immunostaining detection using Odyssey Li-Cor 5% non-fat milk in Phosphate Saline Buffer (PBS; 137 mM NaCl, 3 mM KCl, 8 mM Na<sub>2</sub>HPO<sub>4</sub>·2H<sub>2</sub>O and 2 mM NaH<sub>2</sub>PO<sub>4</sub>·xH<sub>2</sub>O) and PBS containing 5% non-fat milk and 0.1% Tween 20 were used as blocking and washing buffer (and for antibody dilution), respectively. IR Dye 800 CW anti-rabbit and IR Dye 680 RD anti-mouse secondary IgGs were diluted 1:10,000. Their intensities were acquired using a Li-Cor Bioscience Odyssey CLx infrared imaging system (Li-Cor Bioscience, Cornaredo, Milan, Italy).

If necessary, membranes were stripped to detach bound antibodies by washing with glycine 0.2 M buffer, pH 2.2.

### *Immunolabeling of live cells and cell fixation*

We firstly washed cells with PBS containing 0.1 mM CaCl<sub>2</sub>, 1 mM MgCl and 1% HS (PBS++ 1% HS) for Oli-neu, 1% BSA for HEK293 cells (PBS++ 1% BSA), then, incubated them for 35min at 4°C with  $\alpha\text{Nt-GPR17}$  or anti-FLAG epitope ( $\alpha\text{FLAG}$ ) antibodies diluted in PBS++ 1% HS or 1% BSA (refer to Table 1 for antibody dilutions). Antibody excess was removed by washing

with PBS++ 1% HS/BSA at 4°C and samples were incubated in complete Sato/DMEM medium containing 100µM UDP-Gluc at 37°C 10% CO<sub>2</sub> to induce receptor internalization. Internalization was induced for 20min, after that endocytosis was blocked by taking samples to 4°C. When required we used 50 mM glycine buffer (pH 2.8) to detach antibody at cell surface, while we allow receptor distribution into endosomal pathways by re-incubating samples in complete Sato or DMEM medium without agonist at 37°C, 10% CO<sub>2</sub>. After PBS washing, samples were fixed with 4% paraformaldehyde in phosphate buffer (pH 7.3) containing 4% sucrose (incubation for 10 and 15 min for Oli-neu and HEK293 cells, respectively), and processed for immunofluorescence as following described.

### *Immunofluorescence*

We permeabilized fixed cells for 5min (10 minutes for HEK293) with PBS containing 0.3% Triton X-100 (0.1% Triton X-100 was used for samples fixed after *in vivo* labeling). Cells were then incubated for 30min in 0.1 M glycine (pH 7.4) to neutralize aldehyde complexes. The following washes and antibody dilution were done using 10 mM PBS containing 450 mM NaCl and 0.2% gelatin (IF buffer). Incubations of primary and secondary antibodies conjugated to the appropriate fluorophores were done for 2hr and 45min at room temperature (RT), respectively. Primary antibody dilutions are summarized in Table 1, while secondary antibodies were diluted 1:200. We finally reduced saline concentration by washing with PBS and swiftly with distilled H<sub>2</sub>O, and mounted coverslips on slides using Mowiol 4-88 (Polyscience). For goat anti-SNX27 primary antibody detection we used a donkey anti-goat IgG conjugated with biotin (1:200 dilution, 45min incubation), which was then revealed using an AlexaFluor® 488 –conjugated streptavidin (1:200 dilution, 45min incubation). Endogenous biotin and avidin were blocked using avidin/biotin blocking kit (Vector Laboratories, Burlingame, California).

### *Mouse colony (in collaboration with the laboratory of Prof. Renata Bartesaghi of the University of Bologna)*

Ts65Dn female mice were purchased from Jackson Laboratories (Bar Harbour, ME, USA) and mated with C57BL/6JEi x C3SnHeSnJ (B6EiC3) F1 males to maintain the original genetic background (partial trisomy of chromosome 16; Reeves et al., 1995). Analysis of mice karyotypes was done by qRT-PCR, as reported in Liu et al., 2003. Postnatal day zero (P0) was used to refer to the date of birth, in accordance with common conventions. Animals health and comfort were always cared and were under the control of veterinary service. Animals underwent a 12:12 hr dark/light cycle and were always supplied with water and food *ad libitum*. Bologna University Bioethical

Committee oversaw that experiments were in accordance with Italian and European Community law for the use of experimental animals. All efforts were made to minimize both the number of animals required and animal suffering.

*Immunohistochemistry (in collaboration with the laboratory of Prof. Maria Pia Abbracchio and the group of Prof. Stefania Ceruti, Università degli Studi di Milano)*

Brain sections of euploid or Ts65Dn mice at 45 post-natal days were kindly provided by the laboratory of Prof. Renata Bartesaghi (University of Bologna) and were prepared as described in Guidi et al., 2014. Samples were provided as free-floating or paraffin-embedded sections and were processed for immunohistochemistry in accordance with the protocol described in Boda et al., 2011. PBS containing 5% normal goat serum and 0.3% Triton-X 100 was used for primary and secondary antibody incubations. Primary antibodies were incubated overnight at 4°C while secondary antibodies were incubated for 1hr at RT. Primary antibody dilutions are summarized in Table 1, while secondary antibodies, covalently conjugated with appropriate fluorophores, were diluted 1:600. For GPR17 immunostaining was used the high-sensitivity Tyramide Signal Amplification kit (Perkin Elmer, Monza, Italy) in accordance with manufacturer's instructions. Nucleus staining was done by means of Hoechst 33258 dye (Life Technologies) diluted 1:10,000 in PBS 1:1 methanol, samples were incubated for 20min at RT. Slides were mounted using Fluorescent Mounting Medium (Dako Italia, Milan, Italy). MBP staining was performed on paraffin-embedded samples. After paraffin embedding removal using xylene, and samples re-hydration by means of a graded concentration ethanol scale, samples were rinsed in water and a procedure of antigen retrieval was done. For antigen retrieval samples were maintained in sodium citrate buffer (10 mM sodium citrate containing 0.05% Tween 20, pH 6) and underwent four 4 seconds-cycles of heating in a microwave oven at 800W, separated by 1min of cooling. Samples were then rinsed in PBS containing 0.05% Tween 20 and processed for immunostaining using Tyramide Signal Amplification kit (Thermo Scientific, Rockford, Illinois) following manufacturer's instructions, with exception for nonspecific antigenic sites blockage that was done overnight at 4°C.

*Total RNA purification, retrotranscription and qRT-PCR*

For total RNA extraction we cultured cells in 60 mm Petri dishes as described above. Cells were then harvested maintaining samples on ice, centrifuged for 5min at 4,000 rpm and 4°C and resuspended in appropriate volume (1 mL for cells derived from a 60 mm Petri dish) of TriFast reagent (Euroclone, Pero, Milan). RNA, DNA and protein separation was obtained by adding chloroform in a 1:5 volume ratio, followed by incubation at RT and centrifugation for 15min at

12.000xg. The hydrophilic fraction was collected and RNA was concentrated by sequential precipitation using 2-propanol and washes with ethanol 75% in diethylpyrocarbonate (DEPC)-treated water. Finally, RNA was rinsed in DEPC-water and concentration and purity were determined by analysis at the spectrophotometer. The following RNA retrotranscription and qRT-PCR reactions were done using Exiqon miRCURY LNA™ Universal RT microRNA PCR Starter Kit (Exiqon, Vedbaek, Danmark) following manufacturer's instructions, except for sample volumes which were 20 µL both for retrotranscription (final concentration 1 µg/µL) and qRT-PCR reactions. For qRT-PCR amplification cDNA templates were diluted 1:20 (Oli-neu RNA extracts) and 1:40 (fibroblasts RNA extracts). PCR amplification and samples analysis were done using a QuantStudio5 Thermocycler and QuantStudio5 software (Applied Biosystems, Foster City, California).

#### *Image acquisition and analysis*

We acquired immunofluorescence micrographs using a Nikon E600 microscope, a Zeiss Axiovert 200 confocal microscope equipped with a Perkin Elmer UltraVIEW acquisition system, or a Zeiss LSM510 Meta microscope, and by means of Zeiss plan-NEOFLUAR 63x or 40x objectives. When multiple staining were done images from different emission specters were acquired separately and superimposed in the aftermath. When images had to be compared we used the same parameters of acquisition. Images were exported as TIFF files and Photoshop (Adobe Systems, Mountain View, CA, USA) and ImageJ software were used for following processing and analysis. GPR17 distribution in endocytic compartments was quantified by measuring the intensity of  $\alpha$ Nt-GPR17 and  $\alpha$ FLAG immunostaining in samples fixed before UDP-Gluc stimulation, after receptor internalization and glycine washes, and finally after incubation at 37°C in the absence of agonist. Cells expressing comparable levels of transfected proteins were chosen for analysis. Results are the mean of at least three independent experiments for each condition and approximately 100 cells for each experiment were analyzed. For the quantification of GPR17 and CC1-positive cell number in brain hemispheres, images were acquired at 10X magnification using a Zeiss Axiovert 8400 microscope equipped with a CCD camera. ImageJ was used to count cells, whose number was then normalized on the number of counted fields. At least 50 fields (869,14 µm wide and 650,28 µm high) for each sample were examined (total area 565,186.5 µm<sup>2</sup>). The quantification of MBP and MAG expressing cell number and of MBP immunoreactivity in brain sections was done on stitched composite images acquired using the stitch option of Volocity acquisition system. Zeiss Plan-NEOFLUAR 25x/0.80 objective and PRIOR Proscan 3 motorized xy-stage were used for sample scanning. For the analysis of MBP in brain hemispheres, comparable sections were chosen. The

whole hemispheres were automatically acquired and stitched using Volocity software and a focus map created for acquisition of the best focus for each field. Composite stitches images were then exported as TIFF files, processed and analyzed using Photoshop and ImageJ. Selected areas of cortex and corpus striatum were converted in binary images using an automatic thresholding function of ImageJ software and quantification was done on approximately equal areas: 4.95 mm<sup>2</sup> and 5.07 mm<sup>2</sup> respectively for euploid and Ts65Dn in the cortex, while for the corpus striatum the analyzed area was of 5.90 mm<sup>2</sup> for both euploids and Ts65Dn.

### *Statistical analysis*

GraphPad Prism software was used for statistical analysis. When two treatments were compared the results from independent experiments were collected as raw quantitative data and used to calculate mean values, that were then subjected to two-tailed unpaired Student's t-test to assess statistical significance. One-way ANOVA with Tukey's test was used when comparing three or more groups. Results are expressed as percentage of control samples, apart for degradation assay for which we used t=0 control set to 100% for normalization, and rescue experiment for which we used shSCR/pcDNA3 co-transfected sample set to 100% for normalization. With exception for preliminary data regarding the effects of mir-155 overexpression on OL differentiation (Fig. 14B), for which statistical significance is not reported, at least three independent experiments were conducted for each analysis. The exact number of experiments conducted for each analysis is reported as "n" in figure legends.

## RESULTS

### **A PDZ-binding motif is specifically required for endosomes to plasma membrane recycling of GPR17**

Our preliminary data suggested the involvement of the GPR17 PDZ-binding motif in the control of receptor endocytic trafficking. To understand in detail the function of this domain, we decided to define which endosomal pathway the PDZ-binding motif mutation disrupts. We took advantage of the receptor *in vivo* labeling with  $\alpha$ Nt-GPR17 antibody to track the endocytosis and endosomal sorting of wild type GPR17 (GPR17-wt) and GPR17-SELA mutant (Table 2) and then compared receptor transport by immunofluorescence staining and confocal microscopy imaging. HEK293 were transiently transfected with the two GPR17 isoforms. Labeling of live cells with  $\alpha$ Nt-GPR17 was performed 48hr later to allow protein expression. For this analysis labeling was performed at 4°C to maintain cell metabolism blocked and avoid constitutive internalization of labeled receptors (Fratangeli et al., 2013). Notably, quantification of receptor immunoreactivity revealed no significant differences between the amounts of GPR17-wt and SELA present in the plasma membrane of transfected cells (Fig. 1A, E and I). This result indicates that comparable amounts of GPR17-wt/GPR17-SELA are delivered to the cell surface demonstrating that GPR17 synthesis and transport through the biosynthetic pathway are not affected by mutation of the PDZ-binding motif. Thus, we speculated that PDZ-binding motif disruption affected GPR17 internalization and/or transport through the endocytic pathway. To test this hypothesis we stimulated GPR17 endocytosis by incubating transfected HEK293 cells (after labeling at 4°C with  $\alpha$ Nt-GPR17) at 37°C in DMEM medium containing 100  $\mu$ M GPR17 agonist UDP-Gluc (Fratangeli et al., 2013). After 30min, UDP-Gluc containing medium was removed and cells were washed with acid glycine buffer (pH 2.8) to strip antibodies bound to receptors still present at the cell surface. Samples were then fixed and processed for immunofluorescence staining with an anti-rabbit IgG conjugated to Cy2. Analysis of immunofluorescence micrographs showed that upon agonist-induced endocytosis GPR17-wt and GPR17-SELA were both detected in intracellular vesicles (Fig. 1B and F), in line with our previous data showing that upon stimulation GPR17 is rapidly internalized in EE where partially co-localizes with TfR (Fratangeli et al., 2013 and preliminary results). Interestingly, quantification of receptor immunoreactivity using ImageJ software indicated there was no significant difference between the amounts of internalized GPR17-wt and GPR17-SELA (Fig. 1L). This result led us to conclude that GPR17 PDZ-binding motif disruption did not alter receptor internalization. We then allowed internalized receptors to distribute into endosomal compartments by incubating cells in the absence of UDP-Gluc for either 10 or 20 min

(37°C, 10% CO<sub>2</sub>), times previously described to allow GPR17 sorting into either degradative or recycling pathways (Fratangeli et al., 2013). Accordingly, already after 10min intracellular GPR17-wt staining was significantly reduced due to receptor transport to lysosome or recycling to plasma membrane. On the contrary GPR17-SELA was retained into intracellular compartments for a longer period than GPR17-wt (Fig. 1C, D, G and H). Quantification of immunofluorescence intensities confirmed that ~30% more GPR17-SELA than wt receptor was still present inside the cells 20min after agonist removal (Fig. 1L). These results, together with a growing number of evidences showing that PDZ-binding motifs are involved in the regulation of GPCR recycling (Romero et al., 2011), led us to speculate that the C-terminal PDZ-binding motif is required for GPR17 recycling to the plasma membrane.

To definitively clarify this aspect we took advantage of an isoform of GPR17 expressing a Flag-tag epitope in the extracellular domain (FLAG-hGPR17-wt) and mutagenized it to add a C-terminal alanine (FLAG-hGPR17-SELA; Table 2). This allowed us to repeat the above described experiment and follow the endocytic transport of GPR17 in live cells using a monoclonal antibody directed against the Flag-epitope ( $\alpha$ FLAG antibody) with a stronger affinity for antigen compared to  $\alpha$ Nt-GPR17. Using  $\alpha$ FLAG antibody we were able to unveil that internalized FLAG-hGPR17-wt was partially recycled to the plasma membrane once cells were re-incubated at 37°C upon UDP-Gluc removal and glycine-buffer washing. On the contrary, almost no GPR17-SELA was re-exposed at the cell surface (Fig. 2C and C').

Taken together, these results demonstrate that GPR17 PDZ-binding motif is required for GPR17 plasma membrane recycling through a putative interaction with PDZ domain-containing proteins.



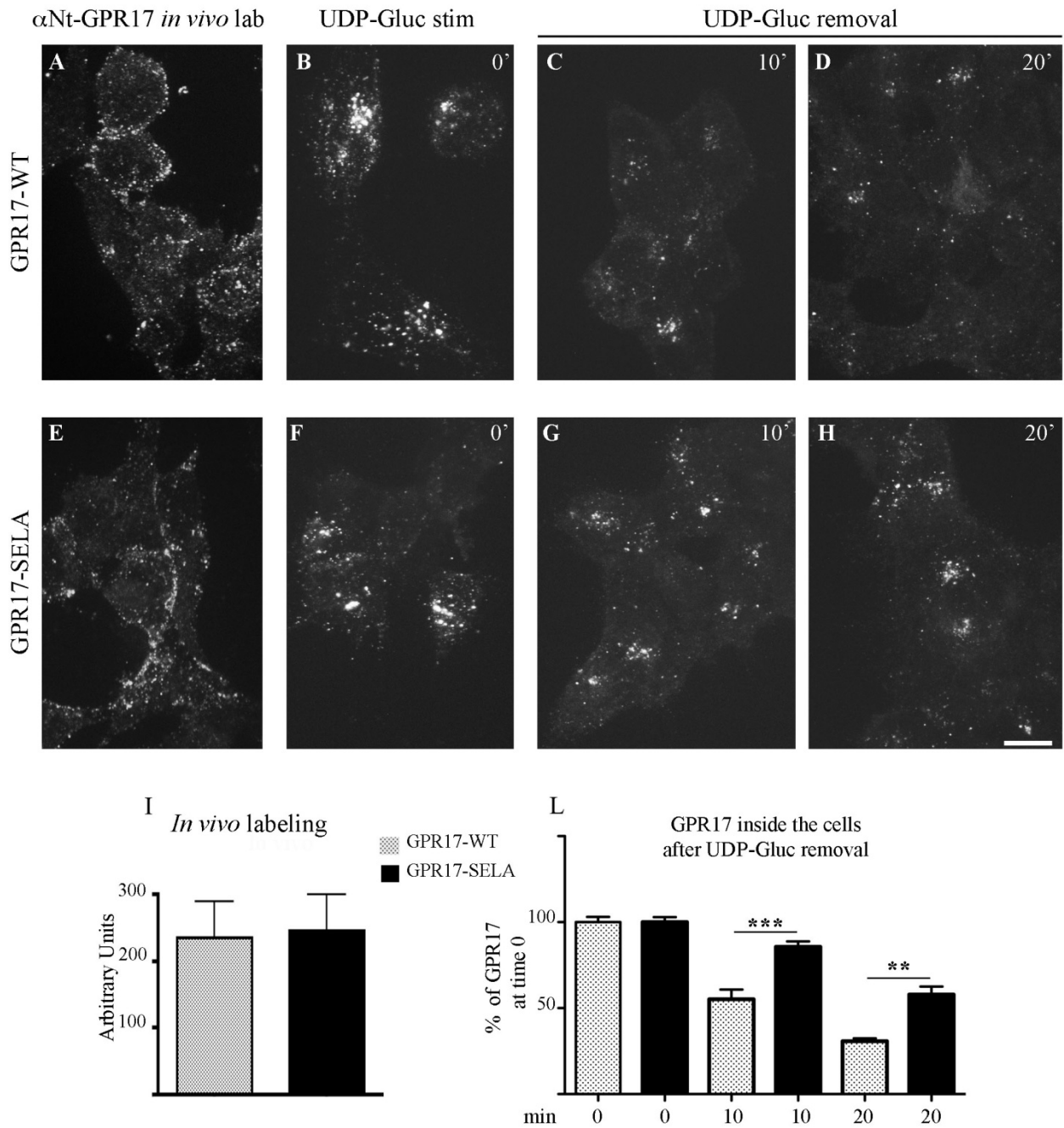


**Figure 1. GPR17-SELA is retained intracellularly after agonist removal.**

**A, E** Representative immunofluorescence micrographs showing surface GPR17 labeling of HEK293 cells with affinity-purified  $\alpha$ Nt-GPR17 after transfection with either GPR17-wt or GPR17-SELA. **B, F** Representative immunofluorescence micrographs showing internalization of GPR17-wt or SELA. Upon stimulation with 100  $\mu$ M UDP-Gluc, cells were washed with glycine buffer (pH 2.8) to remove antibodies bound to the remaining cell surface-exposed receptors, and then fixed (0 min). **C, D, G, H** Representative immunofluorescence micrographs showing that more GPR17-SELA than wt receptors are retained in the cells following 10 and 20 min of agonist removal. **A-H** Scale bar: 10  $\mu$ m. **I** Quantitative analysis of the intensity of GPR17 immunoreactivity detected on

plasma membrane of transfected cells after labeling (see A and E panels) as determined using ImageJ software. The values are expressed as arbitrary units and represent the mean value  $\pm$  s.e.m., n=10 cells transfected with GPR17-wt and 12 cells transfected with GPR17-SELA. **L** Quantitative analysis of the intensity of GPR17 immunoreactivity in transfected cells at 0, 10 and 20 min after agonist removal. The data are expressed as the percentage of immunoreactivity detected after agonist-induced internalization (time 0 set to 100%). The mean value  $\pm$  s.e.m. detected in 93 (0min), 79 (10min), and 104 (20min) GPR17-wt transfected cells or 113 (0min), 110 (20min) and 98 (20min) GPR17-SELA transfected cells are shown. \*\*\*P=0.0007; \*\*P=0.0051 unpaired two-tailed Student's t-test.

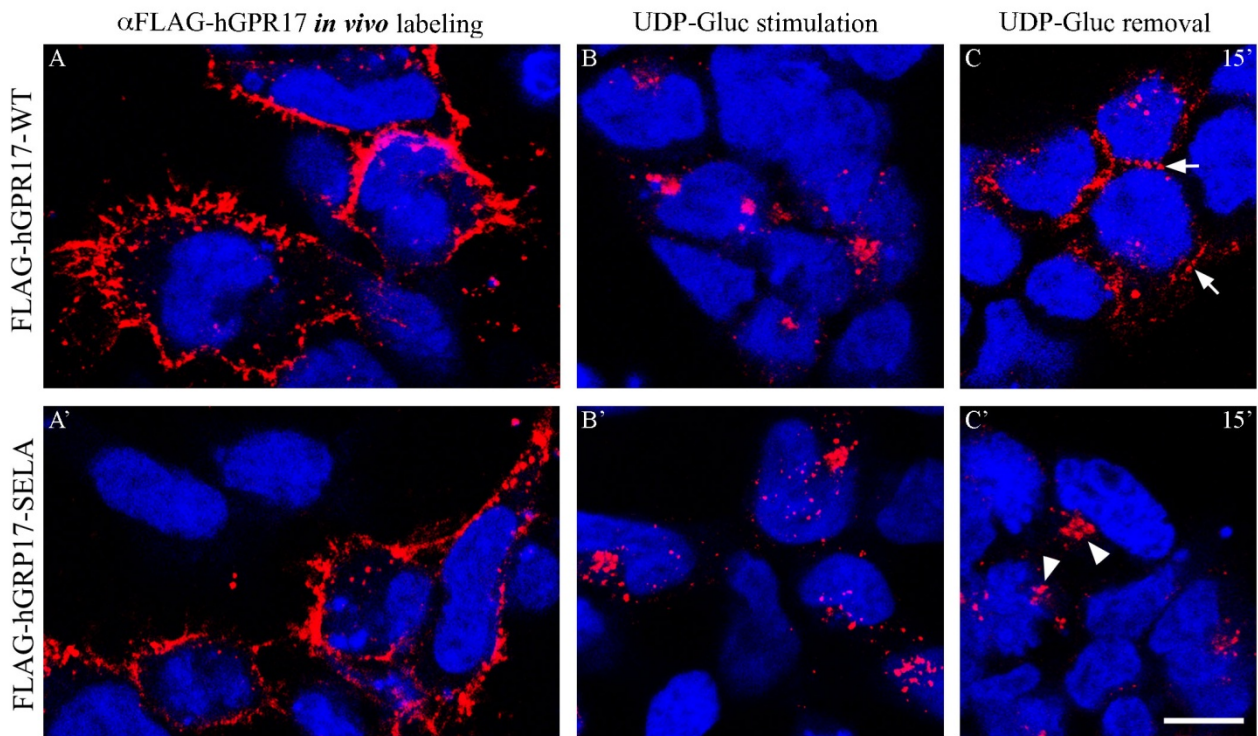


**Figure 2. The recycling of GPR17-SELA is impaired.**

**A-C'** Representative micrographs of HEK293 cells transfected with FLAG-hGPR17-wt or FLAG-hGPR17-SELA showing: A, A' the surface localization of wt and mutant GPR17 after labeling at 4°C with a monoclonal antibody against the Flag epitope; B, B' GPR17 intracellular staining after UDP-Gluc stimulation and C, C' 15min after agonist removal. Note in C recycling of wt receptor to the cell surface (arrows) whereas FLAG-hGPR17-SELA is mainly retained in the cells (C', arrow heads). DAPI nuclear labeling is shown in blue. Scale bar: 10  $\mu$ m.

## **SNX27 interacts with GPR17 at the level of endosomal compartments**

By means of pulldown experiments we had obtained preliminary evidences suggesting an interaction between SNX27 and the C-terminal domain of GPR17 (Prel.Fig. 3). SNX27 is an accessory protein of the retromer complex shown to mediate recruitment of cargos expressing a type I PDZ-binding motif, and their sorting into endosomal tubular-domains committed to membrane recycling (Temkin et al., 2011). To further demonstrate a role for SNX27 in the regulation of GPR17 intracellular trafficking we confirmed its expression in primary cultures of OLs. To this aim, Oli-neu and primary OL cultures were fixed and then double-immunolabeled using antibodies directed against SNX27 and OL lineage markers such as OLIG2. Images obtained with a spinning disk confocal microscope revealed that SNX27 is expressed by oligodendroglial cells where it decorates intracellular dot-like structures distributed in the cytoplasm and in the perinuclear region (Fig. 3), a pattern in line with that reported in literature (Joubert et al., 2004; Lauffer et al., 2010).

We then asked whether SNX27 and GPR17 co-localize at these intracellular vesicles (i.e. early/recycling endosomes). To address this issue we again used  $\alpha$ Nt-GPR17 antibody to label endogenous GPR17 in live Oli-neu or primary OLs, and to detect receptor distribution in the endosomal pathways. Oli-neu or OPCs were exposed to CM or neurobasal medium (Fumagalli et al., 2011) to induce cells differentiation and GPR17 expression. We then labeled at 4°C cell-surface receptors of living cells and either i) incubated samples at 37°C to track GPR17 constitutive endocytic trafficking (Fratangeli et al., 2013); or ii) stimulated receptor endocytosis using UDP-Gluc and allowed endosomal distribution by incubating cells at 37°C 10% CO<sub>2</sub> in the absence of the agonist. We finally washed cells with glycine buffer and fixed samples. Cells were then double-immunolabeled with a goat polyclonal anti-SNX27 antibody (followed by an anti-goat biotin-conjugated antibody and a streptavidin conjugated to Cy2) and anti-rabbit IgG conjugated to Cy3 to detect GPR17. Images acquired by confocal microscopy clearly showed that upon constitutive (Fig. 4C) or agonist-mediated internalization (Fig. 4A and B) GPR17 and SNX27 co-localize in vesicular structures scattered in the cytosol of Oli-neu and primary differentiating OPCs. These findings, joined to the previous evidences obtained by pulldown analysis (Prel.Fig. 3), strongly suggested SNX27-GPR17 interaction in OL endosomes.

To gain more insights on the mechanistic details of GPR17-SNX27 binding, we cloned SNX27 cDNA into a pRSET B vector and used the construct to transform BL21DE3 *E. coli* bacteria and purify SNX27 from bacteria extracts. SNX27 expression was induced using IPTG. In order to purify the protein, we took advantage of a poly-histidine tag at the N-terminal of SNX27,

which results from its cloning into pRSET B vector backbone. Nickel-conjugated resin beads were then used to separate histidine-tagged SNX27 (his-SNX27) from bacteria lysates. His-SNX27 was eluted in phosphate saline buffer (PBS) and incubated with either CT and  $\Delta$ CT peptides (Fig. 5A). After extensive washing we eluted bound proteins with glycine buffer (pH 2.2) and analyzed purified his-SNX27 affinity for CT and  $\Delta$ CT peptides by Western blotting. As reported in figure 5, while we detected his-SNX27 in samples eluted from CT resin, his-SNX27 was not isolated by  $\Delta$ CT peptide (Fig. 5C), suggesting a direct interaction between SNX27 and GPR17 C-terminal.

Based on the observation reported by Lauffer and colleagues who demonstrated that mutation of histidine residue 112 in SNX27 PDZ binding groove disrupts the interaction with  $\beta_2$ AR receptor (Lauffer et al., 2010), we decided to test whether PDZ domain disruption affects also interaction with GPR17. This histidine residue is supposed to coordinate the hydroxyl group of S/T residue P<sub>2</sub> of type I PDZ-binding motif (Fig. 5B and Hanyaloglu and von Zastrow, 2008), but differently from murine SNX27, in SNX27 human orthologue (which we used in our experiments) H<sup>112</sup> is found at position 114 (H<sup>114</sup>). Thus, we mutagenized H<sup>114</sup> by substitution with an alanine (his-SNX27-H114A) and analyzed its interaction with GPR17 C-terminal by pulldown. Results clearly showed that H<sup>114</sup> disruption abolished his-SNX27 isolation with CT peptide (Fig. 5D), demonstrating that interaction specifically occurs between the GPR17 PDZ-binding motif and the PDZ domain of SNX27.

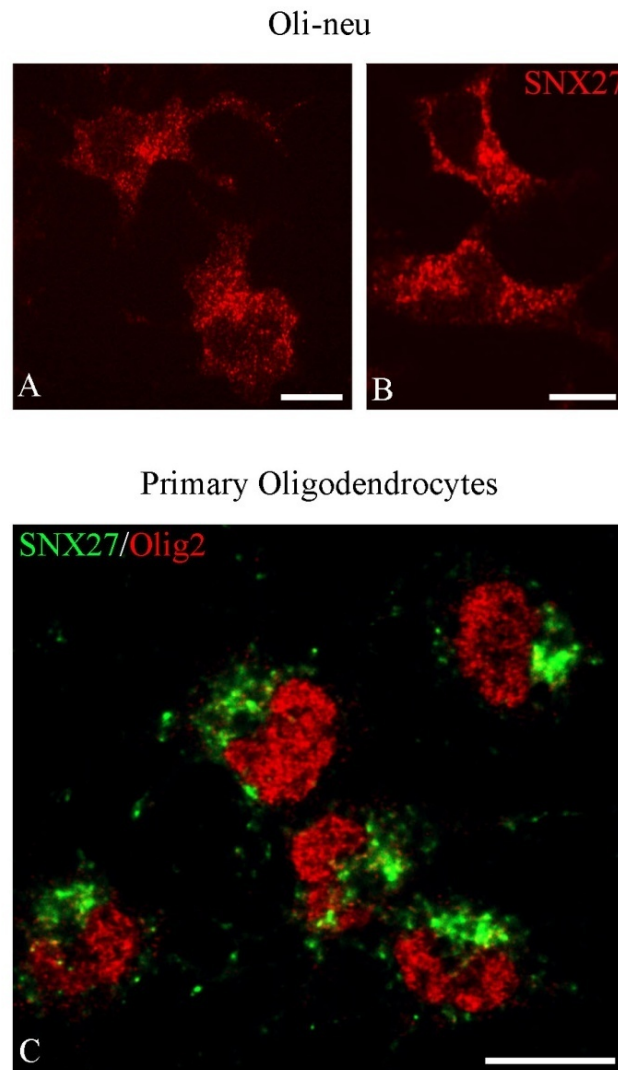


**Figure 3. SNX27 is expressed in cells of the OL lineage.**

**A, B** Representative micrographs showing the distribution of SNX27 in undifferentiated Oli-neu cells after labeling with a polyclonal antibody directed against SNX27. **C** Primary OL cultures were double-immunolabeled with antibodies against SNX27 and the TF OLIG2. Note that SNX27 shows a punctate intracellular distribution. Scale bars: 10  $\mu$ m.

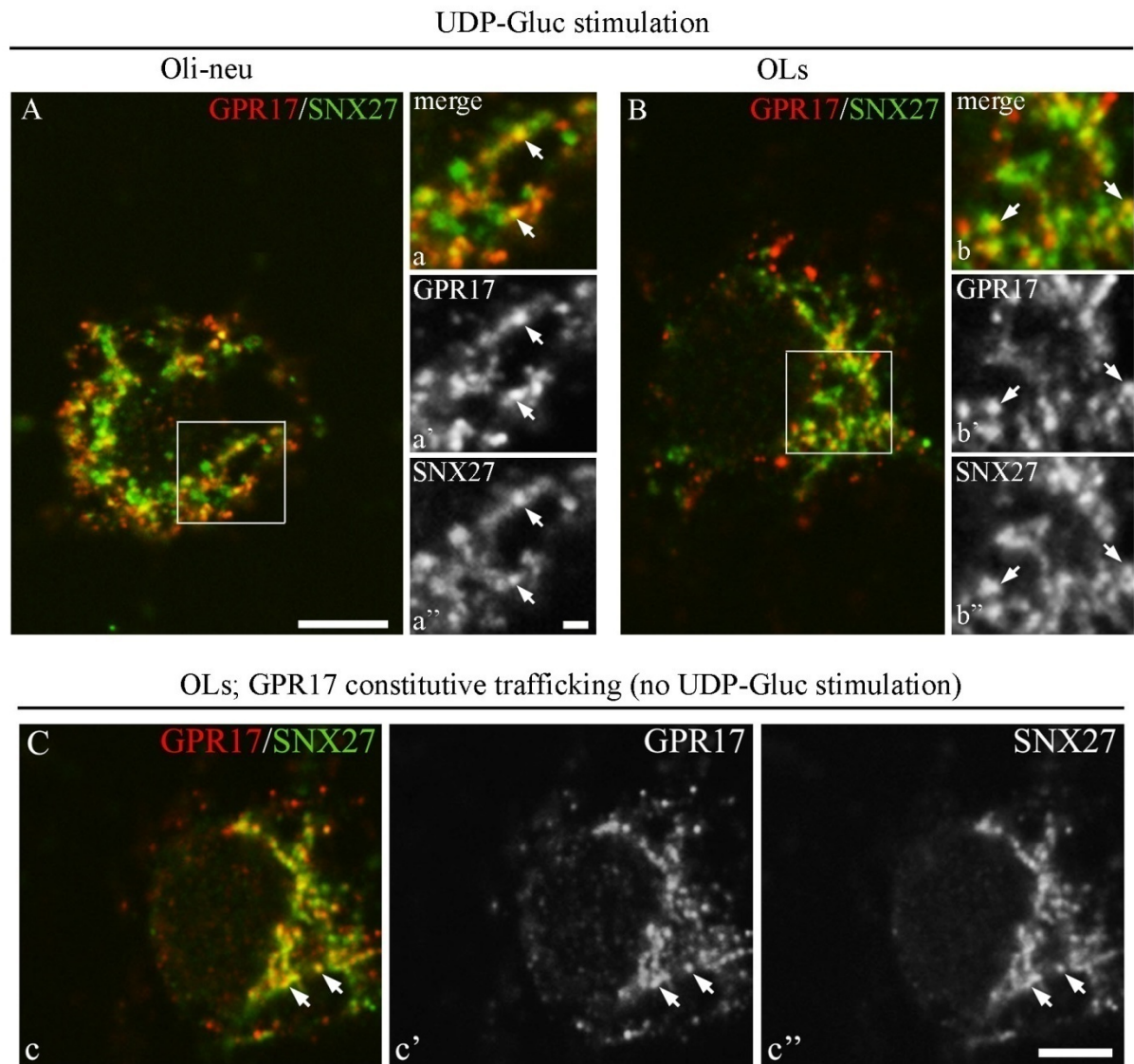


**Figure 4. Endocytosed GPR17 co-localizes with SNX27 in early endosomes.**

**A-C** Representative immunofluorescence micrographs showing co-localization of SNX27 with endogenous GPR17 after internalization. Oli-neu cells (A) and primary OPC cultures (B, C), after differentiation in immature oligodendroglial cells, were incubated at 4°C with affinity-purified  $\alpha$ Nt-GPR17 antibodies and then either unstimulated (C) or stimulated with 100  $\mu$ M UDP-Gluc (A and B). Cells were then washed with glycine buffer to remove labeling from plasma membrane receptors, fixed and double-immunostained with an anti-rabbit IgG conjugated to Cy3 to detect GPR17, and a goat polyclonal antibody against SNX27. Merged images are shown in A, a, B, b and C/c. Note that GPR17 partially co-localizes with SNX27 in vesicles scattered in the cytoplasm (arrows). Scale bars: A, c''=5  $\mu$ m; a''=1  $\mu$ m.

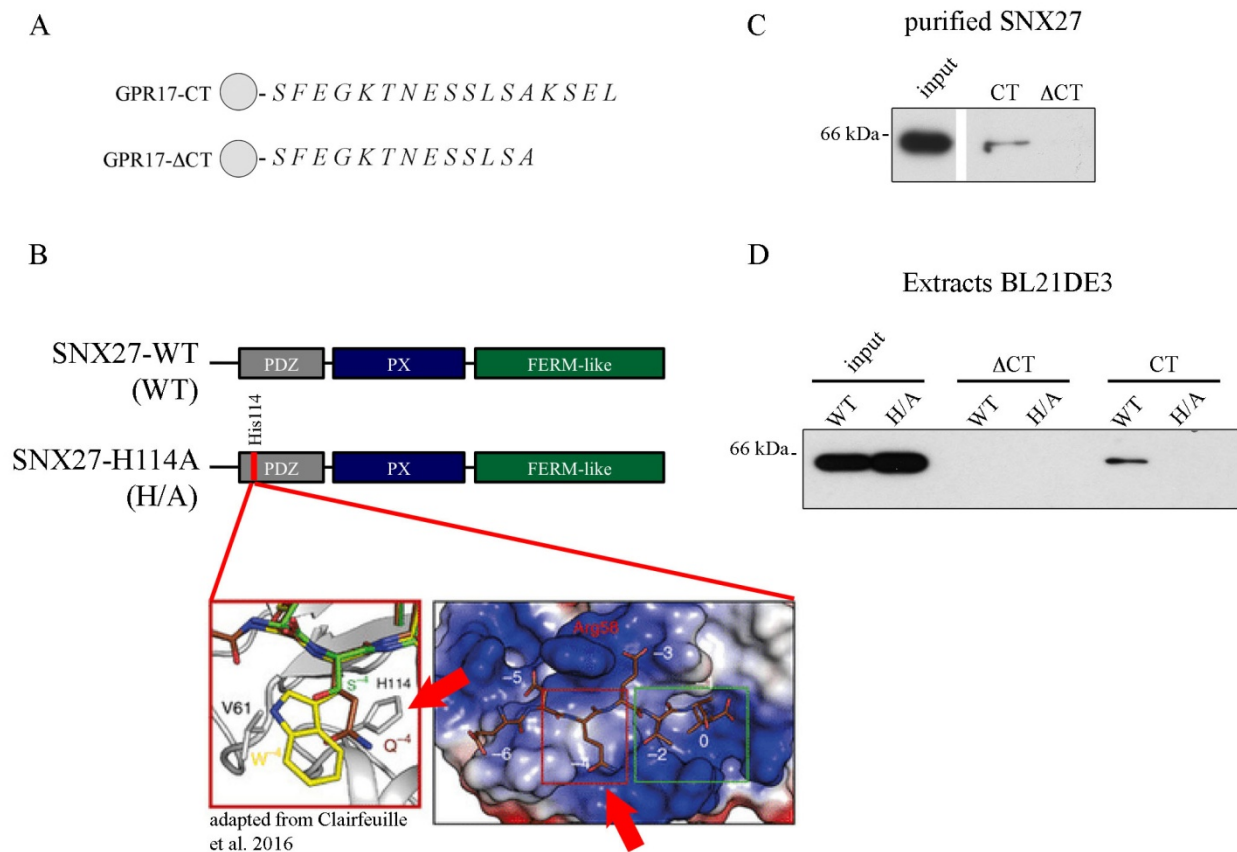


**Figure 5. Interaction *in vitro* of GPR17 PDZ-binding motif and SNX27 PDZ domain.**

**A** Schematic representation of peptides corresponding to the C-terminal tail of GPR17 with (CT) or without ( $\Delta$ CT) the PDZ-binding motif, conjugated to Sepharose 4B resin beads and used in pull-down experiments. **B** Schematic representation of the SNX27-PDZ region and position of the His<sup>114</sup> residue mutagenized to alanine (his-SNX27-H114A or H/A). **C**, **D** CT or  $\Delta$ CT beads (10  $\mu$ L) were incubated with purified his-SNX27 (**C**) or lysates from BL21DE3 (**D**) expressing wild-type his-SNX27 (WT) or his-SNX27-H114A (H/A). Proteins eluted from the Sepharose matrices and aliquots of purified his-SNX27 or bacterial lysates (input) were analyzed by Western blotting. Blots representative of three independent experiments are shown.



## **SNX27 regulates GPR17 recycling and levels of expression**

Given the role of GPR17-PDZ binding motif in receptor recycling and its interaction with SNX27, we asked whether SNX27 has a role in GPR17 recycling to the plasma membrane. To address this issue we used a short-hairpin RNA (shRNA) targeting SNX27 mRNA to silence SNX27 expression and analyze the effects on GPR17 trafficking. In preliminary experiments we tested four constructs expressing GFP as a reporter gene and distinct shRNAs targeting different sequences of SNX27 mRNA. We selected the construct that had the highest efficiency in down-regulating SNX27 (SNX27 was reduced to  $33.36\% \pm 14.44\%$  with respect to shRNA-scrambled transfected control set to 100%; Fig. 7A). For the analysis of GPR17 trafficking, Oli-neu cell line was used as a more physiological model in respect to HEK293 cells. However, on the hypothesis that altered endosomal sorting of GPR17 between recycling and degradation in lysosome would lead to an increased degradation of GPR17 (as observed for other receptors; Lauffer et al., 2010), we co-transfected Oli-neu with FLAG-hGPR17-wt and shRNA-SNX27 or shRNA-scrambled (shRNA-Scr, control). 48hr later live cells were labeled at 4°C using  $\alpha$ FLAG antibody, incubated with UDP-Gluc to promote internalization of labeled receptors and washed with acid glycine. Finally, we allowed endosomal sorting of labeled receptors by re-incubating cells at 37°C in the absence of UDP-Gluc. Cells were fixed during the different steps of the experiment (i.e. labeling, internalization and UDP-Gluc removal) and analyzed by immunofluorescence.  $\alpha$ FLAG antibody was detected using anti-mouse IgG conjugated with Cy3 fluorophore, while we used a polyclonal anti-NG2 antibody to decorate cell membrane. Examination of immunofluorescence micrographs and quantitative analysis of fluorescence intensities were conducted on cells expressing comparable amounts of GFP. Quantitative analysis of GPR17 immunoreactivity revealed that comparable levels of GPR17 were labeled at cell surface (Fig. 6A a-a'' and d-d'') and internalized after UDP-Gluc stimulation (Fig. 6A b-b'', e-e'' and B) in shRNA-SNX27 and shRNA-Scr transfected cells. On the other hand, 15min after UDP-Gluc removal, we saw a redistribution of FLAG-hGPR17-wt staining from intracellular compartments to the plasma membrane in scrambled-transfected control, also confirmed by co-localization with NG2 proteoglycan (Fig. 6A c-c'' arrows, and B). This redistribution (i.e. recycling) was almost completely abolished by SNX27 silencing, leading to increased FLAG-GPR17-wt retention into intracellular compartments (Fig. 6A f-f'', and B). These observations strongly suggested that SNX27 is required for GPR17 recycling to the plasma membrane.

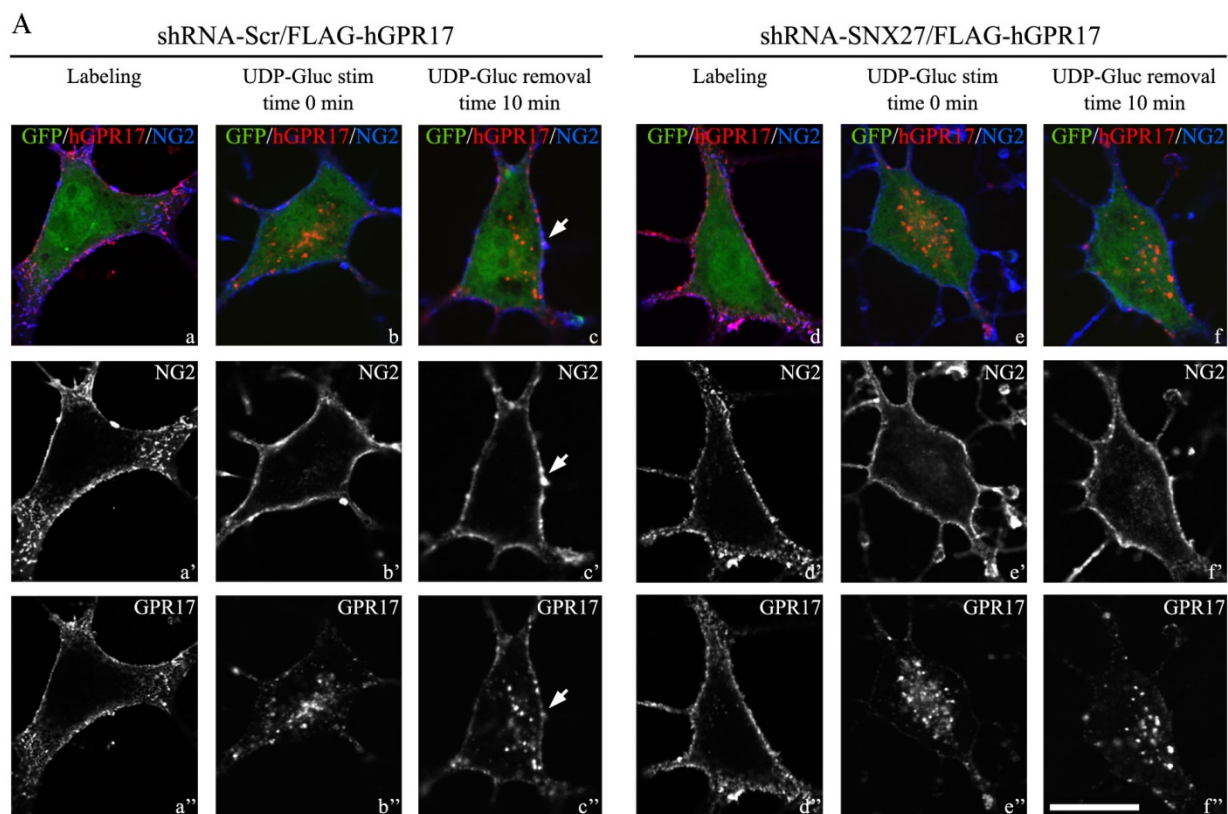
Once internalized in the EE receptors may undergo sorting to different pathways. The LE/lysosome pathway, however, seems to be the dominant destiny of cargos that prolong their stay

in EE because are not transported into other membrane micro-domains committed to different pathways (Gruenberg J., 2001; Hanyaloglu and von Zastrow, 2008). As already described in previous works for  $\beta_2$ AR and glutamate receptors, by inhibiting receptor recycling, SNX27 down-regulation could result in an accumulation of cargos in the EE that ultimately leads to their sorting to lysosomal degradation (Lauffer et al., 2010; Wang et al., 2013). To test this hypothesis also for GPR17 we transfected Oli-neu cells with either shRNA-Scr or shRNA-SNX27 and, 24hr after transfection, differentiate cells using CM. Oli-neu exposure to CM promotes cell exit from proliferating state and entering in the differentiation process. Differentiating Oli-neu express GPR17 in a manner that resembles that of OPCs during differentiation. In particular, GPR17 reaches the peak of expression within 48hr after exposure to CM (refer to “Cell culture” paragraph in Materials and Methods and Meth.Fig. 1). We therefore decided to evaluate GPR17 expression levels at this time point. Thus, after transfection and differentiation, samples were lysed and processed for immunoblotting analysis. Interestingly, we found a reduction of nearly 50% ( $49\% \pm 8.64\%$  with control set to 100%;  $n=3$  independent experiments) in GPR17 amounts in shRNA-SNX27-transfected samples in comparison to shRNA-Scr controls, suggesting that SNX27 silencing affects GPR17 expression stability (Fig. 7A). Notably, no changes were found in proteins known to undergo intracellular trafficking and recycling but that do not express a PDZ-binding motif (cadherins; Le et al., 1999) and also in markers of cellular structures known to be required for intracellular trafficking (i.e. actin cytoskeleton and the GS28 marker of Golgi apparatus) (Fig. 7A).

These observations strengthened the assumption that only recycling pathway was impaired by SNX27 silencing. As a further confirm that GPR17 decrease was, at least partially, due to an increased sorting to lysosome we try to rescue GPR17 levels using ammonium chloride ( $\text{NH}_4\text{Cl}$ ), a known inhibitor of lysosome-associated protease activity. Results indicated that treatment with  $\text{NH}_4\text{Cl}$  determined increased levels of GPR17 in both SNX27-silenced and control samples, but a significantly higher increase was observed in samples down-regulated for SNX27, demonstrating that an higher rate of receptor sorting into the degradative pathway was present (Fig. 7B).

Finally, we tested whether rescue of SNX27 expression caused a recovery of GPR17. To this aim we co-transfected shRNA-SNX27 or scrambled control with the human isoform of SNX27 (hSNX27-Myc). This isoform carries single-nucleotide-polymorphisms (SNPs) in the sequence targeted by shRNA-SNX27 and is shRNA-insensitive (data not shown). Western blot analysis of GPR17 expression confirmed a partial, although significant, recovery of receptor levels with respect to samples co-transfected with shRNA-SNX27 and pcDNA3 vector backbone used as a control (Fig. 7C). Data are expressed as a percentage of shRNA-Scr/pcDNA3 co-transfected samples set to 100%.

Taken together these observations demonstrate that GPR17 recycling is specifically regulated by SNX27, and that this process is required for the maintenance of GPR17 levels of expression.



**B Quantitative Analysis of GPR17 Plasma Membrane Recycling**

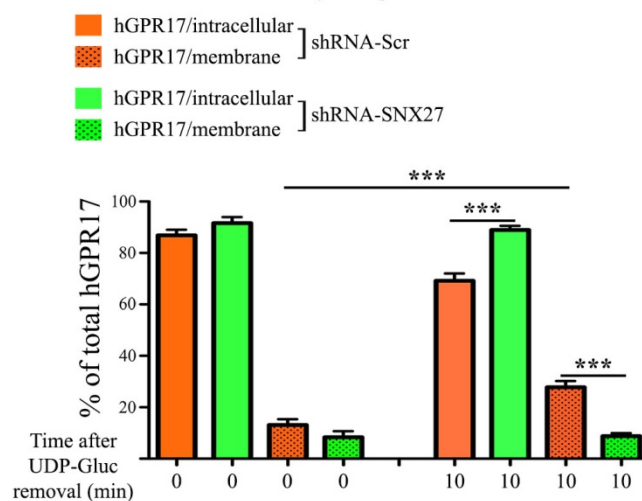


**Figure 6. SNX27 down-regulation inhibits GPR17 recycling**

**A** Oli-neu cells were co-transfected with plasmids encoding FLAG-hGPR17 and shRNA-SNX27 or shRNA-Scr. Cells were fixed i) after labeling at 4°C with the  $\alpha$ FLAG antibody (Labeling, a-a'', d-d''), or ii) after a subsequent incubation with UDP-Gluc followed by glycine washing (UDP-Gluc stim, time 0 min; b-b'', e-e''), or iii) after agonist removal (UDP-Gluc removal, time 10 min; c-c'', f-f''). Cells were then double-immunolabeled with anti-mouse IgG conjugated to Cy3 to detect FLAG-hGPR17, and with an anti-NG2 antibody to decorate plasma membranes.

Immunofluorescence micrographs show that in co-transfected Oli-neu (identified by GFP and FLAG immunolabeling) and expressing a scrambled shRNA, FLAG-hGPR17 is re-exposed to the cell surface (c-c'', arrows). On the contrary in cells silenced for SNX27, FLAG-hGPR17 is not recycled to the plasma membrane (f-f''). Scale bar = 10  $\mu$ m. **B** Cells with similar GFP intensity were acquired and subjected to quantitative analysis. The graphs show the quantification of the intensity of immunoreactivity detected inside the cells and at the cell membrane after UDP-Gluc stimulation (UDP-Gluc stim, time 0) or after stimulation followed by 10min of agonist removal. The data are expressed as the percentage of total immunoreactivity (plasma membrane plus intracellular staining set to 100%) detected after each selected time point and are the mean values  $\pm$  s.e.m. of 25 to 32 transfected cells for each condition from two experiments. \*\*\*P<0,001 two-tailed unpaired Student's t-test.

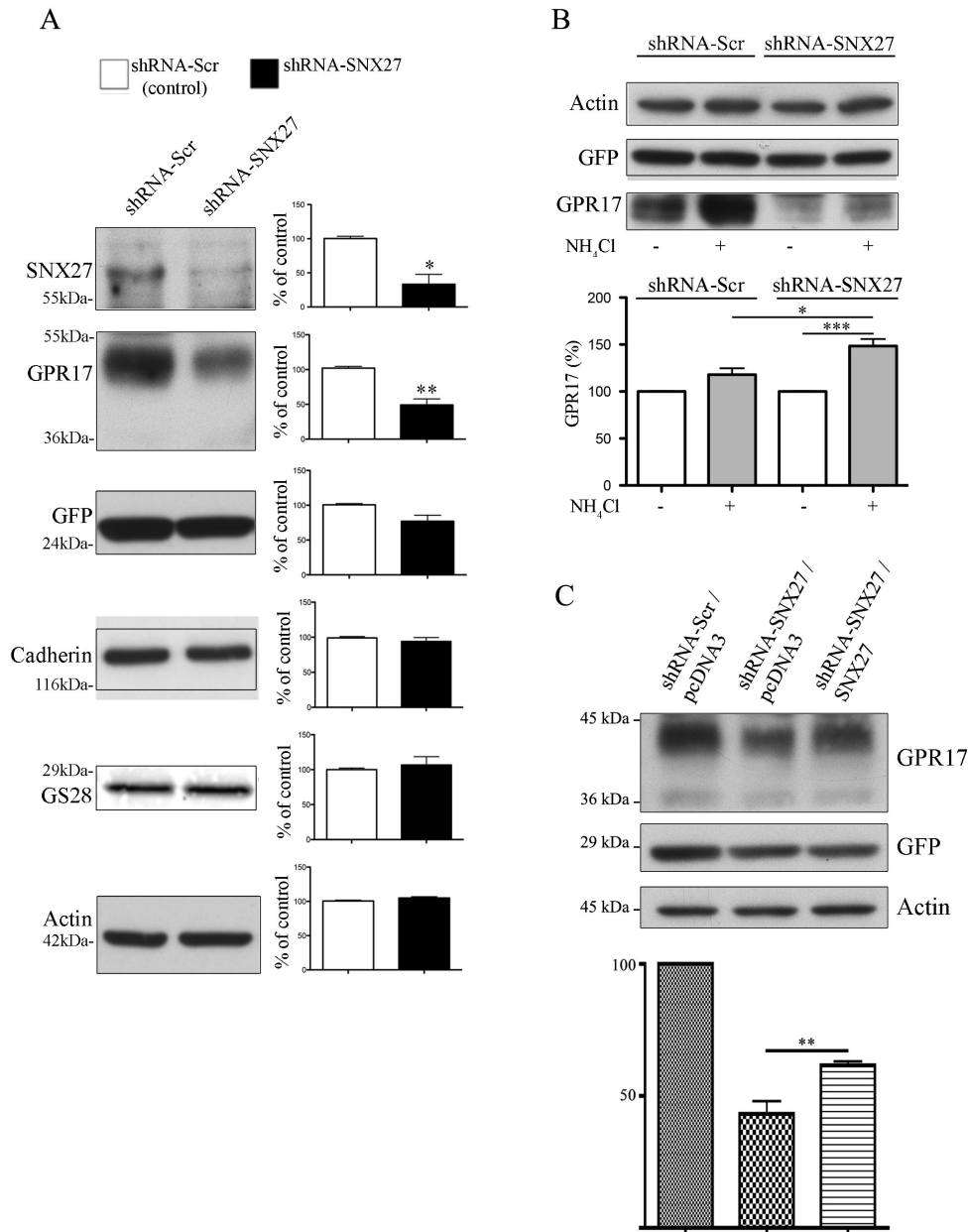


**Figure 7. SNX27 knock-down affects the stability of GPR17.**

**A** SNX27 silencing significantly reduces the levels of GPR17 in Oli-neu cells transfected with shRNA-SNX27 or scrambled shRNA. After transfection followed by incubation in CM to induce differentiation and GPR17 expression, cells were homogenized and protein extracts analyzed by Western blotting. Blots representative of three independent experiments are shown. For quantitative analyses, the signal intensity of the different proteins was standardized to the signal intensity of actin and expressed as a percentage of the amount of protein detected in shRNA-Scr (control, 100%). Mean values  $\pm$  s.e.m. are shown ( $n=3$ ;  $*P=0.011$ ,  $**P=0.0042$  unpaired two-tailed Student's t-test). **B** Oli-neu cells expressing shRNA-Scr or shRNA-SNX27 were pre-incubated for 1hr with cycloheximide (500  $\mu$ M) and then 30min with UDP-Gluc (100  $\mu$ M), followed by 30min of recycling in the presence (+) or absence (-) of NH<sub>4</sub>Cl (20 mM) to block lysosomal degradation.

Samples were analyzed by Western blotting. Mean values  $\pm$  s.e.m., n=3 are indicated; P values were calculated using one-way ANOVA with the Tukey test: \*P<0.05; \*\*\*P<0.001. C Oli-neu cells were transfected either with shRNA-Scr or shRNA-SNX27 and the empty pcDNA3 vector or with shRNA-SNX27 and a plasmid encoding a shRNA-insensitive isoform of SNX27. Cell extracts were analyzed by Western blotting. For quantification we measured the signal intensity of the different proteins and standardized values on the signal intensity of actin. Results are expressed as a percentage of the amount of protein detected in shRNA-Scr/pcDNA3 co-transfected control set to 100%. Mean values  $\pm$  s.e.m. are shown (n=4; \*\*P<0.01, unpaired two-tailed Student's t-test).

## SNX27 is required for the correct kinetics of OL differentiation

Given the important role of GPR17 in OL differentiation (Chen et al., 2009; Fumagalli et al., 2011), and our results describing the role of SNX27 in the recycling of GPR17, we decided to investigate whether SNX27 dysregulation may have some implications on OL differentiation. To address this issue we took advantage of Oli-neu cell model, a well-characterized *in vitro* system for the study of OL differentiation (Fratangeli et al., 2013; Simon et al., 2016). Oli-neu is a cell line derived from murine OPCs immortalized by an activated neu tyrosine kinase (Jung et al., 1995). As previously described (see Materials and Methods) when cultured in Sato medium Oli-neu remain in a proliferating condition and do not undergo differentiation. Under this condition undifferentiated Oli-neu express very low levels of GPR17 and no myelin proteins (Meth.Fig. 1 and Fratangeli et al., 2013). On the other hand, when exposed to CM, Oli-neu begin to differentiate toward a more mature phenotype following the different phases of physiological OL differentiation (Fratangeli et al., 2013). GPR17 is a well-established marker of differentiation transition from committed OPCs (NG2<sup>+</sup> O2<sup>+</sup> O4<sup>+</sup> MBP<sup>-</sup> cells) to pre-myelinating (PLP/DM20<sup>+</sup> MBP<sup>-</sup> cells) OLs (Boda et al., 2011). A similar expression pattern is also observed during Oli-neu differentiation: when exposed to CM, Oli-neu begin to express GPR17 and its expression increases until reaches a peak between 48 and 72 hr of differentiation. At these time points nearly 90% (48hr) or 70% (72hr) of the cells are GPR17-positive (Meth.Fig. 1). As observed in *in vivo* OL differentiation (Boda et al., 2011), GPR17 expression in Oli-neu is then down-regulated in concomitance with cell entrance in the terminal maturation phases and the expression of myelin proteins MAG and MBP. Given the well-established kinetics of Oli-neu differentiation, we compared the differentiation of cells transfected with either shRNA-SNX27 or shRNA-Scr by measuring the levels of GPR17 and myelin proteins. After transfection, cells were exposed to CM and examined after 48hr, a time point when high levels of GPR17 and low MBP/MAG expression are expected. As reported in figure 8, images, acquired by means of a spinning disk confocal microscope, showed that scrambled-transfected control cells (identified by GFP expression) exhibited a branched morphology and expressed high levels of GPR17, while did not co-express MAG and MBP myelin markers. This is in line with a pre-myelinating stage of differentiation, as also previously reported (Fig. 8A a-b''; Fratangeli et al., 2013). On the contrary, GPR17 expression was significantly reduced in shRNA-SNX27-transfected cells, paralleled by a higher expression of both MBP and MAG myelin proteins (Fig. 8A c-d''). Specifically 33.6%±2.57% of GFP-expressing cells were MBP-positive in SNX27-silenced samples while 12%±2.86% MBP-positive cells were counted in control (Fig. 8B). Quantitative analysis of MAG expression by Western blotting of cell extracts also confirmed a 4-fold increase of MAG levels in SNX27-silenced samples with respect to scrambled-treated cells (control) (Fig. 8C). These



data suggest that in differentiating Oli-neu SNX27 knock-down and consequent GPR17 down-regulation (due to lysosomal degradation) correlate with a precocious entering of pre-myelinating OLs in the myelinating phase.

To translate these results in a more physiological model, we repeated this analysis in primary cultures of OPCs. Western blot analysis of differentiated OPC extracts confirmed a significant reduction of GPR17 expression ( $69.77 \pm 8.39$ ) in samples knocked down for SNX27 compared to controls (Fig. 8D). This was accompanied by an increased trend in the number of MAG-expressing cells that we found in shRNA-SNX27-transfected samples in respect to scrambled control, as revealed by confocal microscopy (Fig. 8D), suggesting a precocious expression of myelin markers, in accordance with what observed for Oli-neu cell line.

Overall, these observations indicate that loss of SNX27 results in GPR17 down-regulation and concomitant accelerated OL maturation in Oli-neu and differentiating OPCs.

We further investigated the effects of SNX27 knock-down on OL development by analyzing the activation of pathways associated to OL differentiation and GPR17 signaling. In particular, the levels of GRK2, of mTOR (mammalian Target of Rapamycin) and its activated form phospho-mTOR (Tyler et al., 2011), and the nuclear/cytosolic localization of Id2 TF (Chen et al., 2009) were analyzed in either shRNA-SNX27 or shRNA-Scr transfected Oli-neu. mTOR/GRK2 pathway was shown to control both GPR17 endocytosis and downstream signaling (Tyler et al. 2011; Daniele et al., 2014; Fumagalli et al., 2015) while Id2 is a known inhibitor of OL maturation, which was also suggested to mediate GPR17 effects (Chen et al., 2009). Our analysis revealed no significant alterations in mTOR pathway activation or GRK2 expression between shRNA-SNX27-transfected and control samples (Fig. 9A). However, we observed a redistribution of Id2 TF from the nucleus to the cytosol in SNX27-silenced cells ( $23.48\% \pm 5.53\%$  nuclear;  $76.93\% \pm 5.94\%$  cytosolic) compared to shRNA-Scr-transfected controls ( $44.77\% \pm 0.70\%$  nuclear;  $55.23\% \pm 0.71\%$  cytosolic;  $n=2$  independent experiments) (Fig. 9B). These results further sustain the hypothesis that down-regulation of GPR17 signaling pathway is at least one of the mechanisms responsible of accelerated OL differentiation kinetics observed upon SNX27 knock-down and suggest that Id2 nucleus to cytosol translocation may act as a downstream signal that allows OPC differentiation.

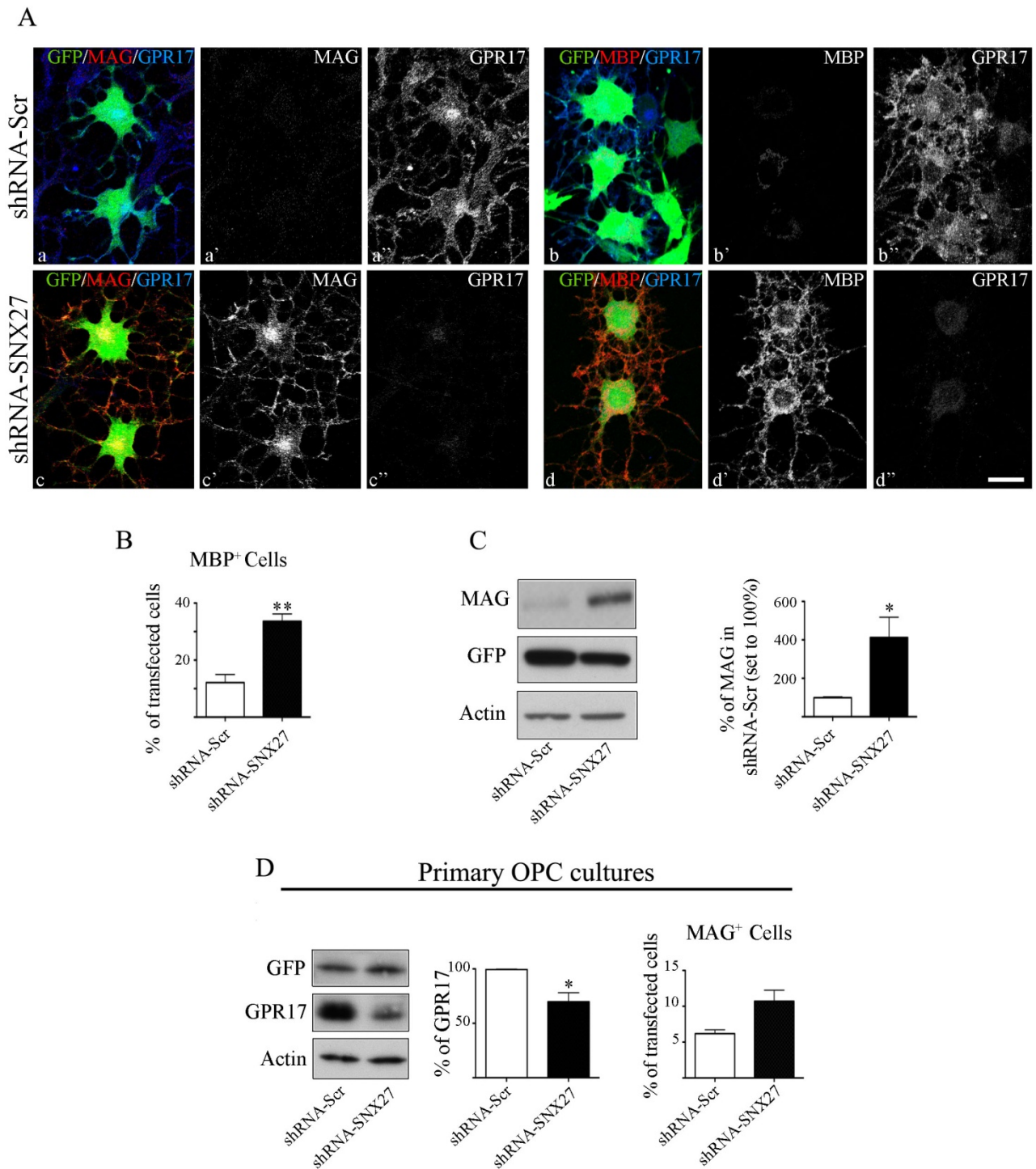


**Figure 8. SNX27 silencing accelerates OL differentiation.**

**A** Representative immunofluorescence micrographs showing elevated MAG and MBP expression concomitantly with GPR17 down-regulation in SNX27-silenced Oli-neu (shRNA-SNX27) compared to control cells (shRNA-Scr). **B** Quantitative analysis of immunolabeled cells demonstrated that the percentage of MBP-positive cells was significantly higher in shRNA-SNX27-

transfected Oli-neu compared with shRNA-Scr-transfected cells. Mean values  $\pm$  s.e.m., n=505 cells transfected with shRNA-Scr and 523 cells transfected with shRNA-SNX27 were examined. \*\*P=0.005, two-tailed unpaired Student's t-test. **C** Western blotting analysis using anti-MAG antibody of cell lysates (30  $\mu$ g of proteins) of Oli-neu transfected with shRNA-Scr or shRNA-SNX27 and the respective quantitative analysis (graph; mean values  $\pm$  s.e.m. n=3, \*P=0.042 two-tailed unpaired Student's t-test). **D** SNX27 knock-down accelerates down-regulation of GPR17 and differentiation of OPCs. Primary mouse OPCs were transfected with shRNA-Scr or shRNA-SNX27, induced to differentiate, and analyzed either by Western blotting or immunofluorescence. Quantitative analysis of Western blots revealed a significant decrease of GPR17 in cultures after SNX27 silencing (mean values  $\pm$  s.e.m., n=3, \*P=0.012 two-tailed unpaired Student's t-test), whereas an increased number of MAG-expressing cells was detected in OPC cultures transfected with shRNA-SNX27. Mean values  $\pm$  s.e.m., n=1170 cells transfected with shRNA-Scr and 1226 cells transfected with shRNA-SNX27. \*P =0.050, two-tailed unpaired Student's t-test.

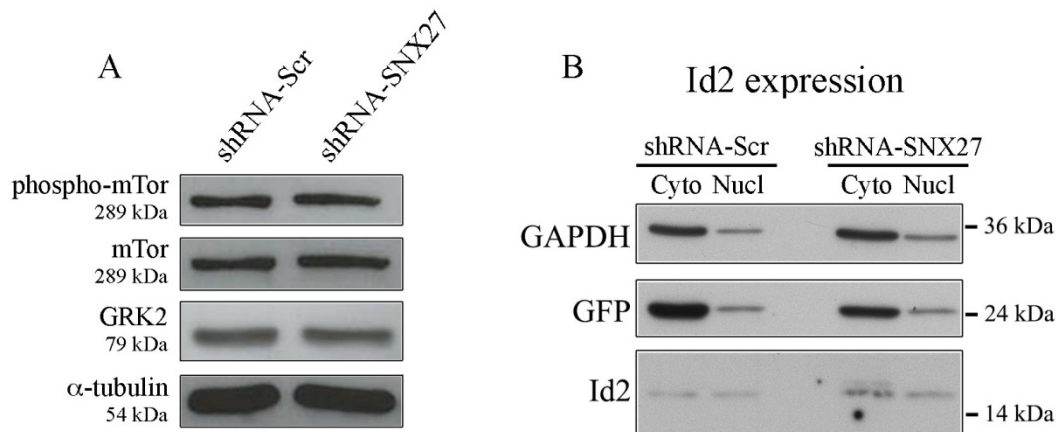


**Figure 9. SNX27 silencing modifies the nuclear/cytoplasmic distribution of Id2 but does not affect the mTOR and GRK2 levels.**

**A** Equal amounts of cell extracts (30  $\mu$ g) from Oli-neu cells transfected with either shRNA-Scr or with shRNA-SNX27 were analyzed by Western blotting. No changes were detected in GRK2 expression, and in the phosphorylation/activation of mTOR at Ser2448. One representative experiment is shown. **B** Cytoplasmic (Cyto) and nuclear (Nucl) fractions were prepared from transfected Oli-neu cells. Equal amounts of proteins were subjected to Western blotting analysis with antibodies against GAPDH, GFP and Id2.

## **Altered OL differentiation and myelin defects in Ts65Dn mouse model of DS correlate with a decrease of SNX27 levels**

Recent studies in human DS brains and Ts65Dn mouse brains (the most used murine model of DS; Reeves et al., 1995) have demonstrated that trisomy-linked overexpression of mir-155 and consequent down-regulation of C/EBP $\beta$ , a TF required for the expression of SNX27, result in reduced levels of SNX27 (Wang et al., 2013). SNX27 deficiency was shown to alter synaptic transport of AMPA and NMDA receptors which finally contributes to the cognitive impairment observed in DS patients (Wang et al., 2013). Based on these observations we thought to be interesting to analyze GPR17 expression and OL differentiation in DS using the Ts65Dn model. Firstly, we confirmed literature data and found SNX27 deficit in Ts65Dn hippocampal extracts compared to euploid controls (Fig. 10A). Moreover, by means of qRT-PCR and Western blot analysis, respectively, we showed mir-155 overexpression and defective levels of SNX27 in primary cultures of fibroblasts derived from post-mortem trisomic human embryos compared to euploid controls (Fig. 10B and C). This suggests an inter-species and inter-tissue conservation of the mir-155/ C/EPB $\beta$  / SNX27 regulatory pathway described in Ts65Dn by Wang and colleagues (Wang et al., 2013). In collaboration with the laboratories of Prof. R. Bartsaghi (University of Bologna) and Prof. S. Ceruti (Università degli Studi di Milano), we then analyzed GPR17 expression and OL development by immunolabeling of coronal sections of brain hemispheres from 45-days-old Ts65Dn and euploid mice. Firstly, the total number of oligodendrocytes was examined by immunostaining of OLIG2 TF, which is broadly expressed in oligodendroglial lineage and is one of the trisomic genes (Mitew et al., 2014). In all the areas analyzed (i.e. hippocampus, dorsal prefrontal cortex and thalamus) Ts65Dn mice expressed a higher number OLIG2-positive cells, indicating an overall increase of oligodendroglial cells (data not shown). Remarkably, despite a global increase in OLs, the number of GPR17-positive cells was significantly reduced in Ts65Dn brain, both in the whole hemisphere and in the thalamus and cortex, with a trend also in the hippocampus (Fig. 11A and B).

To continue our analysis we evaluated the levels of markers of more advanced stages of differentiation. As a first step we stained brain sections with anti-CC1 antibody which is known to decorate mature OLs (Luo et al., 2014; Sachs et al., 2014). Analysis of immunolabeled sections showed a significant increase of CC1-positive OLs in trisomic brains, in the whole hemisphere as well as in the different examined areas (thalamus, dorsal prefrontal cortex, hippocampus, Fig. 11C and D). This result, together with the previously data on GPR17, demonstrates that, although the whole population of OLs is increased in trisomic brains, there is an alteration of OL development. Moreover, the analysis of OL differentiation in Ts65Dn brains suggested that an accelerated

maturation of OLs correlates with a decreased expression of GPR17 in brains characterized by low levels of SNX27.

Despite these data, hypomyelination has been reported in human DS brains (Abraham et al., 2012). Based on this observation we decided to evaluate the expression of MBP (a myelin protein expressed in more mature OLs than CC1 antigen; Boda et al., 2011; Zhang et al., 2014) in Ts65Dn brains. Remarkably, immunochemical staining of brain coronal sections followed by densitometric analysis revealed a significant decrease of MBP immunoreactivity, that involved both the white (corpus callosum; Fig. 12) and the grey matter (cortex and nucleus striatum; Fig. 13A-F). The result was also confirmed by Western blotting analysis of hippocampal extracts for both the two major isoforms of MBP protein (45% and 55% reduction of the 14kDa and 18.5/17kDa isoforms, respectively; Fig. 13G).

In conclusion our analyses showed that in Ts65Dn brain alterations in OL development lead to a final impairment of myelin formation. Deeper analyses are required to establish whether cell-autonomous or non-cell-autonomous mechanisms (or a contribution of both) are responsible for the myelination deficits observed in DS and Ts65Dn brains. In addition, it would be also important to understand whether OL maturation in DS brains begins with a sustained shift towards proliferation followed by a partial maturation (as OLIG2 and CC1 increases suggest) and whether (and which) other pathways may intervene to determine the final myelin impairment at later stages.

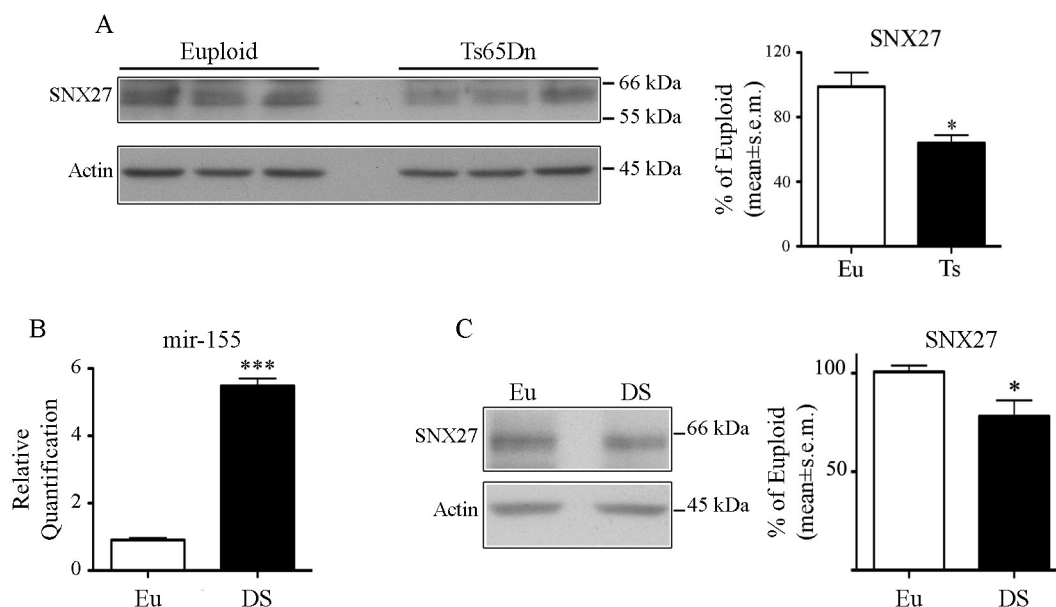


**Figure 10. Levels of SNX27 are decreased in Ts65Dn mouse brains and human trisomic fibroblasts.**

**A** Left, Western blot analysis of SNX27 and actin expression in brain protein lysates of 3 animals per genotype (i.e., euploid and Ts65Dn). Right, quantitative analysis of SNX27 signal intensity normalized to actin and expressed as percentage of euploid brain (Eu: euploid; Ts: Ts65Dn). Mean values  $\pm$  s.e.m. are shown;  $n=3$  mice for each genotype;  $*P<0.05$ , unpaired two-tailed Student's t-test. **B, C** Analysis of mir-155 and SNX27 expression in human euploid (Eu) and trisomic (DS) fibroblasts. **B** Total RNA extracts were prepared from primary cultures of either DS fibroblasts and euploid controls. Mir-155 expression was analyzed by qRT-PCR. Samples were analyzed in triplicates. The  $2^{-\Delta C_t}$  values obtained from euploid (Eu) or trisomic (DS) fibroblast were normalized on the amount of RNA spike-ins and are expressed as fold of increase over euploid (mean values  $\pm$  s.e.m.,  $***P<0.0001$ ). **C** Blots of SNX27 and actin immunostaining (left) and quantitative analysis (right) of SNX27 signal intensity normalized to actin and expressed as percentage of euploid. Mean values of three independent analysis  $\pm$  s.e.m. are shown,  $*P<0.05$ , unpaired two-tailed Student's t-test.

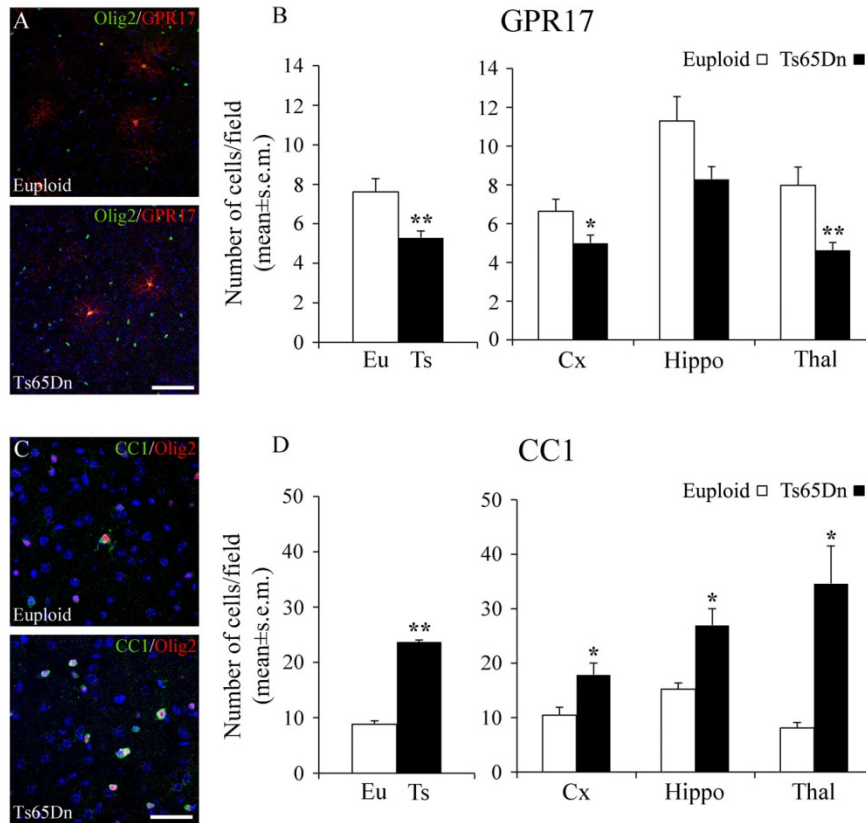


**Figure 11. Reduced expression of GPR17 correlates with increased expression of a marker of mature OLs in the brains of Ts65Dn mice.**

**A, C** Immunohistochemical analysis of GPR17 or CC1 in OLs (identified by co-localization with OLIG2) of brain slices from euploid and Ts65Dn mice. Scale bars = 100  $\mu$ m. **B, D** Quantification of the number of GPR17-positive cells (B) and CC1-positive cells (D) in the whole brain hemisphere (left panels) and in selected brain areas (right panels). The number of cells was normalized to the total number of counted optical fields/condition. Results are the mean  $\pm$  s.e.m., n=10 slices for GPR17 and 4 slices for CC1, from 4 animals each of euploid (Eu) and Ts65Dn (Ts) mice in the case of GPR17. \*P<0.05 and \*\*P<0.01, unpaired two-tailed Student's t-test.



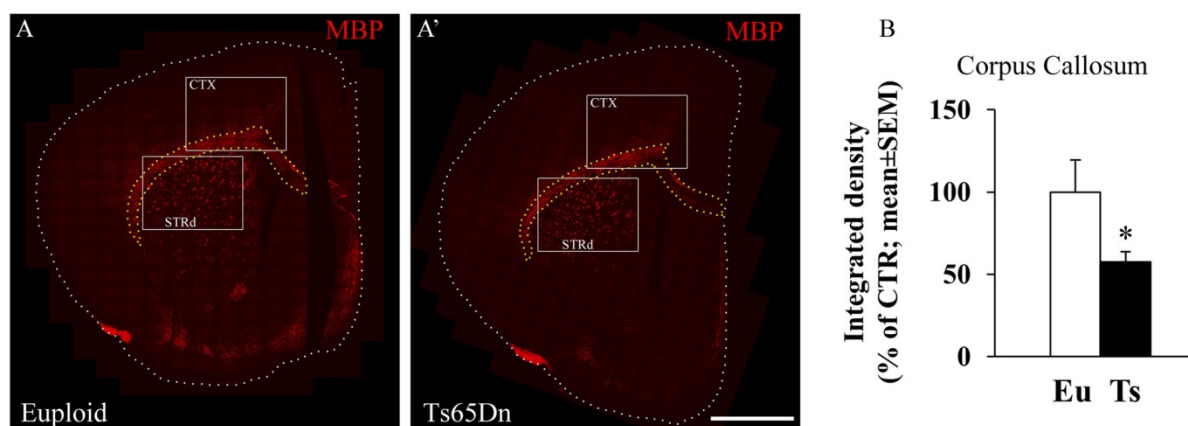


**Figure 12. Decreased expression of MBP in the corpus callosum of Ts65Dn mice.**

**A, A'** Composite images of brain slices from euploid (A) and Ts65Dn (A') mice immunostained for MBP and collected using an Axiovert 200 (Zeiss) confocal system equipped with a spinning disk. We exploited the stitch option of the Volocity acquisition setup and a motorized xy-stage (see Materials and Methods for details). The dotted white lines delimit the brain hemispheres. MBP immunoreactivity has been evaluated in the corpus callosum (i.e., the area between yellow dotted lines) by densitometric analysis with the ImageJ program. The white frames delimit the areas of cortex (CTX) and dorsal striatum (STRd) selected for further quantification (see Fig. 13). Scale bar = 1 mm. **C** Histogram shows MBP expression in the corpus callosum of euploid (Eu) and Ts65Dn (Ts) brains expressed as percentage  $\pm$  s.e.m. of euploid set to 100%. 4 brain slices from 3 mice for each genotype have been analyzed. \* $P < 0.05$ , unpaired two-tailed Student's t-test.

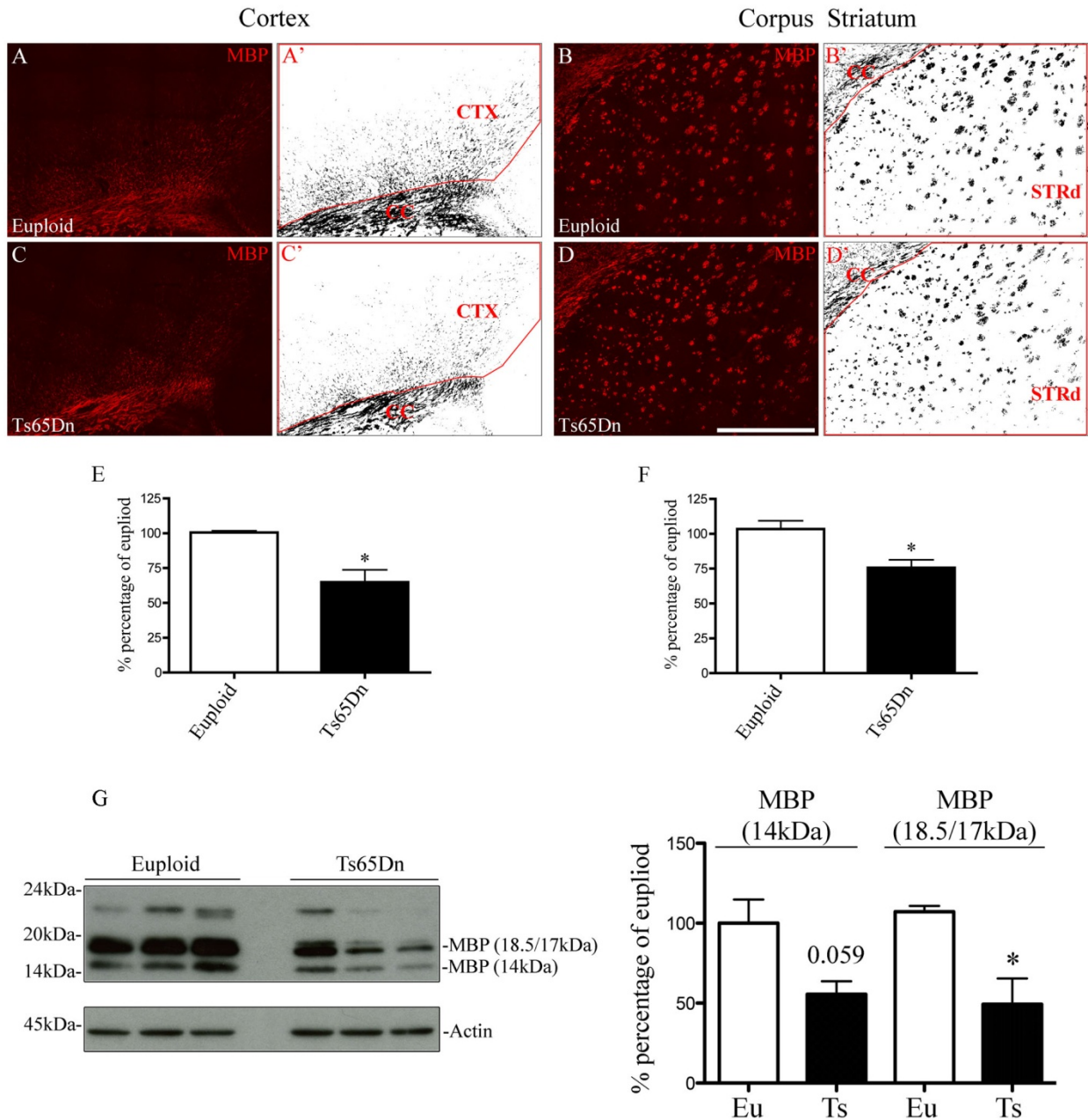


**Figure 13. Decreased myelination in the cortex, dorsal striatum and hippocampus of Ts65Dn mice.**

**A-D'** MBP expression was examined in regions of cortex (A, C) and dorsal striatum (B, D) (refer also to Fig. 12). The selected areas were converted in binary format (A', B', C', D') and the regions between the red lines were analyzed using ImageJ program. Six brain slices from three animals for each genotype were used and equal areas for cortex (CTX; euploid = 4.95mm<sup>2</sup>; Ts65Dn = 5.07mm<sup>2</sup>) or dorsal striatum (STRd; euploid = 5.90mm<sup>2</sup>; Ts65Dn = 5.90mm<sup>2</sup>) were examined. Scale bar = 450  $\mu$ m. **E, F** Histograms show the mean intensity  $\pm$  s.e.m. of MBP expression as

percentage of euploid,  $n=6$ ;  $*P<0.05$ , unpaired two-tailed Student's t-test. **G** Western blotting analysis of MBP expression in the hippocampus. Left, hippocampal lysates from three animals for each genotype were analyzed by Western blotting. Right, histograms showing the quantification of the two major isoforms of MBP (polypeptides of 14kDa and 18.5/17kDa). Results are expressed as the percentage  $\pm$  s.e.m. of euploid set to 100%;  $n=3$ ,  $*P<0.05$ , unpaired two-tailed Student's t-test.

## **mir-155 overexpression inhibits Oli-neu differentiation**

To extend our analysis and begin to understand the mechanisms that underlie myelination impairment in DS, we decided to investigate the role of mir-155 in OLs. Analysis of online database revealed that it may targets a number of different genes expressed in oligodendroglial cells. As a first step, we analyzed mir-155 expression in undifferentiated and 48hr-differentiated Oli-neu by qRT-PCR. Our results demonstrated that mir-155 is expressed in oligodendroglial cells, though at very low levels (Fig 14A). This observation is consistent with previous data showing mir-155 expression in human OPCs (Leong et al., 2014). Based on this result showing low levels of mir-155 in OLs, we speculated that was more informative to mimic the pathological conditions reported in DS patients, and thus we investigated the effect of mir-155 overexpression on Oli-neu differentiation. To this aim, we used a construct generated by O'Connel and colleagues that contains a mir-155 expressing cassette downstream of a GFP stop codon to allow concomitant expression of mir-155 and GFP, used as transfection reported gene (from here on referred to as pMGP155; O'Connel et al., 2009). The vector backbone was used as a control (pMGP). Oli-neu cells were transiently transfected with either pMGP or pMGP155 and induced to differentiate by exposure to CM. Samples were then processed for immunofluorescence or Western blot analyses. Confocal microscopy analysis, showed that mir-155 overexpressing cells (recognized by GFP expression) exhibited an altered cell morphology, with a less-branched shape and fewer thinner extensions compared to untransfected or pMGP-transfected controls (Fig. 14C). These morphological changes were accompanied by reduced levels of GPR17 (Fig. 14C) that did not correlate with increased expression of myelin proteins. On the contrary, expression of neither MAG nor MBP were observed in pMGP155-transfected cells (Fig. 14C and data not shown for MAG). Western blot analysis of 48 and 72 hr -differentiated cell extracts confirmed GPR17 and MAG down-regulation upon mir-155 overexpression (Fig. 14B), although in the specific case of GPR17, less pronounced difference was observed at 72hr of differentiation (Fig. 14B), when GPR17 constitutive expression is expected to diminish (Fratangeli et al., 2013). These results, though preliminary, suggest that mir-155 overexpression inhibits Oli-neu differentiation, with cells maintained in an immature state that may precede GPR17 expression. This effect is different from that observed for SNX27 down-regulation. Accordingly, we did not find a reduction of SNX27 levels in mir-155 overexpressing samples compared to pMGP controls analyzed by Western blotting (Fig. 14B).

These data suggest that other, and yet to be determined, mir-155 target genes (beside C/EBP $\beta$ ) may be involved in determining the impaired OL differentiation observed in DS brains.

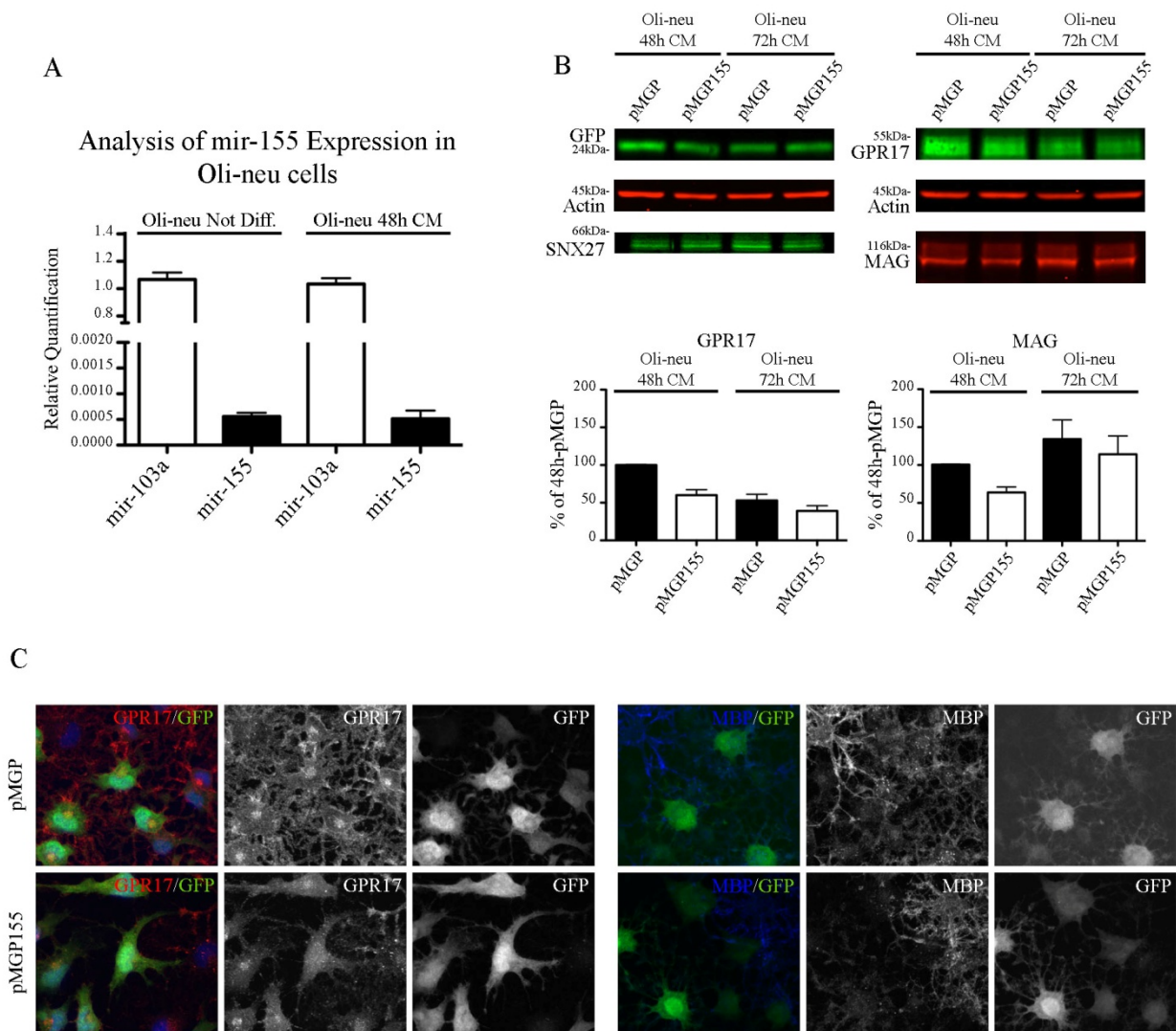


**Figure 14. Overexpression of mir-155 in Oli-neu induces down-regulation of GPR17 and myelin proteins in the early phases of differentiation.**

**A** mir-155 expression in undifferentiated and 48hr-differentiated Oli-neu was analyzed by qRT-PCR. Total RNA extracts were prepared from Oli-neu cultured for 48hr in either Sato medium or in CM. Samples were then analyzed in triplicates. Values obtained by qRT-PCR amplification were expressed as  $2^{-\Delta Ct}$  using microRNA-103a (mir-103a) housekeeping microRNA for normalization. Results are expressed relative to mir-103a and are the mean values  $\pm$  s.e.m.. **B**, **C** Oli-neu cultures were transfected with control-empty plasmid (pMGB) or a plasmid coding for mir-155 (pMGP155) and cultured for 48hr or 72hr in CM. **B** Cell extracts were analyzed by Western blotting for GFP, GPR17, SNX27 and MAG expression. Blots representative of two independent experiments are shown. For quantitative analyses, the signal intensity of GPR17 and MAG was standardized to the intensity of actin and expressed as a percentage of the amounts of proteins detected in the 48hr pMGB-transfected samples (control). Mean values  $\pm$  s.e.m. are shown. **C** pMGP or pMGP155 transfected Oli-neu cells, cultured in CM, were fixed after 48hr and double-immunostained for GPR17 and MBP. Transfected cells are identified by GFP expression.

## DISCUSSION

To shed light on the mechanisms underlying GPR17 expression and function in OL maturation, we have recently analyzed receptor endocytic trafficking based on observations that receptor levels at the plasma membrane and, consequently, receptor signaling, are determined by the balance between receptor *de novo* synthesis and endocytosis (Hanyaloglu and von Zastrow, 2008). In previous works we described that GPR17 undergoes either constitutively or agonist (UDP-Gluc and LTD<sub>4</sub>) -induced endocytosis. We demonstrated that GPR17 is internalized via clathrin-mediated endocytosis and subsequently sorted at the level of EE between two opposite destinies: while a portion enters the lysosomal pathway for degradation, a smaller amount is recycled to the plasma membrane via the Rab4-dependent recycling pathway (Fratangeli et al., 2013). In this study, we deepen our analysis and demonstrate that GPR17 C-terminal PDZ-binding motif is required for receptor recycling via interaction with SNX27. This interaction mediates GPR17 recruitment into recycling tubules by the so called “SNX27-retromer complex” (Temkin et al., 2011; Gallon and Cullen, 2015). In addition, we report strong evidences that loss of SNX27 unbalances GPR17 endosomal sorting leading to an increased receptor degradation and precocious down-regulation, with consequences for OL differentiation.

GPR17 is expressed by a specific sub-population of differentiating OPCs with a kinetics that is finely regulated during differentiation (Boda et al., 2011 and 2015). Its expression begins when OPCs exit mitosis and become cells committed to differentiation, and is sustained until OL pre-myelinating stages. However, GPR17 down-regulation is fundamental to complete cell maturation (Chen et al., 2009). Such expression kinetics is in agreement with the proposed role of GPR17 as an intrinsic timer of OL differentiation. GPR17 expression maintains differentiating OPCs in an immature state until external/intrinsic signal(s) induces cells to form myelin (Chen et al., 2009). This function is in line with observations that OL development is a highly regulated process, temporally and spatially restricted, which needs to act in concert with CNS development (Mitew et al., 2014 and refs therein). Given these evidences, we here propose that a GPR17 increased degradation may be at least one of the mechanisms that underlie accelerated OL differentiation observed after SNX27-silencing.

Our results may have some implications for pathologies where OL degeneration or altered metabolism/development is observed (i.e. demyelinating diseases and neurological disorders; Fields, 2008). In this regard, it is important to note that abnormally up-regulated amounts of GPR17 are observed *in vivo* in various models of neurodegenerative diseases characterized by myelin loss (Fumagalli et al., 2015 and refs therein). A condition that is thought to make diseases significantly worse by contributing to block OPC *de novo* differentiation and myelin repair (Hennen et al., 2013).

Furthermore, GPR17 was proposed to orchestrate CNS response to injuries by acting on differential cell types during tissue damage development and repair (Lecca et al., 2008). In addition, Viganò and colleagues suggested that in the adult brain GPR17 contributes to the maintenance of a reserve pool of committed but still undifferentiated OL precursors which is activated in response to brain injuries (Viganò et al., 2015). Given these observations and the extreme need for new therapeutic approaches for the treatment of demyelinating and ischemic/traumatic diseases of the CNS, there is now great interest in GPR17 as a pharmacological target and many efforts are made to establish the mechanisms controlling its expression (Hennen et al., 2013; Fumagalli et al., 2015). In this context, our data suggest that the targeting of GPR17-endosomal sorting is as a potential new therapeutic strategy. The pharmacological targeting of endosomal transport has been already used for the treatment of infections by parasites such as *Plasmodium* and consequent Malaria disease (van Weert et al., 2000). A second example is the therapeutic use of the Wnt effector Dishevelled to disrupt PDZ domain interactions and, consequently, Wnt signaling. An approach that was proposed for the treatment of prostate cancer (Grandy et al., 2009). In addition, recent evidences reporting the role of endosomal transport alterations in neurodegenerative disfunctions, have promoted the development of new biotechnological approaches (Gallon and Cullen, 2015).

Finally, our findings also extend knowledge on SNX27 physiological roles, showing for the first time that SNX27 is expressed in oligodendroglial lineage, and that has a crucial role in OL differentiation.

## **SNX27 interacts with the PDZ-binding motif of GPR17 and is required for receptor recycling to the plasma membrane**

We here bring many evidences sustaining the hypothesis that GPR17 C-terminal PDZ-binding motif is required for receptor sorting into the recycling pathway. First of all, our detailed analysis of receptor endocytic trafficking revealed that GPR17 PDZ-binding motif integrity is necessary for receptor recycling. Upon transient transfection, equal amounts of wild type and mutant receptors were labeled at the cell surface and were internalized due to agonist stimulation, thus excluding alterations of biosynthesis and biosynthetic transport and clathrin mediated internalization. On the contrary, we found GPR17 mutants trapped in EE (Fratangeli et al., 2013) 10min after agonist removal, thus suggesting that receptor endocytic traffic was compromised. By means of a Flag-tagged construct and  $\alpha$ FLAG antibody we were able to follow GPR17-wt recycling to plasma membrane in live cells, a process disrupted by mutation of PDZ-binding motif. Quantitative analysis of wild type or mutant GPR17 demonstrated that PDZ-binding motif disruption determined an increase of approximately 30% of receptor retained in intracellular

compartments, in line with our previous data showing that after endocytosis ~30% of internalized GPR17 is recycled to the plasma membrane (Fratangeli et al., 2013).

Based on these observations, we looked for candidate partners for GPR17 among PDZ proteins described to regulate receptor recycling. Our studies demonstrate that SNX27 is directly involved in GPR17 recruitment into recycling endosomes. SNX27 is known to bind type I PDZ-binding motifs (Rincon et al., 2007; Gallon et al., 2014). Accordingly, GPR17 C-terminal region directly interacts with the PDZ domain of SNX27. Two evidences support this conclusion: i) purified SNX27 (and not only SNX27 present in Oli-neu total protein extracts) is specifically isolated by the peptide containing the GPR17 PDZ-binding motif; and ii) no interaction was observed when a single histidine residue (H<sup>114</sup>) in the SNX27 PDZ binding groove was mutagenized, demonstrating that the PDZ domain of SNX27 is directly involved in mediating GPR17 PDZ ligand binding.

We next contextualized the interaction in a physiological setting by showing that GPR17 encounters SNX27 during its endocytic transport in the endosomal compartments of Oli-neu and primary OLs. This occurs when GPR17 internalization is promoted by UDP-Gluc treatment as well as in the absence of agonist stimulation, consistent with our findings that GPR17 may undergo also constitutive endocytosis (Fratangeli et al., 2013). SNX27 is a cytosolic protein that is recruited to endosomal membranes since expresses a PX domain, which determines its affinity for PI3P-enriched endosomal membranes (Rincon et al., 2007). In these organelles SNX27 is specifically localized into Rab4-positive domains due to its interaction with the retromer/WASH complexes (McGough et al., 2014; Lee et al., 2016). Consistently, GPR17 was also shown to traffic through Rab4-positive compartments (Fratangeli et al., 2013).

Loss of SNX27 affects GPR17 recycling, leading to retention of receptor into endosomal compartments. Accordingly with data showing that prolonged retention in the EE favors protein cargo delivery to degradative compartments (note that EE undergo a constant process of remodeling and maturation, Scott et al., 2014), we demonstrated that the levels of endogenous GPR17 are significantly reduced in Oli-neu after SNX27 silencing. Remarkably, shRNA-SNX27 transfection does not alter the expression of either proteins involved in the correct functioning of intracellular trafficking (actin) or proteins that do not depend on SNX27 for their recycling (cadherins), thus showing that shRNA-SNX27 specifically targets SNX27. Our data also prove that GPR17 undergoes to partial lysosomal degradation in SNX27-silenced Oli-neu. However, on the basis of the partial recovery of GPR17 expression upon lysosomal inhibition we speculate that GPR17 enters other degradative pathways, for example proteasomes. In this context, it is interesting to note



that Wang and colleagues, showed that AMPA and NMDA receptor degradation after SNX27 silencing is rescued by both lysosomal and proteasomal inhibitors (Wang et al, 2013).

Finally, we can also conclude that SNX27 is indeed responsible of correct GPR17 recycling, since receptor levels are partially rescued when SNX27-silenced Oli-neu (mouse) are co-transfected with a shRNA-insensitive SNX27 isoform (human-SNX27). The partial recovery of GPR17 levels may be due i) either to a different affinity of human-SNX27 for murine GPR17 ii) or to interference of SNX27-overexpression with endocytic homeostasis, as already described by other groups (Lauffer et al, 2010; Munoz and Slesinger, 2014).

In conclusion we have demonstrated that after endocytosis GPR17 can be recycled at the cell surface via interaction with SNX27-retromer complex. Inhibition of the pathway determines the premature down-regulation of the receptor.

## **Loss of SNX27 accelerates OL differentiation kinetics**

SNX27 down-regulation results in an accelerated maturation of differentiating OLs, an effect that we propose to be mediated, at least in part, by GPR17 precocious down-regulation.

OL differentiation, altered by SNX27/GPR17 down-regulation, seems to concern mainly the kinetics of the process. The synthesis of myelin proteins, at least in OL cultures, is not altered but only early, and OLs do not exhibit apparent defects in maturation. In addition, SNX27 silencing *per se* is not sufficient to trigger proliferating OPCs (i.e. Oli-neu cultured in Sato medium) towards a pro-differentiating condition (data not shown), meaning that a different stimulus is required to initiate differentiation process and/or that SNX27 exerts its effects by acting on target proteins that are expressed during OL differentiation but absent in immature OPCs. Our data are consistent i) with the role of GPR17 as “intrinsic timer” of OL maturation (Chen et al., 2009) and ii) with the kinetics of GPR17-expression in OL development (Boda et al., 2011; Fratangeli et al., 2013). Remarkably, GPR17 decrease after SNX27-silencing is accompanied by increased translocation of Id2 from nucleus to cytosol, in line with results by Chen and colleagues, who proposed Id2 as one of the effectors acting downstream of GPR17 activation (Chen et al., 2009). Id2 is a known inhibitor of OL differentiation that accumulates in the nucleus and sequesters OLIG2 TF, thus hampering pre-myelinating cells to express MAG and MBP myelin proteins (Chen et al., 2009).

Despite the data suggesting that SNX27 alters OL development by regulating GPR17 recycling, we cannot exclude that other molecules may be involved. SNX27 has been described in HeLa cells to regulate the trafficking of approximately hundred different cargos and is considered a general hub regulating the recruitment of cargos that express a type I PDZ-binding motif and that

requires retromer complexes to recycle via the fast pathway (Steinberg et al., 2013). Some SNX27-regulated cargos are known to be expressed by OLs. AMPA and NMDA receptors, for example, are expressed, though at low levels, in OL lineage (Hossain et al., 2014; Li et al., 2013). However, it is important to note that their roles in OL differentiation are still controversial with contradictory results reported in particular between *in vivo* and *in vitro* studies (Emery, 2010).

An accurate endosomal sorting has relevant implications for development as shown in other cell lines and tissues. An example is the Frizzled alternative degradation or retrograde transport upon Wnt-induced endocytosis. When the balance between these two pathways is compromised embryonic development alternations have been observed (Seto and Bellen, 2006; Yu et al., 2007). A second example is the lysosomal-mediated down-regulation of erythropoietin receptor, which is a prerequisite to allow erythrocyte precursors complete maturation (Walrafen et al., 2005). On the basis of the observation of the dramatic effects of its knockout, it has been proposed that also SNX27 is required for the correct development of many different tissues: SNX27 deficient mice exhibit severe growth retardation and die within few weeks after birth (Cai et al., 2011).

Taken together, our data highlight the importance of SNX27 expression for OL differentiation via mechanisms that include the regulation of GPR17 recycling. It would be important to reveal whether SNX27 expression decreases during OL maturation in parallel with GPR17 down-regulation, thus further supporting its physiological role in GPR17 expression. Unfortunately, we still have not answered this question. Our preliminary data in Oli-neu suggested that SNX27 expression does not undergo to significant changes during cell differentiation (data not shown). However, online databases reporting gene expression profiling during OL development show that SNX27 transcription is reduced during the differentiation progression (Zhang et al., 2014), in line with the requirement of promoting GPR17 degradation when immature OLs enter terminal maturation. Moreover a recent work by Tian and colleagues has reported that arrestin domain-containing protein 3 (ARRDC3) competes with SNX27 for  $\beta_2$ AR engagement and negatively regulates receptor entrance into recycling tubules, with the final result of maintaining  $\beta_2$ AR in the EE for a prolonged period (Tian et al., 2016). Interestingly, ARRDC3 transcript increases during OL maturation (Marques et al., 2016), raising the possibility that ARRDC3 competition with SNX27 may contribute to GPR17 down-regulation.

## **OL development in SNX27-deficient Ts65Dn brains**

Since SNX27 expression may be involved in OL differentiation we considered the possibility of a dysregulation of OL differentiation in pathological conditions characterized by altered levels of SNX27. A growing number of data indicate that alterations of retromer complex

components (i.e. VPS26 and VPS35 as well as SNX27) are associated to the pathogenesis of some neurodegenerative conditions. With regards to the retromer, it has been shown that in line with its function in the retrograde transport of amyloid precursor protein (APP), reduced levels of expression of both VPS26 and VPS35 subunits are present in brain areas vulnerable to Alzheimer's disease (Small et al., 2005). In addition, mutations that disrupt VPS35 interaction with WASH complex were shown to be risk factors for the pathogenesis of Parkinson's disease (Vilariño-Güel et al., 2011; Zimprich et al., 2011). A mutation/deletion in SNX27 human gene on the other hand, has recently been reported and associated to a familiar form of infantile myoclonic epilepsy and neurodegeneration (Damseh et al., 2015). Finally, recent observations have shown that SNX27 deficiency contributes to cognitive impairment in DS patients by altering the expression of AMPA and NMDA receptors in hippocampal neuron synapses (Wang et al., 2013). On the basis of this observation and our previous data, we investigated OL differentiation in trisomic brains. Using Ts65Dn mouse model of DS, we show alterations in the number of pre-myelinating/mature OLs in different brain regions of trisomic mice. In spite of an overall increase in OLIG2-expressing cells, which suggests an higher number of OLs in Ts65Dn mice brains than in euploids, we report that the number of GPR17-expressing cells are reduced, whereas the number of CC1-positive cells (mature, but not myelinating OLs; Boda et al., 2011; Viganò et al., 2016) is increased. These results are consistent with our *in vitro* findings, indicating a correlation between OL accelerated maturation and GPR17 down-regulation in a context of reduced SNX27 expression. Despite these observations, and in accordance with the condition observed in trisomic brains (Abraham et al., 2012), hypo- and not hyper-myelination was found in Ts65Dn brains, as revealed by immunochemistry and immunoblotting analyses of MBP. This result seems to contradict our *in vitro* findings that indicate an accelerated OL differentiation with any defects in myelin protein synthesis. However, it has been reported that DS brains are characterized by a reduced number of neurons (Contestabile et al., 2007; Guidi et al., 2008; Guidi et al., 2014). Thus, it can be hypothesized that the defects in myelin formation (despite the accelerated maturation of OLs) may be due to the presence of a reduced number of axonal targets.

A thorough analysis would be required to contextualize our results in the complex scenario that DS pathogenesis implies. DS is a highly complex pathological condition, with different factors involved. In this context it is important to note that recent data from Olmos-Serrano and collaborators demonstrate the presence of myelin defects in DS brain (in line with our results) but suggest that these defects may depend on cell autonomous mechanisms related to an altered expression pattern of a cluster of genes required for OPC maturation (Olmos-Serrano et al., 2016).

## **mir-155 up-regulation inhibits OL differentiation**

To gain more insights in the complexity of OL degeneration in DS, we decided to extend our analysis on the molecular mechanisms underlying SNX27 down-regulation. As reported by Wang and colleagues SNX27 deficit depends on the down-regulation of C/EBP $\beta$  TF which is inhibited by the trisomy-linked overexpression of mir-155 (Wang et al., 2013). In line with previous data (Leong et al., 2014) we demonstrated that mir-155 is expressed in oligodendroglial lineage, though at very low levels. This result prompted us to test *in vitro* the effects of mir-155 overexpression using Oli-neu, thus mimicking DS condition. Mir-155 overexpression determines a strong inhibition of OPC differentiation (in line with data of Olmos-Serrano and colleagues, 2016) that finally results in a decreased expression of both GPR17 and myelin proteins, MAG and MBP. In addition, mir-155 overexpression seems to exert an effect also on undifferentiated Oli-neu, leading to a morphological change that resembles that of differentiating cells but without reaching a mature state, since markers of differentiating phases are not expressed (data not shown). On the other hand, transfected cells retain expression of the OPC markers (OLIG2 and NG2) and do not express markers of different lineage (i.e. GFAP) suggesting that they maintain their lineage specification (data not shown).

Apparently, we did not observe a significant decrease of the SNX27 levels in Oli-neu (reduction of approximately 10%) upon overexpression of mir-155. Further experiments are needed to confirm the result and to understand the reasons. One possible explanation is that C/EBP $\beta$  TF is expressed in a very low amount in oligodendroglial lineage cells, as reported by different online databases of gene expression profile during OL differentiation (Zhang et al., 2014; Marques et al., 2016), suggesting that in OLs SNX27 expression may be regulated by different TFs, not affected by mir-155. This partially explains the discrepancy observed between the effects of mir-155 overexpression and the accelerated OL maturation that results from SNX27 silencing.

In the light of these data, we planned to identify mir-155 targets in OLs responsible for the observed effects. To this aim we took advantage of miRTarBase online database (<http://mirtarbase.mbc.nctu.edu.tw/>) to obtain a list of all validated targets of human and murine mir-155. After removal of targets with weak functional evidences, we classified the remaining on the basis of i) their expression during OL differentiation (performed using the mentioned online databases; Zhang et al., 2014; Marques et al., 2016); ii) the number of references reporting their targeting by mir-155 (used as a criterion to assess the strength of the datum); iii) the expression profile in DS brains (used as a criterion for putative functional correlations), performed using the online database generated by Olmos-Serrano and colleagues (Olmos-Serrano et al., 2016); iv) literature evidences reporting associations with OLs.

The result of this *in silico* analysis was the identification of 15 mir-155 targets (Table 3) that have a well-established association to mir-155 and an expression profile that correlates with putative roles in mediating the pathological effects of mir-155 up-regulation in DS brain. Some of these targets will undergo to experimental validation in order to understand their possible physiological and pathological roles in OLs.

## CONCLUSIONS

Our study of the molecular mechanisms underlying GPR17 intracellular trafficking demonstrates a new role for SNX27 in the regulation of GPR17 recycling and in OL differentiation. SNX27 is a well-described mediator of receptor sorting into the fast recycling pathway, but had never been described in OLs. We show that by direct binding with GPR17 PDZ-binding motif, SNX27 prevents receptor degradation, thus contributing to maintain correct levels of GPR17 expression, which is a crucial requisite for OL correct kinetics of differentiation. Furthermore, we described altered OL differentiation and myelin defects in Ts65Dn brain, which correlates with that observed in human DS patients. This suggests that in addition to the well-characterized impairments in neuronal functions, other defects (for example in myelination) may be involved in the pathogenesis of the cognitive deficits that characterize DS. We also propose that up-regulation of mir-155 may be involved not only in neuronal defects (Wang et al., 2013), but also in inhibition of OL maturation and hypomyelination found in trisomic brains. We now propose a list of putative new targets, beside C/EBP $\beta$  / SNX27, that could be used as a starting point to understand mir-155 pathological functions.

These results, apart from contributing to better understand GPR17 and SNX27 physiological functions, deepen our knowledge on the mechanisms that control OL differentiation, and may serve for a better understanding of pathological conditions characterized by myelin degeneration or OL differentiation impairment. Finally, we hope they could be exploited for the development of new strategies to promote myelination repair in demyelinating and neurological diseases.

# ACKNOWLEDGMENTS

I am grateful to Dr. Patrizia Rosa (CNR's Institute of Neuroscience of Milan), who gave me the opportunity to do my PhD project in her laboratory, and constantly supported my work.

I also thank Prof. Panerai and Prof. Corsini (Università degli Studi di Milano), for their help during my PhD studies and precious advices.

I have to thank Prof. Bartesaghi (University of Bologna), who kindly provided Ts65Dn brain samples, Prof. Abbracchio and Prof. Ceruti (Università degli Studi di Milano), who helped me for the immunohistochemical analyses, Prof. Nitsch (University of Napoli Federico II) for kindly providing me DS fibroblasts, and Dr. Benfante (CNR's Institute of Neuroscience of Milan) for her help in the qRT-PCR analyses.

I finally would like to thank my colleagues Veronica, Marta, Nicol and Fabiola, whose contributions were very important for my results.

## REFERENCES

- Abraham H., Vincze A., Veszpremi B., Kravjac A., Gomori E., Kovacs G. and Seress L., Impaired myelination of the human hippocampal formation in Down Syndrome; *International Journal of Developmental Neuroscience*; 2012; 30:147-158.
- Bissing C. and Gruenberg J.; Lipid sorting and multivesicular endosome biogenesis; *Cold Spring Harbor Perspectives in Biology*; 2013; 5(10):a016816.
- Blackstone C., O’Kane J.C. and Reid E.; Hereditary spastic paraplegias: membrane traffic and the motor pathway; *Nature Reviews Neuroscience*; 2011; 12(1):31-42.
- Bockaert J., Dumuis A., Fagni L. and Marin P.; GPCR-GIP networks: a first step in the discovery of new therapeutic drugs?; *Current Opinion in Drug Discovery and Development*; 2004; 7(5):649-657.
- Boda E., Viganò F., Rosa P., Fumagalli M., Labat-Gest V., Tempia F. and Abbracchio M.P.; The GPR17 receptor in NG2 expressing cells: focus on in vivo cell maturation and participation in acute trauma and chronic damage; *Glia*; 2011; 59:1958-1973.
- Boda E., Di Maria S.; Rosa P., Taylor V., Abbracchio M.P. and Buffo A.; Early phenotypic asymmetry of siter oligodendrocyte progenitor cells after mitosis and its modulation by aging and extrinsic factors; *Glia*; 2015; 63:271-286.
- Cai L., Loo L.S., Atlashkin V., Hanson B.J. and Hong W.; Deficiency of sorting sexin 27 (SNX27) leads to growth retardation and elevated levels of N-methyl-D-aspartate receptor 2C (NR2C); *Molecular and Cellular Biology*; 2011; 31(8):1734-1747.
- Carlton J., Bujny M., Rutherford A. and Cullen P.; Sorting nexins – unifying trends and new perspectives; *Traffic*; 2005; 6:75-82.
- Ceruti S., Villa G., Genovese T., Mazzon E., Longhi R., Rosa P., Bramanti P., Cuzzocrea S. and Abbracchio M.P.; The P2Y-like receptor GPR17 as a sensor of damage and a new potential target in spinal cord injury; *Brain*; 2009; 132(Pt 8):2206-2218.

Chen Y., Wu H., Wang S., Koito H., Li J., Ye F., Hoang J., Escobar S.S., Gow A., Arnett H.A., Trapp B.D., Karandikar N.J., Hsieh J. and Lu Q.R.; The oligodendrocyte-specific G protein-coupled receptor GPR17 is a cell-intrinsic timer of myelination; *Nature Neuroscience*; 2009; 12:1398-1406.

Ciana P., Fumagalli M., Trincavelli M.L., Verderio C., Rosa P., Lecca D., Ferrario S., Parravicini C., Capra V., Gelosa P., Guerrini U., Belcredito S., Cimino M., Sironi L., Tremoli E., Rovati G.E., Martini C. and Abbracchio M.P.; The orphan receptor GPR17 identified as a new dual uracil nucleotides/cysteinyl-leukotrienes receptor; *EMBO Journal*; 2006; 25:4615-4627.

Clairfeuille T., Mas C., Chan A.S., Yang Z., Tello-Lafoz M., Chandra M., Widagdo J., Kerr M.C., Paul B., Merida I., Teasdale R.D., Pavlos N.J., Anggono V. and Collins B.M.; A molecular code for endosomal recycling of phosphorylated cargos by the SNX27-retromer complex; *Nature Structural and Molecular Biology*; 2016; 23(10):921-932.

Contestabile A., Fila T., Ceccarelli C., Bonasoni P., Bonapace L., Santini D., Bartesaghi R. and Ciani E.; Cell cycle alteration and decreased cell proliferation in the hippocampal dentate gyrus and in the neocortical germinal matrix of fetuses with Down syndrome and in Ts65Dn mice; 2007; *Hippocampus*; 17:665-678.

Cullen P.J. and Korswagen H.C.; Sorting nexins provide diversity for retromer-dependent trafficking events; *Nature Cell Biology*; 2011; 14(1):29-37.

Damseh N., Danson C.M., Al-Ashhab M., Abu-Libdeh B., Gallon M., Sharma K., Yaacov B., Coulthard E., Caldwell M.A., Edvardson S., Cullen P.J. and Elpeleg O.; A defect in the retromer accessory protein, SNX27, manifests by infantile myoclonic epilepsy and neurodegeneration; *Neurogenetic*; 2015; 16:215-221.

Daniele S., Trincavelli M.L., Fumagalli M., Zappelli E., Lecca D., Bonfanti E., Campiglia P., Abbracchio M.P. and Martini C.; Does GRK- $\beta$  arrestin machinery work as a “switch on” for GPR17-mediated activation of intracellular signaling pathways?; *Cell Signaling*; 2014; 26:1310-1325.

De Biase L.M., Nishiyama A. and Bergles D.E.; Excitability and synaptic communication within oligodendrocyte lineage; *Journal of Neuroscience*; 2010; 30(10):3600-3611.



De Biase L.M., Kang S.H., Baxi E.G., Fukaya M., Pucak M.L., Mishina M., Calabresi P.A. and Bergles D.E.; NMDA receptor signaling in oligodendrocyte progenitors is not required for oligodendrogenesis and myelination; *Journal of Neuroscience*; 2011; 31:12650-12662.

Di Paolo G. and De Camilli P.; Phosphoinositides in cell regulation and membrane dynamics; *Nature*; 2006; 443(12):651-657.

Donowitz M., Cha B., Zachos N.C., Brett C.L., Sharma A., Tse C.M. and Li X.; NHERF family and NHE3 regulation; *Journal of Physiology*; 2005; 567(Pt. 1):3-11.

Duglas J.C., Cuellar T.L., Scholze A., Ason B., Ibrahim A., Emery B., Zamanian J.L., Foo L.C., McManus M.T. and Barres B.A.; Dicer1 and miR-219 are required for normal oligodendrocyte differentiation and myelination; *Neuron*; 2010; 65:597-611.

Elkin S.R., Lakoduk A.M., Schmid S.L.; Endocytic pathways and endosomal trafficking: a primer; *Wiener Medizinische Wochenschrift (1946)*; 2016; 166(7-8):196-204.

Emery B.; Regulation of oligodendrocyte differentiation and myelination; *Science*; 2010; 330(6005):779-782.

Fields R.D.; White matter in learning, cognition and psychiatric disorders; *Trends in Neuroscience*; 2008; 31:361-370.

Fratangeli A., Parmigiani E., Fumagalli M., Lecca D., Benfante R., Passafaro M., Buffo A., Abbracchio M.P. and Rosa P.; The regulated expression, intracellular trafficking and membrane recycling of the P2Y-like receptor GPR17 in Oli-neu oligodendroglial cells; *Journal of Biological Chemistry*; 2013; 288:5241-5256.

Fumagalli M., Daniele S., Lecca D., Lee P.R., Parravicini C., Fields R.D., Rosa P., Antonucci F., Verderio C., Trincavelli M.L., Bramanti P., Martini C. and Abbracchio M.P.; Phenotypic changes, signaling pathway, and functional correlates of GPR17-expressing neural precursor cells during oligodendrocyte differentiation; *Journal of Biological Chemistry*; 2011; 286:10593-10604.

Fumagalli M., Bonfanti E., Daniele S., Zappelli E., Lecca D., Martini C., Trincavelli M.L. and Abbracchio M.P.; The ubiquitin ligase mdm2 controls oligodendrocyte maturation by intertwining mTOR with G protein-coupled receptor kinase 2 in the regulation of GPR17 receptor desensitization; *Glia*; 2015; 63(12):2327-2339.

Gallon M., Clairfeuille T., Steinberg F., Mas C., Ghai R., Sessions R.B., Teasdale R.D., Collins B.M. and Cullen P.J.; A unique PDZ domain and arrestin-like fold interaction reveals mechanistic details of endocytic recycling by SNX27-retromer; *PNAS*; 2014; 111(35):E3604-3613.

Gallon M. and Cullen P.J.; Retromer and sorting nexins in endosomal sorting; *Biochemical Society Transactions*; 2015; 43(1):33-47.

Grandy D., Shan J., Zhang X., Rao S., Akunuru S., Li H., Zhang Y., Alpatov I., Zhang X.A., Lang R.A., Shi D.L. and Zheng J.J.; Discovery and characterization of a small molecule inhibitor of the PDZ domain of dishevelled; *Journal of Biological Chemistry*; 2009; 284:16256–16263.

Grant B.D. and Donaldson J.G.; Pathways and mechanisms of endocytic recycling; 2009; 10(9):597-608.

Gruenberg J; The endocytic pathway: a mosaic of domains; *Nature Review Molecular Cell Biology*; 2001; 2(10):721-730.

Guidi S., Bonasoni P., Ceccarelli C., Santini D., Gualtieri F., Ciani E. and Bartesaghi R.; Neurogenesis impairment and increased cell death reduce total neuron number in the hippocampal region of fetuses with Down syndrome; *Brain Pathology*; 2008; 18:180-197.

Guidi S., Stagni F., Bianchi P., Ciani E., Giacomini A., De Franceschi M., Moldrich R., Kurniawan N., Mardon K., Giuliani A., Calzà L. and Bartesaghi R.; Prenatal pharmacotherapy rescues brain development in a Down's syndrome mouse model; 2014; *Brain*; 137:380-401.

Hanyaloglu A.C. and von Zastrow M.; Regulation of GPCRs by endocytic membrane trafficking and its potential implications; *Annual Review of Pharmacology and Toxicology*; 2008; 48:537-568.

Harris Z.L. and Lim A.W.; Mechanism and role of PDZ domains in signaling complex assembly; *Journal of Cell Science*; 2001; 114:3219-3231.

He L. and Lu R.Q.; Coordinated control of oligodendrocyte development by extrinsic and intrinsic signaling cues; *Neuroscience Bulletin*; 2013; 29(2):129-143.

Hennen S., Wang H., Peters L., Merten N., Simon K., Spinrath A., Blattermann S., Akkari R., Schrage R., Schroder R., Schulz D., Vermeiren C., Zimmermann K., Kehraus S., Drewke C., Pfeifer A., Konig G.M., Mohr K., Gillard M., Muller C.E., Lu Q.R., Gomeza J. and Kostenis E.; Decoding signaling and function of the orphan G protein-coupled receptor GPR17 with a small-molecule agonist; *Science Signaling*; 2013; 6:1-16.

Hossain S., Liu H.N., Fragoso G. and Almazan G.; Agonist-induced downregulation of AMPA receptors in oligodendrocyte progenitors; *Neuropharmacology*; 2014; 79:506–514.

Houtari J. and Helenius A.; Endosome maturation; *EMBO Journal*; 2011; 30:3481-3500.

Irannejad R., Tsvetanova N.G., Lobingier B.T. and von Zastrow M.; Effects of endocytosis on receptor-mediated signaling; *Current Opinion in Cell Biology*; 2015; 35:137-143.

Johannes L. and Popoff V.; Tracing the retrograde route in protein trafficking; *Cell*; 2008; 135:1175-1187.

Joubert L., Hanson B., Barthet G., Sebben M., Claeysen S., Hong W., Marin P., Dumuis A. and Bockaert J.; New sorting nexin (SNX27) and NHERF specifically interact with the 5-HT<sub>4(a)</sub> receptor splice variant: roles in receptor targeting; *Journal of Cell Science*; 2004; 117:5367-5379.

Jung M., Krämer E., Grzenkowski M., Tang K., Blakemore A., Aguzzi A., Khazaie K., Chlichlia K., von Blankenfeld G. and Kettenmann H.; Lines of murine oligodendroglial precursor cells immortalized by an activated neu tyrosine kinase show distinct degrees of interaction with axons in vitro and in vivo; *European Journal of Neuroscience*; 1995; 7:1245-1265.

Lau A.G. and Hell R.A.; Oligomerization of NHERF1 and NHERF2 PDZ domains: differential regulation by association with receptor carboxyl-termini and by phosphorylation; *Biochemistry*; 2001; 40(29):8572-8580.

Lauffer B.E.L., Melero C., Temkin P., Lei C., Hong W., Kortemme T. and von Zastrow M.; SNX27 mediates PDZ-directed sorting from endosomes to the plasma membrane; *Journal of Cell Biology*; 2010; 190(4):565-574.

Le T.L., Yap A.S. and Stow J.L.; Recycling of E-cadherin: a potential mechanism for regulating cadherin dynamics; *Journal of Cell Biology*; 1999; 146:219–232.

Lecca D., Trincavelli M.L., Gelosa P., Sironi L., Ciana P., Fumagalli M., Villa G., Verderio C., Grumelli C., Guerrini U., Tremoli E., Rosa P., Cuboni S., Martini C., Buffo A., Cimino M. and Abbracchio M.P.; The recently identified P2Y-like receptor GPR17 is a sensor of brain damage and a new target for brain repair; *PLoS One*; 2008; 3(10):e3579.

Lecca D., Marangon D., Coppolino G.T., Mendez A.M., Finardi A., Costa G.D., Martinelli V., Furlan R. and Abbracchio M.P.; mir-125a-3p timely inhibits oligodendroglial maturation and is pathologically up-regulated in human multiple sclerosis; *Scientific Reports*; 2016; 6:34503.

Lee S., Chang J. and Blackstone C.; FAM21 directs SNX27-retromer cargoes to the plasma membrane by preventing transport to the Golgi apparatus; *Nature Communications*; 2016; 7:10939.

Leong S.Y., Rao V.T., Bin J.M., Gris P., Sangaralingam M., Kennedy T.E and Antel J.P.; Heterogeneity of oligodendrocyte progenitor cells in adult human brain; *Annals of Clinical and Translational Neurology*; 2014; 1(4):272-283.

Li C., Xiao L., Liu X., Yang W., Shen W., Hu C., Yang G. and He C.; A functional role of NMDA receptor in regulating the differentiation of oligodendrocyte precursor cells and remyelination; *Glia*; 2013; 61:5732–5749.

Li H., Lu Y., Smith H.K. and Richardson W.D; Olig1 and Sox10 interact synergistically to drive myelin basic protein transcription in oligodendrocytes; *Journal of Neuroscience*; 2007; 27(52):14375-14382.

Liu D.P., Schmidt C., Billings T. and Davisson M.T.; Quantitative PCR genotyping assay for the Ts65Dn mouse model of Down syndrome; *Biotechniques*; 2003; 35:1170-1174.

Lopez Juarez A., He D. and Lu R.Q.; Oligodendrocyte progenitor programming and reprogramming: toward myelin regeneration; *Brain Research*; 2016; 1638(Pt B):209-220.

Lu R.Q., Sun T., Zhu Z., Ma N., Garcia M., Stiles C.D. and Rowitch D.H.; Common developmental requirement for Olig function indicates a motor neuron/oligodendrocyte connection; *Cell*; 2002; 109(1):75-86.

Lunn M.L., Nassirpour R., Arrabit C., Tan J., McLeod I., Arias C.M., Sawchenko P.E., Yates J.R. 3rd and Slesinger P.A.; A unique sorting nexin regulates trafficking of potassium channels via PDZ domain interaction; *Nature Neuroscience*; 2007; 10(10):1249-1259.

Luo F., Burke K., Kantor C., Miller R.H. and Yang Y.; Cyclin-dependent kinase 5 mediates adult OPC maturation and myelin repair through modulation of Akt and GSK-3 $\beta$  signaling; *Journal of Neuroscience*; 2014; 34:10415-10429.

Marques S., Zeisel A., Codeluppi S., van Bruggen D., Falcao A.M., Xiao L., Li H., Häring M., Hochgerner H., Romanov R.A., Gyllborg D., Munoz-Manchado A.B., La Manno G., Lönnerberg P., Floriddia E.M., Rezayee F., Ernfors P., Arenas E., Hjerling-Leffer J., Harkany T., Richardson W.D., Linnarsson S. and Castelo-Branco G.; Oligodendrocyte heterogeneity in the mouse juvenile and adult central nervous system; *Science*; 2016; 352(6291):1326-1329.

Mayoral S.R. and Chan J.R.; The environment rules: spatiotemporal regulation of oligodendrocyte differentiation; *Current Opinion in Neurobiology*; 2016; 39:47-52.

McGough I.J., Steinberg F., Gallon M., Yatsu A., Ohbayashi N., Heesom K.J., Fukuda M. and Cullen P.J.; Identification of molecular heterogeneity in SNX27-retromer-mediated endosome-to-plasma-membrane recycling; *Journal of Cell Science*; 2014; 127(Pt 22):4940-4953.

McMillan K.J., Gallon M., Jellet A.P., Clairfeuille T., Tilley F.C., McGough I., Danson C.M., Heesom K.J., Wilkinson K.A., Collins B.M. and Cullen P.J.; Atypical parkinsonism-associated

retromer mutant alters endosomal sorting of specific cargo proteins; *Journal of Cell Biology*; 2016; 214(4):389-399.

Medina-Rodriguez E., Arenzana F.J., Bribian A. and de Castro F.; Protocol to isolate a large amount of functional oligodendrocyte precursor cells from the cerebral cortex of adult mice and humans; *PLoS One*; 2013; 8:e81620.

Mitew S., Hay C.M., Peckam H., Xiao J., Koenning M. and Emery B., Mechanisms regulating the development of oligodendrocytes and central nervous system myelin; *Neuroscience*; 2014; 276:29-47.

Munoz M.B. and Slesinger P.A.; Sorting nexin 27 regulation of G protein-gated inwardly rectifying K<sup>+</sup> channels attenuates in vivo cocaine response; *Neuron*; 2014; 82(3):659-669.

Nisar S.P., Cunningham M., Saxena K., Pope R.J., Kelly E. and Mundell S.J.; Arrestin scaffolds NHERF1 to the P2Y12 receptor to regulate receptor internalization; *Journal of Biological Chemistry*; 2012; 287:24505-24015.

O'Connell R.M., Chaudhuri A.A., Rao D.S. and Baltimore D.; Inositol phosphatase SHIP1 is a primary target of miR-155; *PNAS*; 2009; 106(17):7113-7118.

Olmos-Serrano J.L., Kang H.J., Tyler W.A., Silbereis J.C., Cheng F., Zhu Y., Pletikos M., Jankovic-Rapan L., Cramer N.P., Galdzicki Z., Goodliffe J., Peters A., Sethares C., Delalle I., Golden J.A., Haydar T.F. and Sestan N.; Down syndrome developmental brain transcriptome reveals defective oligodendrocyte differentiation and myelination; *Neuron*; 2016; 89:1-15.

Pfeffer S.R.; A nexus for receptor recycling; 2013; 15(5):446-448.

Reeves R.H., Irving N.G., Moran T.H., Wohn A., Kitt C., Sisodia S.S., Schmidt C., Bronson R.T. and Davisson M.T.; A mouse model of Down syndrome exhibits learning and behaviour deficits; *Nature Genetics*; 1995; 11:177-184.

Richardson W.D., Kessaris N. and Pringle N.; Oligodendrocyte wars; *Nature Review Neuroscience*; 2006; 7(1):11-8.

Rincon E., Santos T., Avila-Flores A., Albar J.P., Lalioti V., Lei C., Hong W. and Merida I.; Proteomic identification of sorting nexin 27 as a diacylglycerol kinase  $\zeta$ -associated protein; *Molecular and Cellular Proteomics*; 2007; 6(6):1073-1087.

Romero G., von Zastrow M. and Friedman P.A.; Role of PDZ proteins in regulating trafficking, signaling, and function of GPCRs: means, motif, and opportunity; *Advances in Pharmacology*; 2011; 62:279-314.

Sachs H.H., Bercury K.K., Popescu D.C., Narayanan S.P. and Macklin W.B.; A new model of cuprizone-mediated demyelination/remyelination; *ASN Neuro*; 2014; 6(5):1759091414551955.

Scita G. and Di Fiore P.P.; The endocytic matrix; *Nature*; 2010; 463:464-473.

Scott C.C., Vacca F. and Gruenberg J.; Endosome maturation, transport and functions; *Seminars in Cell and Developmental Biology*; 2014; 31:2-10.

Seaman M.N.J.; The retromer complex – endosomal protein recycling and beyond; *Journal of Cell Science*; 2012; 125:4693-4702.

Seto E.S. and Bellen H.J.; Internalization is required for proper wingless signaling in *Drosophila melanogaster*; *Journal of Cell Biology*; 2006;173:95-106.

Sheng M. and Sala C.; PDZ domains and the organization of supramolecular complexes; *Annual Review Neuroscience*; 2001; 24:1-29.

Simon K., Hennen S., Merten N., Blattermann S., Gillard M., Kostenis E. and Gomeza J.; The orphan G protein-coupled receptor GPR17 negatively regulates oligodendrocyte differentiation via *Gai/o* and its downstream effector molecules; *Journal of Biological Chemistry*; 2016; 291(2):705-718.

Small S.A., Kent K., Pierce A., Leung C., Kang M.S., Okada H., Honig L., Vonsattel J.P. and Kim T.W.; Model-guided microarray implicates the retromer complex in Alzheimer's disease; *Annals of Neurology*; 2005; 58:909-919.

Small S.A. and Petsko G.A.; Retromer in Alzheimer disease, Parkinson disease and other neurological disorders; *Nature Review Neuroscience*; 2015; 16(3):126-132.

Somkuwar S.S, Staples M.C., Galitano M.H., Fannon M.J. and Mandyam C.D., Role of NG2 expressing cells in addiction: a new approach for an old problem; *Frontiers in Pharmacology*; 2014; 5:279.

Steinberg F., Gallon M., Winfield M., Thomas E.C., Bell A.J., Heesom K.J., Tavaré J.M. and Cullen P.J.; A global analysis of SNX27-retromer assembly and cargo specificity reveals a function in glucose and metal ion transport; *Nature Cell Biology*; 2013; 15:461-471.

Temkin P., Lauffer B., Jäger S., Cimermancic P., Krogan N.J. and von Zastrow M.; Snx27 mediates retromer tubule entry and endosome-to-plasma membrane trafficking of signaling receptors; *Nature Cell Biology*; 2011; 13(6):715-721.

Tian X., Irannejad R., Bowman S.L., Du Y., Puthenveedu M.A., von Zastrow M. and Benovic J.L.; The  $\alpha$ -arrestin ARRDC3 regulates the endosomal residence time and intracellular signaling of the  $\beta$ 2-adrenergic receptor; *Journal of Biological Chemistry*; 2016; 291(28):14510-14525.

Traiffort E., Zakaria M., Laouarem Y. and Ferent J.; Hedgehog: a key signaling in the development of oligodendrocyte lineage; *Journal of Developmental Biology*; 2016; 4(28).

Tyler W.A., Jain M.R., Cefelli S.E., Li Q., Ku L., Feng Y., Li H. and Wood T.L.; Proteomic identification of novel targets regulated by the mammalian target of rapamycin pathway during oligodendrocyte differentiation; *Glia*; 2011; 59(11):1754-1769.

van Weert A.W., Geuze H.J., Groothuis B. and Stoorvogel W.; Primaquine interferes with membrane recycling from endosomes to the plasma membrane through a direct interaction with endosomes which does not involve neutralization of endosomal pH nor osmotic swelling of endosomes; *European Journal of Cell Biology*; 2000; 79(6):394-399.



Viganò F., Schneider S., Cimino M., Bonfanti E., Gelosa P., Sironi L., Abbracchio M.P. and Dimou L.; GPR17 expressing NG2-glia: oligodendrocyte progenitors serving as a reserve pool after injury; *Glia*; 2016; 64(2):287-299.

Vilariño-Güell C., Wider C., Ross O.A., Dachsel J.C., Kachergus J.M., Lincoln S.J., Soto-Ortolaza A.I., Cobb S.A., Wilhoite G.J., Bacon J.A., Behrouz B., Melrose H.L., Hentati E., Puschmann A., Evans D.M., Conibear E., Wasserman W.W., Aasly J.O., Burkhard P.R., Djaldetti R., Ghika J., Hentati F., Krygowska-Wajs A., Lynch T., Melamed E., Rajput A., Rajput A.H., Solida A., Wu R.M., Uitti R.J., Wszolek Z.K., Vingerhoets F. and Farrer M.J.; VPS35 mutations in Parkinson disease; *American Journal of Human Genetics*; 2011; 89:162-167.

Walrafen P., Verdier F., Kadri Z., Chrétion S., Lacombe C. and Mayeux P.; Both proteasomes and lysosomes degrade the activated erythropoietin receptor; *Blood*; 2005; 15:600-608.

Wang S., Sdrulla A.D., Di Sibio G., Bush G., Nofziger D., Hicks C., Weinmaster G. and Barres B.A.; Notch receptor activation inhibits oligodendrocyte differentiation; *Neuron*; 1998; 21:63-75.

Wang X., Zhao Y., Zhang X., Badie H., Zhou Y., Mu Y., Loo L.S., Cai L., Thompson R.C., Yang B., Chen Y., Johnson P.F., Wu C., Bu G., Mobley W.C., Zhang D., Gage F.H., Ranscht B., Zhang Y.W., Lipton S.A., Hong W. and Xu H., Loss of sorting nexin 27 contributes to excitatory synaptic dysfunction by modulating glutamate receptor recycling in Down's syndrome; *Nature Medicine*; 2013; 19(4):473-481.

Wang X., Huang T., Zhao Y., Zheng Q., Thompson R.C., Bu G., Zhang Y.W., Hong W. and Xu H.; Sorting nexin 27 regulates A $\beta$  production through modulating  $\gamma$ -secretase activity; *Cell Reports*; 2014; 9:1023-1033.

Wolf R.M., Wilkes J.J., Chao M.V. and Resh M.D.; Tyrosine phosphorylation of p190 RhoGAP by Fyn regulates oligodendrocyte differentiation; *Journal of Neurobiology*; 2001; 49:62-78.

Xin M., Yue T., Ma Z., Wu F., Gow A. and Lu R.Q.; Myelinogenesis and axonal recognition by oligodendrocytes in brain are uncoupled in *Olig1*-null mice; *Journal of Neuroscience*; 2005; 25(6):1354-1365.

Ye F., Chen Y., Hoang T., Montgomery R.N., Zhao X.H., Bu H., Hu T., Taketo M.M., van Es J.H., Clevers H., Hsieh J., Bassel-Duby R., Olson E.N., Lu R.Q.; HDAC1 and HDAC2 regulate oligodendrocyte differentiation by disrupting the beta-catenin-TCF interaction; *Nature Neuroscience*; 2009; 12:829-838.

Yu A., Rual J.F., Tamai K., Harada Y., Vidal M., He X. and Kirchhausen T.; Association of dishevelled with the clathrin AP-2 adaptor is required for frizzled endocytosis and planar cell polarity signaling; 2007; *Developmental Cell*; 12:129-141.

Yu K., McGlynn S. and Matise M.P. Floor plate-derived sonic hedgehog regulates glial and ependymal cell fates in the developing spinal cord; *Development*; 2013; 140:1594-1604.

Zhang Y., Chen K., Sloan S.A., Bennett M.L., Scholze A.R., O'Keefe S., Phatnani H.P., Guarnieri P., Caneda C., Ruderisch N., Deng S., Leddelow S.A., Zhang C., Daneman R., Maniatis T., Barres B.A. and Wu J.Q.; An RNA-sequencing transcriptome and splicing database of glia, neurons, and vascular cells of the cerebral cortex; *Journal of Neuroscience*; 2014; 34(36):11929-11947.

Zhao X., He X., Han X., Yu Y., Ye F., Chen Y., Hoang T., Xu X., Mi Q.S., Xin M., Wang F., Appel B. and Lu Q.R.; MicroRNA-mediated control of oligodendrocyte differentiation; *Neuron*; 2010; 65(5):612-626.

Zimprich A., Benet-Pagès A., Struhal W., Graf E., Eck S.H., Offman M.N., Haubenberger D., Spielberger S., Schulte E.C., Lichtner P., Rossle S.C., Klopp N., Wolf E., Seppi K., Pirker W., Presslauer S., Mollenhauer B., Katzenschlager R., Foki T., Hotzy C., Reinthaler E., Harutyunyan A., Kralovics R., Peters A., Zimprich F., Brücke T., Poewe W., Auff E., Trenkwalder C., Rost B., Ransmayr G., Winkelmann J., Meitinger T. and Strom T.M.; A mutation in VPS35, encoding a subunit of the retromer complex, causes late-onset Parkinson disease; *American Journal of Human Genetics*; 2011; 89:168-175.

Zuchero J.B. and Barres B.A.; Intrinsic and extrinsic control of oligodendrocyte development; *Current Opinion in Neurobiology*; 2013; 23(6):914-920.

**Table 1. Primary antibodies used in the study.**

anti-GPR17 C-terminal – polyclonal	Raised in rabbit (Fratangeli et al., 2013)	Western blotting (dilution 1.75 µg/µL), immunofluorescence, (dilution 10 µg/µL) and immunohistochemistry (dilution 1:20,000)
anti-GPR17 N-terminal – polyclonal	Raised in rabbit (Fratangeli et al., 2013)	Immunofluorescence of living cells (dilution 10 µg/250 µL)
MAG – monoclonal	Merck Millipore (Billerica, MA)	Western blotting (dilution 1:1,000) and immunofluorescence (dilution 1:200)
Flag tag – monoclonal	Merck Millipore (Billerica, MA)	Immunofluorescence of live cells (dilution 1:150) and fixed samples (dilution 1:250)
Myc tag – monoclonal	Sigma-Aldrich (Milan, IT)	Western blotting (dilution 1:500) and immunofluorescence (dilution 1:300)
MBP – monoclonal	Covance (Milan, IT)	Immunofluorescence (dilution 1:500)
MBP – monoclonal	Merck Millipore (Temecula, CA)	Western blotting (dilution 1:2,000)
TfR – monoclonal	Life Technologies (Monza, IT)	Western blotting (dilution 1:1,000) and immunofluorescence (dilution 1:100)
GFP – polyclonal	Merck Millipore (Billerica, MA)	Western blotting (dilution 1:2,000)
Pan cadherin – monoclonal	Sigma-Aldrich (Milan, IT)	Western blotting (dilution 1:1,000) and immunofluorescence (dilution 1:150)
NHERF – polyclonal	Thermo Scientific (Rockford, IL)	Western blotting (dilution 1:1,000)
NG2 – polyclonal	Merck Millipore (Temecula, CA)	Immunofluorescence (dilution 1:150)
SNX27 – polyclonal	Novus Biologicals (Cambridge, UK)	Western blotting (dilution 1:1,000) and immunofluorescence (dilution 1:100)
SNX27 – polyclonal	Raised in goat. Santa Cruz Biotechnology (Dallas, TX)	Immunofluorescence (dilution 1:400)
Actin - monoclonal	Sigma-Aldrich (Milan, IT)	Western blotting (dilution 1:1,000)
GS28 - monoclonal	Enzo Life Science (Italy)	Western blotting (dilution 1:1,000)
Olig2 – polyclonal	Merck Millipore (Billerica, MA)	Immunohistochemistry (dilution 1:200) and immunofluorescence (dilution 1:150)
CC1 – monoclonal	Merck Millipore (Billerica, MA)	Immunohistochemistry (dilution 1:50)
Id2 – polyclonal	Santa Cruz Biotechnology (Dallas, TX)	Western blotting (dilution 1:400)
GAPDH – monoclonal	Santa Cruz Biotechnology (Dallas, TX)	Western blotting (dilution 1:500)
α-tubulin – monoclonal	Sigma-Aldrich (Milan, IT)	Western blotting (dilution 1:1,500)
GRK2 – polyclonal	Santa Cruz Biotechnology (Dallas, TX)	Western blotting (dilution 1:200)
mTOR – monoclonal	Cell Signaling (Danvers, MA)	Western blotting (dilution 1:1,000)
Phospho-mTOR – monoclonal	Cell Signaling (Danvers, MA)	Western blotting (dilution 1:500)

**Table 2. GPR17 PDZ-binding motif mutants used in the study.**

Name	Sequence
mGPR17-wt	ATG [...]AGT.GCC.CGA.TCC.GAG.CTG.TGA NH [...] S A R <u>S E L</u> *
mGPR17-SELA	ATG [...]AGT.GCC.CGA.TCC.GAG.CTG.GCA.TAA NH [...] S A R S E L A *
FLAG-hGPR17-wt	ATG [...]AGT.GCC.AAG.TCA.GAG.CTG.TGA NH [...] S A K <u>S E L</u> *
FLAG-hGPR17-SELA	ATG [...]AGT.GCC.AAG.TCA.GAG.CTG.GCA.TGA NH [...] S A K S E L A *

**Table 3. Putative mir-155 targets in OL differentiation** (GO was based on NCBI database updated at the 26th of November 2016; in bold are DEX genes from the database of Olmos-Serrano and colleagues, 2016).

<b>Gene Name</b>	<b>Gene Ontology</b>	<b>Species</b>
<b>OPCs</b>		
<b>SOCS1</b>	Insulin-like growth factor receptor binding; kinase inhibitor activity; negative regulator of JAK-STAT cascade	Mouse and Human
HIVEP2	DNA binding; metal ion binding; multicellular organism development; regulation of transcription	Human
MASTL	ATP binding; protein phosphatase 2A binding; protein serine/threonine kinase activity; G2/M transition of mitotic cells; cell division	Human
<b>TAF5L</b>	Contributes to histone acetyltransferase activity; transcription coactivator activity; histone H3 acetylation	Human
TLE4	Chromatin binding; transcription factor activity; Wnt signaling pathway	Human
TRAK1	GABA receptor binding; endosome to lysosome transport; protein O-linked glycosylation	Human
<b>NFOs (Newly Forming Oligodendrocytes)</b>		
<b>LRRC9</b>	NAD <sup>+</sup> ADP ribosyltransferase activity	Human
<b>MFOs (Myelin Forming Oligodendrocytes)</b>		
FAM135A	Carboxylic ester hydrolase activity; cellular lipid metabolic process	Human
MEF2A	RNA polymerase II core promoter proximal region sequence-specific DNA binding; RNA polymerase II transcription factor binding; ERK5 cascade	Human
MEIS1	RNA polymerase II core promoter proximal region sequence-specific DNA binding; chromatin binding; angiogenesis	Human
PCDH9	Calcium ion binding; forebrain development; cell-cell contact zone	Human
PHC2	DNA binding; multicellular organism development; PRC1 complex	Human
RAB11FIP2	RabGTPase binding; establishment of cell polarity; insulin secretion involved in cellular response to glucose stimulus; regulated exocytosis	Human
SECISBP2	mRNA 3'-UTR binding; poly(A) RNA binding; negative regulator of nuclear-transcribed mRNA catabolic process, nonsense-mediated decay; neuron development	Human
<b>MOs (Myelinating Oligodendrocytes)</b>		
CEP41	G2/M transition of mitotic cell cycle; cell surface; cell-cell junction; centriole	Human